ADDIS ABABA UNIVERSITY

SCHOOL OF GRADUATE STUDIES

FACULTY OF TECHNOLOGY

DEPARTMENT OF ELECTRICAL and COMPUTER ENGINEERING

DSP BASED FIELD WEAKENING CONTROL OF PMSM

A thesis submitted to the School of Graduate Studies in partial fulfillment of the requirement for the degree of Master of Science in Electrical and Computer Engineering (Control)

By:

Dereje Shibeshi

Advisor: Dr. Mengesha Mamo

October 2007

Declaration

I, the undersigned declare that this thesis is my original work, and has not been presented for a degree in this or any other university, and all sources of materials used for the thesis have been fully acknowledged.

Dereje Shibeshi	_____
Name	Signature
Addis Ababa	October12, 2007
Place	Date of submission

This thesis has been submitted with my approval as a university advisor

Dr. Mengesha Mamo	_____
Advisor Name	Signature

ADDIS ABABA UNIVERSITY

SCHOOL OF GRADUATE STUDIES

"DSP based field weakening control of PMSM"

By

Dereje Shibeshi

Faculty of Technology

Approval by Board Examiners

Dr. Mengesha Mamo Chairman, Department Graduate Committee	Signature
Dr. Mengesha Mamo Advisor	Signature
Dr. Getachew Alemu Internal Examiner	Signature
Prof. Girma Mullisa External Examiner	Signature

ACKNOWLEDGEMENT

I would like to express my deepest thanks and gratitude to my advisor Dr. Mengesha Mamo for his invaluable advices, comments, encouragement, continuous guidance, remarkable patience and caring support during my graduate studies.

I would also like to thank every staff members of the electrical power department in DEC and AAU for giving me the necessary laboratory equipments and their encouragement.

I also express my love and millions of thanks to my family who provide me basic schooling and my beloved wife, Tizu, whose love and encouragement have been so strategic in completing this thesis. I do want to thank Ato Abraham Belay for purchasing the DSP with its JTAG emulator. Finally I would like to say thanks to different authors who I mentioned in the references, and companies like Texas Instruments and Danotek Motion Technology.

> And to the Father Almighty, may You continue to give me strength and vision that I may follow your path…..to eternal salvation.

TABLE OF CONTENTS **Pages**

1. INTRODUCTION..…….. 1

2. FIELD WEAKENING CONTROL OF PMSM…….…….. 5

2.1 General overview of conventional synchronous motor …..... …….5

2.2 Permanent Magnet Machines ……..…….. …….7

2.3 Classification of permanent magnet motors.……...8

2.3.1 Direction of field flux……..8

2.3.2 Flux density distribution……..……. …..8

2.3.3 Permanent magnet radial field motors…….....9

2.4 Why concentrate this study on PMSM ?…….....11

2.4.1 Advantages of PM machines…….…….....11

2.4.2 Disadvantages of PM machines…….11

2.5 Application…….…….12

2.6 Mathematical Model of PMSM for Field Oriented (Vector) Control……....13

2.6.1 Field Oriented (Vector) control…….....13

2.6.2 Rotating transformation……..……16

2.6.2.1 Space vector definition……...17

2.6.3 Dynamic model of PMSM…….23

2.7 PMSM control structure……..27

2.7.1 Space Vector Pulse Width Modulation (SVPWM…….. ..31

2.7.2 Implementation of Space Vector PWM…….... .41

2.7.3 Position sensor….....52

2.7.4 Current Controlled inverter…… ..55

2.7.5 PI Controller…….....57

2.7.6 Current sensing…….....60

2.8 Field weakening strategies……..... 61

2.8.1 Concept of field weakening operation……... 61

2.8.2 Field-weakening analysis of Permanent Magnet Motors…….... 66

2.8.3 operation in flux weakening region…… 67

2.8.4 Common flux weakening strategies ……... ……. 69
2.8.4.1 Constant voltage constant power control…….. 73
2.8.4.2 Constant current constant power control…….. 75
2.8.4.3 Optimum current vector……... 78

3. SIMULATION AND EXPERIMENTAL SET UP ……...……... 82

3.1Simulation result and discussion……. 82
3.1.1 Simulation for Operation at 150 rad/s (without field weakening).83
3.1.2 Simulation for Operation at Higher Speed of 233 rad/s
(with field weakening)……86

3.2 System hardware and software organization…… 92
3.2.1 System hardware ……. 92
3.2.1.1 The DSP (TDS 2407 EA) in motor control…….. 92
3.2.1.2 A large range of application…….. 97
3.2.2 System software organization……99

4. CONCLUSION……..……..104

4.1 Conclusion……..104
4.2 Recommendation……105

REFERENCES……...106
APPENDIX

LIST OF FIGURES

Figure **Page number**

Figure 1.1 PMSM 'Two rotating stator winding' two phase model……....2

Figure 2.1 Revolving-field synchronous motor..……...……..5

Figure 2.2 Rotor configurations …..…….……..10

Figure 2.3 Summary of classification of AC synchronous machine …….…….10

Figure 2.4 Separately excited DC motor …… ...14

Figure 2.5 Three-phase motor surface mounted PMSM model...……..….16

Figure 2.6 Stator Current Space Vector and Its Projection ……..… 18

Figure 2.7 Three-phase windings and two-axes equivalent (α/β transformation) 20

Figure 2.8 PMSM 'Stator fixed' 2 phase model…..……..… 20

Figure 2.9 (α,β)->(d,q) Projection (Park Transformation)..……..…… 21

Figure 2.10 PMSM rotating two winding stator ……..... 22

Figure 2.11 Equivalent Circuit of a PM Synchronous Motor …..……. ..24

Figure 2.12 PMSM drive system ……29

Figure 2.13 Sensor based Field Oriented Control for PMSM …… ..30

Figure 2.14 Circuit model of a single-phase inverter …… … 32

Figure 2.15 Pulse width modulation …….……32

Figure 2.16 Locus comparisons of SVPWM with sinusoidal-PWM....…….…… 34

Figure 2.17 Three-phase voltage source PWM Inverter…….……. 35

Figure 2.18 Eight switching state topologies of a voltage source inverter …….…. 38

Figure 2.19(a) Topology 1-**V1**(pnn) of a voltage source inverter…..…….……38

Figure 2.19(b) Representation of topology 1 in the α,β plane …...…….…….. 39

Figure 2.20 Basic switching vectors and sectors …….…….. 39

Figure 2.21 Voltage space vector and its components in (α,β)…..…….…….. 42

Figure 2.22 PWM output signals for a reference vector sitting in sector I…..... 44

Figure 2.23 Pole voltage for the ideal SV-modulation …… 46

Figure 2.24 Reference vector as a combination of adjacent vectors at sector I….. 46

Figure 2.25 Reference voltages u_{ref1}, u_{ref2} and u_{ref3} ……... 48

Figure 2.26 Identification of sector the number…….. 49

Figure 2.27 Output voltage vector in the $\alpha\beta$ plane …….. 49
Figure 2.28 Output line voltage in the time domain …… 50
Figure 2.29 Space Vector PWM switching patterns at each sector…….. 51
Figure 2.30 Optical encoder ……..…… 52
Figure 2.31 Incremental and absolute encoder ……..…….. 53
Figure 2.32 Resolver……...…….. 54
Figure 2.33 Voltage source inverter connected with a motor …… 56
Figure 2.34 PI controller……. 57
Figure 2.35 Structure of PI controller……..58
Figure 2.36 Separately excited dc commutator motor drive ……... 62
Figure 2.37 Torque vs. speed capability curve for dc motor drive……64
Figure 2.38 Electrical variables corresponding to (a) as a function of speed …… 64
Figure 2.39 Ideal and practical field weakening characteristics ……..……65
Figure 2.40 Field weakening of permanent magnet motor …… 66
Figure 2.41 Phasor diagram of the PM motor (ideal condition assumed)…… 67
Figure 2.42 Voltage and current limit circle……. 69
Figure 2.43 PMSM voltage d-q vector diagram for a) $i_d=0$, and b) $i_d \neq 0$..... 70
Figure 2.44 PMSM voltage d-q vector diagram for CVCP flux-weakening control…… 75
Figure 2.45 PMSM voltage d-q vector diagram for CCCP flux weakening control.....77
Figure 2.46 PMSM voltage d-q vector diagram for OCV flux-weakening control…….. 80
Figure 3.1(a) The complete simulation set up……..83
Figure 3.1 Motor accelerating to speed 150 rad/se……...…… 84
Figure 3.2 Developed Torque at 150 rad/s ……...…….85
Figure 3.3 Idq current at 150 rad/sec……...85
Figure 3.4 I abc currents as motor accelerating to 150 rad/sec…….. 86
Figure 3.5 Motor accelerating to speed 233 rad/se……...…… 87
Figure 3.6 Developed Torque at 233 rad/s ……...…….88
Figure 3.7 Idq current at 233 rad/sec……...89
Figure 3.8 I abc currents as motor accelerating to 233 rad/sec…….. 90
Figure 3.9 Motor electrical speed when change of torque…….……91
Figure 3.10 Suddenly decreasing the torque from Trated (4 Nmt) to 3.5 Nmt ……....90
Figure 3.11 The speed-torque characteristics curve with and without field weakening Capability…… 91
Figure 3.12 PMSM system control structure…….…….....96

Figure 3.13 Block diagram of TDS 2407 EA…….. 98
Figure 3.14 Complete experimental set up for open loop control……...99
Figure 3.15 General software flow chart ……..……..100
Figure 3.15 The flow and block diagram chart for open loop control of PMSM…….. 101

LIST OF TABLES

Table 2.1 Switching vectors, phase voltages and output line to line voltages…… 37
Table 2.2 Tk and T_{k+1} definition for different sectors in terms of X, Y and Z….. 48

Table 2.3 Switching Time Calculation at Each Sector…….. 51
Table 2.4 Devices power and switching capabilities……. 56
Table 2.5 Summery of PI controller characteristic……..… 59
Table 3.1 Surface mounted permanent magnet motor parameters……..… 82

REFERENCES

1. Tom Denton, "*Automobile Electrical and Electronics System*", 2nd edition, 2000.

2. Dr. P.S. BIMBHRA "*Electric Machinery*" Khanna Publishers, Delhi, seventh-edition, 2004.

3. Richard M.Crowder, "*Electric Drives and Their Control*" Clarendon Press, Oxford Science publication, 1995.

4. Dr. P.S. BIMBHRA "*Power electronics"* Khanna Publishers, Delhi, 1st edition, 2004.

5. Sabri Cetinkunt, "*Mechatronics*" John Wiley and Sons, INC, 1st edition, 2007.

6. Andrzej M. Trzynadlowski, "*Field orientation principle in control of induction motor*" Kluwer Academic Publisher, 1st edition, 1994.

7. Austin Hudhes, "*Electrical motors and Drives*" Newnes publication, 2nd edition, 1993.

8. John Hindmarsh and Aladair Renfrew, "*Electrical machines and drives systems*" Newnes publication, 3rd edition, 1996.

9. D.W.Novotny and T.A Lipo, "*vector control and dynamics of ac drives*" Oxfored science puplication, 1st eition, 1996.

10. Werner Leonhard, "*Control of Electrical Drives*" Springer Press, 2nd edition, 1996.
11. Rolf Iserman, "*Digital control systems*" Springer Press, 2nd revised edition, 1991.
12. William J. Palm, "*control system engineering*" John Wiley and Sons, 1st edition, 1986.

13. Jacqueline Wilkie and Michael Johnson and Reza Katebi, "*Control engineering an introductory course*" Palgrave Macmillan publisher, 1st edition, 2002.

14. Marian P.K and Henryk Tunia, "*Automatic control of Converter-Fed Drives*" PWN-Polish Scientific Publisher,1994.

15. Texas Instruments , " *SVPWM with TMS320C2XX* ", Literature number:SPRA 524,2001.

16. Mengesha Mamo, K.Ide,M. Sawamura and J.Oyama "*Novel rotor position Extraction " based on carrier frequency component method(CFCM) using two reference frame of IPM drives*" IEEE-IE Journal, volume 52, number 2,April 2005.

17. Texas Instruments Inc.," *Implementation of a Speed Field Oriented Control of 3-phase PMSM Motor using TMS320F240* " , www.ti.com, Texas Instruments Literature number SPRA588, Europe, 1999.

18. Freescale semiconductor," *Design of a PMSM servo system using the 56F8357 device*" document number: AN 3301

19. Texas Instruments Inc., "*Clarke and Park Transforms on the TMS320C2xx",* www.ti.com, Texas Instruments Literature number BPRA048, Europe, 1998

20. H. Grotstollen and J.Wiesling, "*Torque Capability and Control of a saturated induction motor over a wide range of flux weakening," IEEE Trans. Ind. Electron. Vol.42,pp.374-381, Aug.1995.*

21. T. M. Jahns, "*Flux-Weakening Region Operation of an Interior Permanent-Magnet Synchronous Motor Drive" IEEE Trans. Indust .Applicat.* vol.23, pp 681-689, July/Aug.1987.

22. J.W. Park, D.H. Koo, and J.M .Kim, "*Improvement of Control Characteristics of Interior Permanent Magnet Synchronous Motor for Electric vehicle*," IEEE Transactions of Industry *Applications*, Vol. 37, No. 6,., pp.1754-1761, Nov/ Dec. 2001.
23. Vedam Subrahmanyam, "*Electrical drives-concepts and appliaction*" Tata McGraw-Hill Publishing Company Limited, 1st edition, 2003.
24. NEC corp., "*An introduction to vector control of AC motor using V850*" documentation number U16483EEIVOAN00, 2002.
25. Dal Y.Ohm, "*dynamic model of permanent magnet synchronous motor*" Drivetech Inc, 2005.
26. Y.H.Chin, J.Soulard, "*a permanent magnet synchronous motor for traction applications of electric vehicle*", 2002.
27. D.S Maric, S.Hiti, C.C.Stancu, J.M.Nagashima, "*two flux weakening schemes for surface mounted permanent magnet synchronous drive-Design and transient response considerations*", 1999.
28. www.ti.com
29. Matlab documentation, release 14.
30. Power electronics, frequency converter DL 2646 technical manual.

ABSTRACT

This thesis deals with control of PMSM (Permanent Magnet Synchronous Motor) with field weakening capability using DSP board and simulation using Matlab/Simulink. The practical part will only cover up to open loop control due to the failure of some I/O pins for PWM output. A PMSM motor model has been analyzed in order to control the motor both in the constant-torque (constant flux) and in the constant-volt-ampere (flux weakening) regions.

A flux-weakening technique is applied when extension of the motor speed beyond base speed is desired. The field-oriented control, with its flux/torque decoupling feature is realized with a digital PWM controller in rotating d-q coordinate system. This kind of control requires a relatively powerful microprocessor along with the relevant peripherals to make vector control a practical proposition. The DSP board used, TDS2407 EA is designed for such drive application.

Simulation results demonstrate that the speed range of the surface mounted PMSM use can be extended up to approximately 350 rpm by field weakening while the speed is limited to 175 rpm without field weakening.

Key words:
PMSM, vector control, field weakening, SVPWM, DSP

CHAPTER-1
INTRODUCTION

The term "field weakening" is used to describe a process by which extended speed range beyond base speed is achieved. The separately excited DC commutator motor drives show an ideal field weakening characteristics. In this motor the field flux ϕ_f produced by the field current I_f is perpendicular to the armature flux ϕ_a produced by the armature current I_a. These fields are decoupled and stationary with respect to each other. Decoupling concept describes controlling field current doesn't have any effect on armature current control in case of having wide range of speed or can simply say independent control of flux or torque producing current. In DC motor, flux due to field current is inversely proportional to speed of a motor. Therefore, in order to have wide speed range beyond base speed, the flux must be weakened by decreasing the field current while the armature voltage is kept constant at rated speed.

In permanent magnet motors the air gap flux is produced by permanent magnet. As the magnet resembles a "fixed excitation" source, the magnetic field can not be varied as in a separately excited DC motor. To weaken the field in permanent magnet synchronous motors (PMSMs) where the excitation is provided by the permanent magnet is not just like separately excited DC motor. The approach commonly used to weaken the field is Field Oriented Control (FOC). Field Oriented Control seeks to recreate orthogonal components of stator currents with respect to rotating reference frame in the AC machine in order to control the torque producing current (I_q) separately from the magnetic flux producing current (I_d) so as to achieve responsiveness of a DC machine. I_d and I_q can be defined as stator current component responsible for producing flux and torque respectively.

Field oriented control algorithm will enable real-time control of torque and rotational speed. This control is based on three major points: the machine current and voltage space vectors, the transformation of a three phase speed and time dependent system into a two

co-ordinate time invariant system (Clarke and Park transformations) and effective Pulse Width Modulation pattern generation. Thanks to these factors, the control of AC machines acquires every advantage of DC machine control but frees itself from the mechanical commutation drawbacks.

Using Clarke transform three-phase stator current can be replaced by two phase orthogonal vectors with respect to stationary reference frame (α-β) and the Park transformation provides us with the direct axis and quadrature axis components (I_d and I_q) of the stator current in a synchronously rotating reference frame. For visualization the three-phase stator winding can ideally be replaced by its two winding equivalent as shown in figure 1.1 where the two windings are rotating with the rotor.

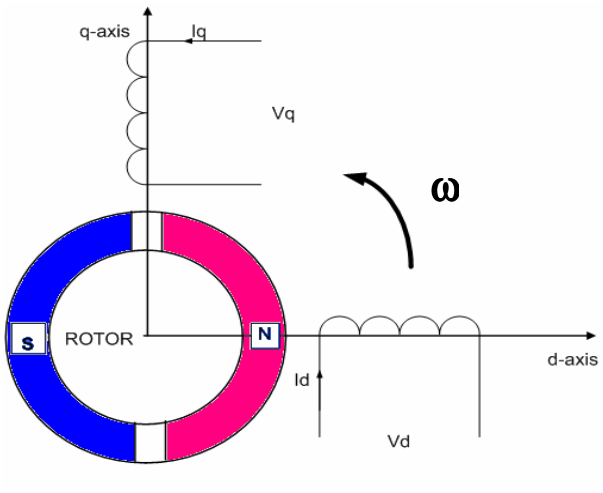

Figure 1.1 PMSM 'two rotating stator winding' 2 phase model

The commonly known technology of field weakening for PMSM is achieved by controlling the direct-axis current component through an inverter. That is, control the stator current in such a manner that an intentional component of mmf which acts in opposition to the permanent magnet field along the magnetic axis (d-axis) is applied there by reducing the field in the air gap.

The torque produced by surface mounted PMSM is proportional to the product of I_q and rotating d-axis flux of the rotor (ψ_m) as they are stationary with respect to each other like DC motor. If negative d-axis current is injected, the air gap flux due to permanent magnet rotor will weaken and the torque will also decrease due to two reasons; first due to decrease in I_q and second due to decrease in air-gap flux. Yet, the torque drop as speed increases is slower than when the field weakening is not implemented. As a result, the speed range beyond its base speed is wider.

Dc motor and induction motor drives, which have dominated the field until now, are being replaced by PMSM and BLDC drives for low power applications. Lowe power is defined here as being less than 10 KW. Some of applications for motors below 10 KW are in home appliances, electric tools and small pumps and fans. The three reasons why this study is concentrated on PMSMs are: First the motor has high efficiency because of low rotor losses, superior power density, high torque to inertia ratio give better dynamic performance etc, second, the falling price of high energy magnets and third reason is of course advent of power and micro-electronics and falling price of micro-controller.

PMSMs are now very popular in a wide variety of industrial applications like automotive control (in electric vehicle), robotics and factory automations, computer and office equipment, household appliances etc.

In conventional vehicle with engine and fuel tank, in order to get very high speed gear must be used to increase the speed. Gear system introduces loss and decrease the overall efficiency. Furthermore, it is additional load to the vehicle. This drawback is overcome by using electric vehicle with field weakening controlled motor. Besides, in the case of spindle drive, the motor should run with a very high speed (that is the maximum speed is up to 9000 – 20,000 rpm) in order to do the mechanical work properly. Here in spindle drive large extended speed range is required.

The field weakening has not been implemented due to time constraint and technical problem.

The contents of this thesis are organized as follows: Chapter 1 provides the background of this project work and an over view of how this thesis report is organized. Chapter 2 presents the reviewed literatures on synchronous motor, rotating transformations and mathematical model of PMSM and principle of field weakening operation and its control. Chapter 3 explains simulation and experimental system with its result. The conclusions are drawn in chapter 4 and the expected work to be completed in the continuing phase of the project is also described.

CHAPTER 2

FIELD WEAKENING CONTROL OF PMSM

Usually, high-performance motor drives require fast and accurate response, quick recovery from any disturbances, and insensitivity to parameter variations. The dynamic behavior of an ac motor can be significantly improved using vector control theory where motor variables are transformed into an orthogonal set of d-q axes such that field current and torque current can be controlled separately. This gives the PMSM machine the highly desirable dynamic performance capability of the separately excited dc machine, while retaining the general advantages of the ac over dc motors.

2.1 General overview of conventional synchronous motor

Synchronous motors have the characteristic of constant speed between no load and full load. They are capable of correcting the low power factor of an inductive load by adjusting the excitation system. They are often used to drive generators. Synchronous motors are designed in sizes up to thousands of horsepower. They may be designed as either single-phase or multiphase machines

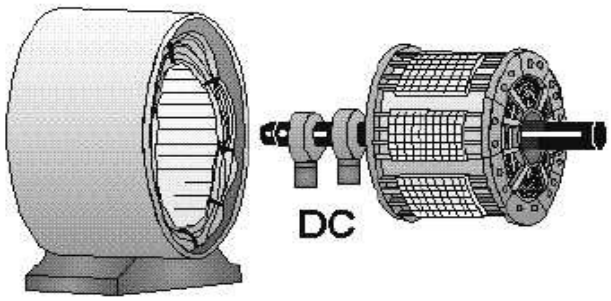

Figure 2.1 Revolving-field synchronous motor

To understand how the synchronous motor works, assume that the application of three-phase ac power to the stator causes a rotating magnetic field to be set up around the rotor. The rotor is energized with dc (it acts like a bar magnet). The strong rotating magnetic field attracts the rotor field activated by the dc excitation if only rotor is running near to synchronous speed by some means. This results in a strong turning force on the rotor shaft. The rotor is therefore able to turn a load as it rotates in step with the rotating

magnetic field. It can also be said that electrical energy is converted to mechanical energy by the magnetic attractive forces between rotor field and a rotating magnetic field induced in the wound stator poles. However, one of the disadvantages of a synchronous motor is that it cannot be started from a standstill by applying three-phase ac power to the stator. When ac is applied to the stator, a high-speed rotating magnetic field appears immediately. This rotating field rushes past the rotor poles so quickly that the rotor does not have a chance to get started due to inertia. In effect, the rotor is repelled first in one direction and then the other. Hence, synchronous motor in its purest form has no starting torque. It has torque only when it is running at synchronous speed. In field oriented control such problem is totally avoided since maximum torque can be achieved with zero speed.[2][7]

For the motor to operate, the rotor should first reach a synchronous speed. This can be done in three ways: by driving the rotor to the synchronous speed (with an external machine), by starting the rotor (which has to be equipped with a starting cage) as in induction motors, or by supplying the stator winding with variable frequency, beginning from zero to the rated frequency. The latter method can be used if the winding is supplied from a frequency converter.

A synchronous machine is an ac machine whose speed under steady state condition is proportional to the frequency of the current in the armature. The magnetic field created by the armature currents rotates at the same speed as that created by field current on the rotor (which is rotating at synchronous speed). The synchronous speed, N_s, is determined by the frequency of the stator supply, f_s and the number of stator poles. Unlike induction motor synchronous motor is excited by a separate DC or permanent magnet source. The stator of the three-phase synchronous motor normally has a sine distributed three-phase winding. When excited with a three-phase supply, a rotating magnetic field is developed. The speed of this field (the synchronous speed) is given by equation 2.1.

$$N_s = \frac{60 f_s}{p} \qquad (2.1)$$

where f_s - frequency of ac supply
p - number of pole pairs
N_s - synchronous speed

From the above equation, synchronous motor speed totally depends on the supply frequency. Therefore, changing the supply frequency means changing the speed.

2.2 Permanent Magnet Machines

A permanent magnet synchronous motor (PMSM) is a motor that uses permanent magnets to produce the air gap magnetic field rather than using electromagnets. These motors have significant advantages, attracting the interest of researchers and industry for use in many applications.

Permanent Magnet Machines for high performance applications have a wound stator, and a permanent magnet rotor assembly and internal or external devices to sense rotor position. The sensing devices provide logic signals for electronically switching the stator windings in the proper sequence to maintain rotation of the magnet assembly. The combination of an inner permanent magnet rotor and outer windings offers the advantages of low rotor inertia, efficient heat dissipation, and reduction of the motor size. Moreover, the elimination of brushes reduces noise, EMI generation and suppresses the need for brush maintenance.[17][18]

The brushless PM synchronous motors involve adjustment of the armature supply frequency, proportionally as the rotor speed is varied, so that the armature field always moves at the same speed as the rotor. The rotating magnetic fields of the stator (armature) and the rotor (excitation) system are then always in synchronous motion producing a steady torque at all operating speeds. This is analogous to the D.C motor in which the armature and excitation fields are synchronous but stationary for all operating speeds.

Brushless (PM) Synchronous motor requires the very accurate measurement of rotor speed and position and the very precise adjustment of the stator frequency. Rotor position

sensing is done by an encoder, resolver… etc which forms part of a control loop of an adjustable frequency inverter feeding the armature winding.

2.3 Classification of permanent magnet motors

2.3.1 Direction of field flux

PM motors are broadly classified by the direction of the field flux. The first field flux classification is radial field motor meaning that the flux is along the radius of the motor. The second is axial field motor meaning that the flux is perpendicular to the radius of the motor. Radial field flux is most commonly used in motors and axial field flux have become a topic of interest for study and used in a few applications.

2.3.2 Flux density distribution

PM motors are classified on the basis of the flux density distribution and the shape of current excitation. They are PMSM and PM brushless motors (BLDC). The PMSM has a sinusoidal-shaped back EMF (it is an induced voltage in the stator by the motion of the rotor) and is designed to develop sinusoidal back EMF waveforms. They have the following:

- Sinusoidal distribution of magnet flux in the air gap
- Sinusoidal current waveforms
- Sinusoidal distribution of stator conductors.

BLDC has a trapezoidal-shaped back EMF and is designed to develop trapezoidal back EMF waveforms. They have the following:

- Rectangular distribution of magnet flux in the air gap
- Rectangular current waveform
- Concentrated stator windings.

2.3.3 Permanent magnet radial field motors

In PM motors, the magnets can be placed in two different ways on the rotor. Depending on the placement they are called either as surface permanent magnet motor (SPM) or interior permanent magnet (IPM) synchronous motor. Surface mounted PM motors have a surface mounted permanent magnet rotor. Each of the PM is mounted on the surface of the rotor, making it easy to build, and specially skewed poles are easily magnetized on this surface mounted type to reduce the magnitude of torque harmonics (ripple) due to the harmonic content of the MMF-waves. This configuration is used for low speed applications because of the limitation that the magnets will fly apart during high-speed operations. These motors are considered to have small saliency, thus having practically equal inductances in both axes. For a surface permanent magnet motor, $L_d = L_q$ [6][9]

The rotor has an iron core that may be solid or may be made of punched laminations for simplicity in manufacturing. Thin permanent magnets are mounted on the surface of this core using adhesives. Alternating magnets of the opposite magnetization direction produce radially directed flux density across the air gap. This flux density then reacts with currents in windings placed in slots on the inner surface of the stator to produce torque. Figure 2.2 (a) shows the placement of the magnet.

Interior PM Motors have interior mounted permanent magnet rotor as shown in figure 2.2 (b). Each permanent magnet is mounted inside the rotor. It is not as common as the surface mounted type but it is a good candidate for high-speed operation. By designing a rotor magnetic circuit such that the inductance varies as a function of rotor angle, the reluctance torque can be produced in addition to the mutual reaction torque of synchronous motors. These motors are considered to have saliency with q axis inductance greater than the d axis inductance ($L_q > L_d$).

In this thesis SPM radial flux machine with classical winding and lamination has been chosen due to the following reasons:

• The SPM drive with a saliency ratio ξ=1 and thus without reluctance torque is simpler to analyze and design than an IPM drive.

• The topology of a radial flux machine with classical winding and lamination has been chosen because of the well-known and established technology.

In figure 2.3 summary of classification of AC synchronous machine has been shown.

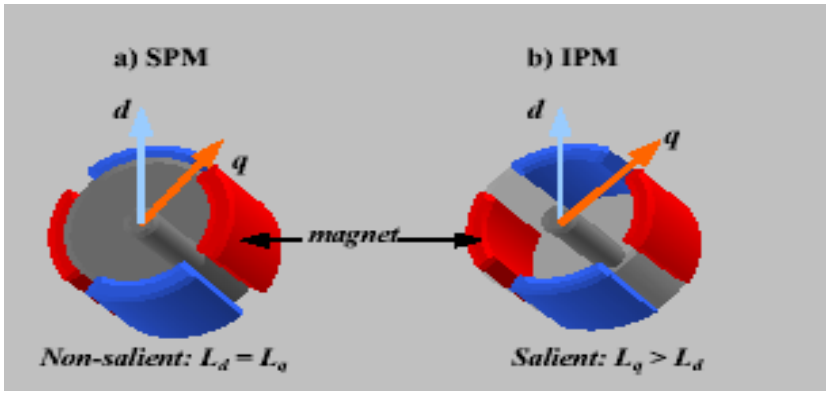

Figure2.2 Rotor configurations studied: a) Surface Mounted PM (SPM); b) Inset PM (IPM)

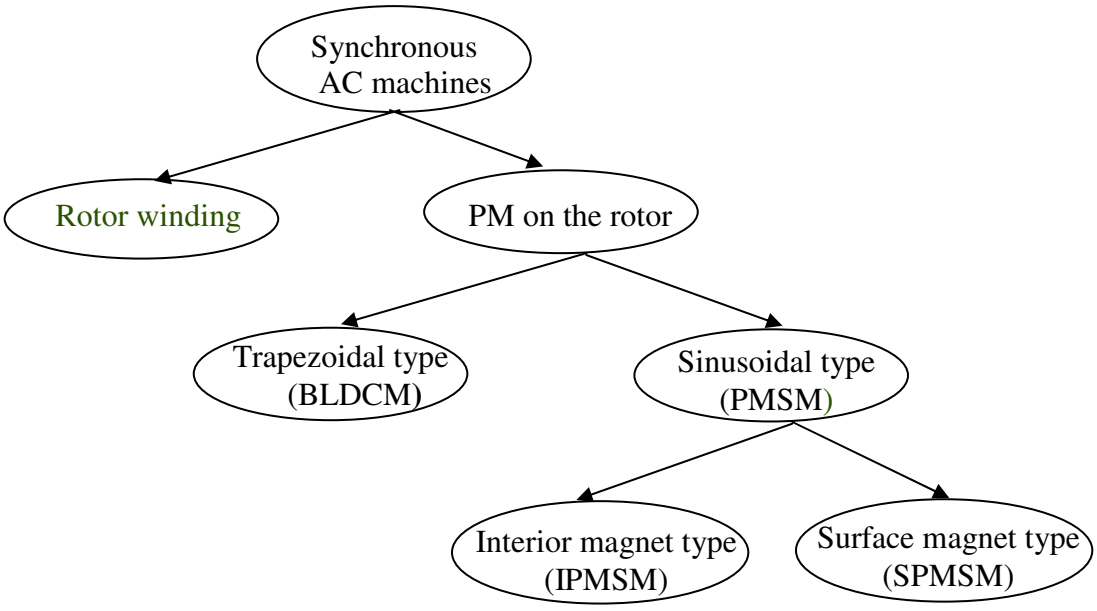

Figure 2.3-Summary of Classification of AC synchronous machines

2.4 Why concentrate this study on PMSM ?

While the transition from single speed to variable speed systems is in progress, another transition is in effect within the field of variable speed motor drives. Direct current and induction motor drives, which have dominated the field until now, are being replaced by PMSM.

2.4.1 Advantages of PM machines

PM machines have many advantages. To mention some;

- they have high torque to inertia (lower weight). That is better dynamic performance than conventional one.
- high power density.
- high efficiency (That is no current in the rotor means no copper loss) and reliability.
- avoidance of brushes and slip rings makes the machine less audible noise, longer life, sparkless (no fire hazard) and high speed.
- efficient heat dissipation.

2.4.2 Disadvantages of PM machines

Even though PM machines have aforementioned merits, they have the following demerits:

- They have complex control.
- There is a possibility of demagnetization of the rotor magnet.
- If demagnetization occurs, there will be a reduction of torque production.
- There is a problem of maintenance of rotor magnet.

2.5 Applications

Among many applications of PM synchronous motor, here are the following:

Robotics and factory automaton (servo drives)

- pick and place robots (Motion control)
- positioning tablets
- automatic guided vehicle

Computer and office equipment

- copier and microfilm machines
- printers/plotters
- tape drivers

Appliances

- washers
- blowers
- compressors

Automotive control

- Power steering
- Anti-lock brakes
- Suspension controls

HVAC

- heating
- ventilation and air conditioning

  etc.

2.6 Mathematical Model of PMSM for Field Oriented (Vector) Control

Although traditional per-phase equivalent circuits have been widely used in steady-state analysis and design of ac machines, it is not appropriate to predict the dynamic performance of the motor. In order to understand and analyze vector control of ac motor drives, a dynamic model is necessary. As the application of ac machines has continued to increase over this century, new techniques have been developed to aid in their analysis. The significant breakthrough in the analysis of three-phase ac machines was the development of the reference frame theory. Using these techniques, it is possible to transform the machine model to another reference frame. By careful choice of the reference frame, it proves possible to simplify vastly the complexity of the mathematical machine model. While these techniques were initially developed for the analysis and simulation of ac machines, they are now invaluable tools in the digital control of such machines. As digital control techniques are extended to control current, torque and flux of ac machines, the need for compact and accurate machine models is obvious. The machine used in this project is a Permanent-Magnet Synchronous Motor (PMSM) with surface mounted permanent magnet on the rotor (SPMSM).

A clear and comprehensive description of the dynamic behavior of ac machines is a key point for their application in speed or torque controlled drive systems. Steady-state analysis of PMSM are typically presented by means of the so called per phase equivalent circuit. However, these models are inadequate when applied to dynamic conditions, as needed in variable frequency drives.

2.6.1 Field Oriented (Vector) control

The Field Oriented Control is an efficient method to control a synchronous motor in adjustable speed drive applications with quickly changing load in a wide range of speeds including high speeds where field weakening is required. It controls the stator currents represented by a vector. This control is based on projections which transform a three phase time and speed dependent system into a two co-ordinate (d and q) time invariant

system. These projections lead to a structure similar to that of a DC machine control. In order for the motor to behave like DC motor, the control needs knowledge of the position of the instantaneous rotor flux or rotor position of permanent magnet synchronous motor. This needs a resolver or an absolute optical encoder. The idea of Field Oriented Control method is to control the current of the machine in space quadrature with the magnetic flux created by the permanent magnets as in the case of DC motors.[9][17][28]

A dc machine consists of a stationary field structure utilizing a stationary dc excited winding or permanent magnets and a rotating armature winding supplied through a commutator and brushes. This basic structure is schematically illustrated in the figure 2.4 along with the resulting orientation of the armature mmf and the field flux. The action of the commutator is to reverse the direction of the armature winding currents as the coils pass the brush position that the armature current distribution is fixed in space no matter what rotor speed exists. As shown in the figure 2.4, the field flux and armature mmf are maintained in a mutually perpendicular orientation independent of rotor speed. The result of this orthogonality is that the field flux is unaffected by the armature current. That is the field flux and the armature mmf are decoupled.

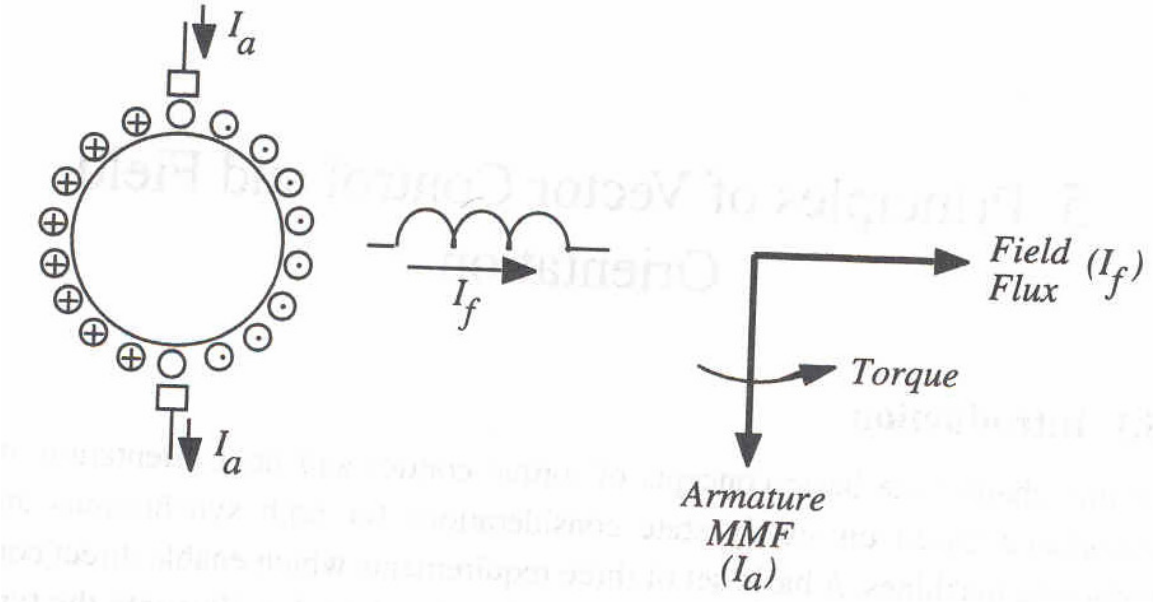

Figure 2.4 separately excited DC motor

Like separately excited DC motor Field Oriented Control seeks to recreate these orthogonal components in AC machines in order to control the torque producing current separately from the magnetic flux producing current so as to achieve the responsiveness of a DC machine.

Field Oriented Controlled machines need two constants as input references; the torque component (aligned with the q axis) and the flux component (aligned with d axis). As Field Oriented Control is simply based on projections, the control structure handles instantaneous electrical quantities. This makes the control accurate in every working operation (steady state and transient).

The goal of Field Oriented Control is to perform real time control of torque variations demand, to control the mechanical speed and to regulate phase currents. To perform these controls, the electrical equations are projected from a three-phase non-rotating frame in to a two coordinate rotating frame. This mathematical projection (Clarke and Park transformation) greatly simplifies the expression of the electrical equations and removes their time and position dependencies.

The advantages of this type of control system are; it has good torque response, accurate speed control and full torque at zero speed. And the demerits of which are feedback is needed, and more cost and the control is complex.

Therefore, Field Oriented Control can be considered as:

- a commercial reality in high performance drive.
- vector control involves control of the spatial orientation of the air gap flux.
- the purpose is to decouple that portion of the stator current involved in producing air gap flux from that portion involved in the direct production of torque, thereby providing independent control of torque and flux.

2.6.2 Rotating transformation

Vector control of an AC motor is analogous to the control of separately excited DC motor. In a DC motor the field flux ϕ_f and armature flux ϕ_a are decoupled and stationary with respect to each other. Therefore, when the armature current is controlled to control the torque the field flux remains unaffected enabling a fast transient response.

Vector control seeks to reconstruct these orthogonal components in the AC machine in order to control the torque producing current separately from the magnetic flux producing current so as to achieve the responsiveness of the DC machine. In order to create the perpendicular components of the stator current of PMSM which is in the form of a vector, concept of rotating transformation is required. In this subsection the Clarke and Park transformation will be explained. Assume that the three phase supply voltage is balanced.

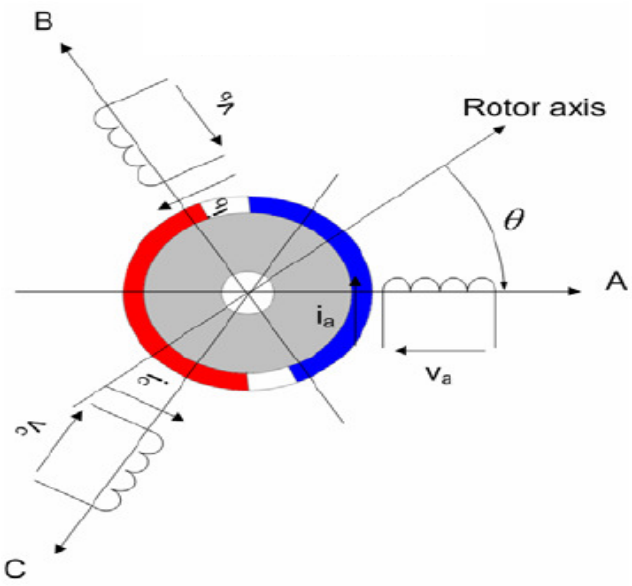

Figure 2.5 Three-phase motor surface mounted PMSM model

The Clarke and Parke transformation is a transformation of coordinates from the three-phase stationary coordinate system to the dq rotating coordinate system.

Considering PMSM or squirrel-cage induction motor, the transformations are usually based on following assumptions:

- Space harmonics of the flux linkage distribution are neglected.
- Slot harmonics and deep bar effects are not considered.
- Iron losses are not taken into account.
- Saturation is neglected.
- Permanent magnets behave linearly.
- Neutral point is isolated.

2.6.2.1 Space vector definition

Assume i_a , i_b and i_c are the instantaneous balanced three phase current:

$$i_a + i_b + i_c = 0$$

It is then possible to define the stator current space vector as follows:

$$\bar{i}_s = k(i_a + a i_b + a^2 i_c) \qquad (2.2)$$

where a and a^2 are the spatial operators

$$a = e^{j2\pi/3}$$

$$a^2 = e^{j4\pi/3}$$

k is the transformation constant, chosen as k = 2/3

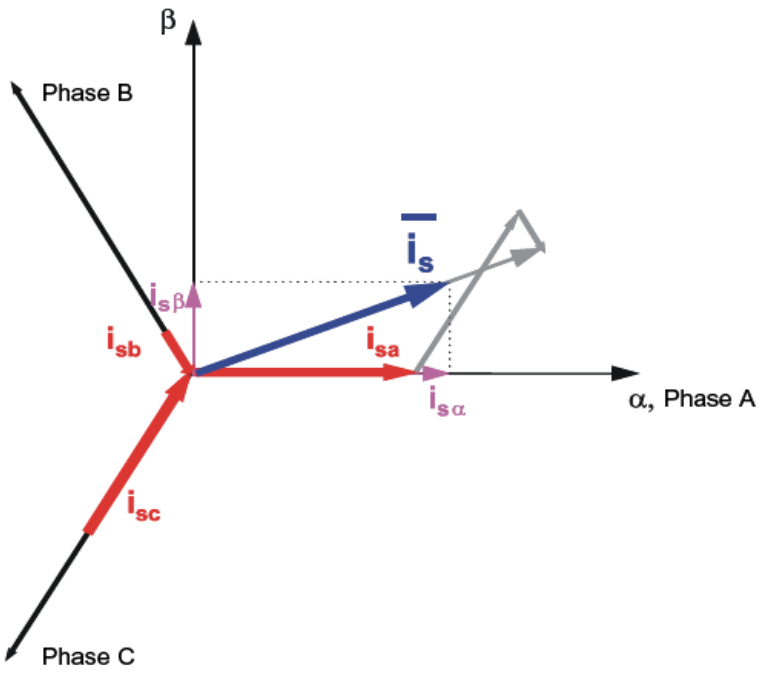

Figure 2.6 Stator Current Space Vector and Its Projection

The transformation is made in two steps:

- A transformation from the three-phase stationary coordinate system to the two phase, so-called αβ, stationary coordinate system is called **Clarke Transformation**.

The idea of Clarke transformation is that the rotating stator current vector that is the sum of the three-phase currents can also be generated by a bi-phased system placed on the fixed axis α and β.

The space vector defined by equation 2.2 can be expressed utilizing two-axis theory. The real part of the space vector is equal to the instantaneous value of the direct-axis stator current component, i_α , and whose imaginary part is equal to the quadrature-axis stator current component, i_β. Thus, the stator current space vector, in the stationary reference frame attached to the stator, can be expressed as:

$$\bar{i}_s = i_\alpha + j i_\beta \tag{2.3}$$

In symmetrical 3-phase machines, the direct and quadrature axis stator currents $i_{s\alpha}$ and $i_{s\beta}$ are fictitious quadrature-phase (2-phase) current components, which are related to the actual 3-phase stator currents as follows:

$$\begin{aligned} i_\alpha &= k(i_a - \frac{1}{2} i_b - \frac{1}{2} i_c) \\ i_\beta &= k \frac{\sqrt{3}}{2}(i_b - i_c) \end{aligned} \tag{2.4}$$

where:

k = 2/3 is a transformation constant and $i_a + i_b + i_c = 0$

In matrix form of a three phase to two phase transformation of the stator current ((a,b,c) to (α,β))

$$\begin{bmatrix} i_\alpha \\ i_\beta \end{bmatrix} = 2/3 \begin{bmatrix} 1 & -1/2 & -1/2 \\ 0 & \frac{\sqrt{3}}{2} & -\frac{\sqrt{3}}{2} \end{bmatrix} \begin{bmatrix} i_a \\ i_b \\ i_c \end{bmatrix} \tag{2.5}$$

For stator voltage the matrix form of a three phase to two phase transformation ((a,b,c) to (α,β)) is

$$\begin{bmatrix} V_\alpha \\ V_\beta \end{bmatrix} = 2/3 \begin{bmatrix} 1 & -\frac{1}{2} & -\frac{1}{2} \\ 0 & \frac{\sqrt{3}}{2} & -\frac{\sqrt{3}}{2} \end{bmatrix} \begin{bmatrix} V_{an} \\ V_{bn} \\ V_{cn} \end{bmatrix} \tag{2.6}$$

Equations (2.5) and (2.6) are valid for balanced system otherwise zero sequence component is introduced.

The simplified diagram of a three-phase ac motor (see figure 2.7) shows only the stator windings for each phase displaced 2π/3 radians in space. The transformation of stator

variables to a 2-phase reference frame (indicated by subscripts α, β), where the coils are perpendicular, guarantees that there is no interaction between perpendicular windings as long as there is no saturation.

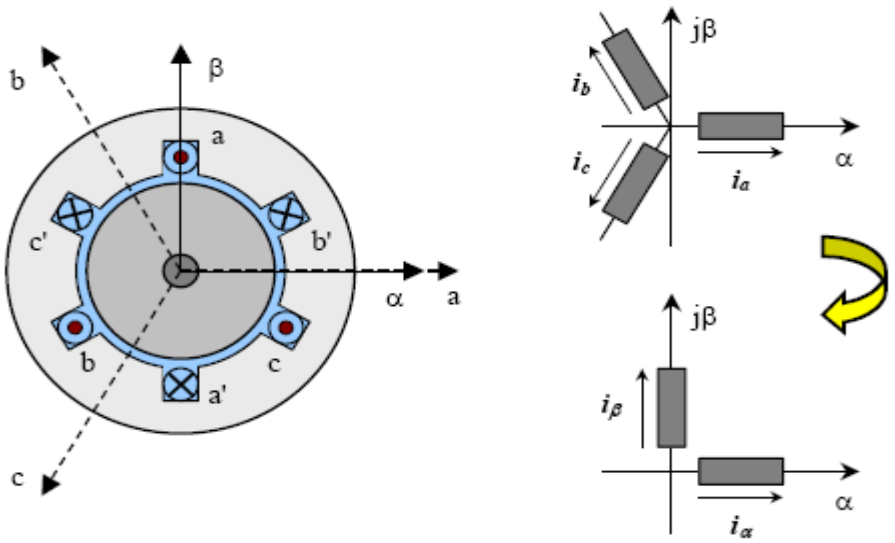

Figure 2.7 Three-phase windings and two-axes equivalent (α/β transformation)

To make more simplified the concept of Clarke transformation, three-phase stator winding of surface mounted PMSM with respect to stationary reference frame can be described by using its two winding equivalent with respect to fixed reference frame as shown in the figure 2.8

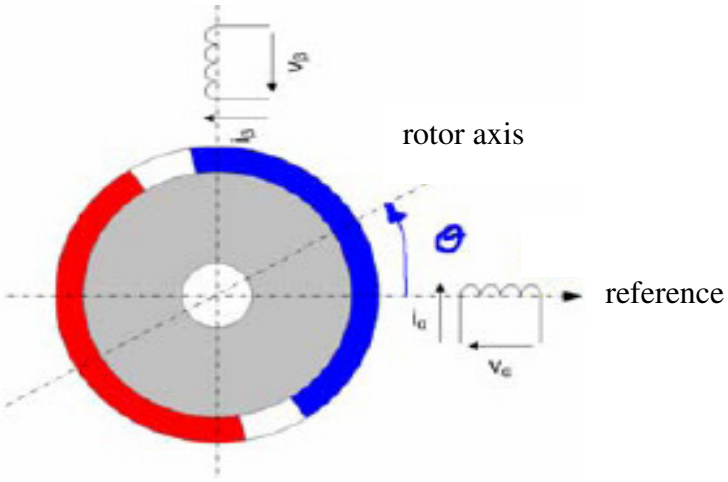

Figure 2.8 PMSM 'Stator fixed' 2 phase model

In this new frame, the expression of the torque is still dependent on the position of the rotor flux, preventing any easy solution of the electrical differential equation. To remove the dependency, the electrical equations are projected in a two-phase (d,q) system that rotates at the speed of the electrical speed of the rotor and where the d-axis is aligned with the electrical position of the rotor flux. In this frame, the electrical expression of the torque becomes independent of the electrical position.

- A transformation from the αβ stationary coordinate system to the d-q rotating coordinate system is called **Park Transformation**.

Vector control is performed entirely in the d-q coordinate system to make the control of PM synchronous motors elegant and easy. Here θ_e is the angle between the d-axis and the stationary α-axis.

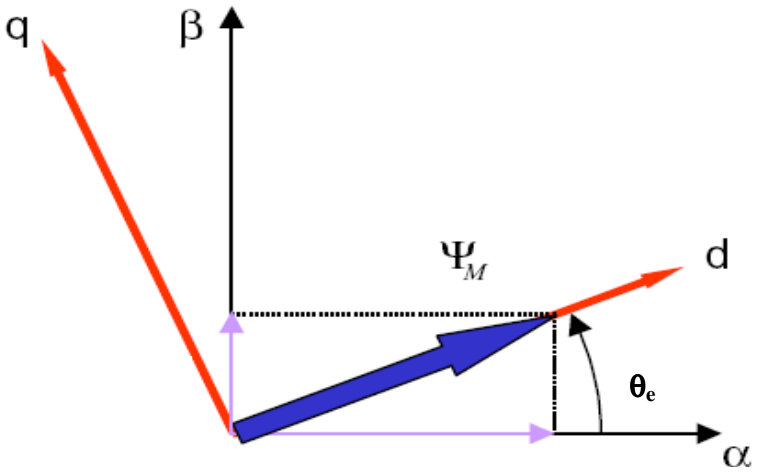

Figure2.9- (α,β)->(d,q) Projection (Park Transformation)

The equation corresponding to this transformation are given by

$$\begin{aligned} i_d &= i_\alpha \cos(\theta_e) + i_\beta \sin(\theta_e) \\ i_q &= -i_\alpha \sin(\theta_e) + i_\beta \cos(\theta_e) \end{aligned} \qquad (2.7)$$

To simplify the concept of this transformation three-phase stator winding with respect to stationary reference frame can be described by using its two winding equivalent with respect to rotating reference frame as shown in the figure 2.10.

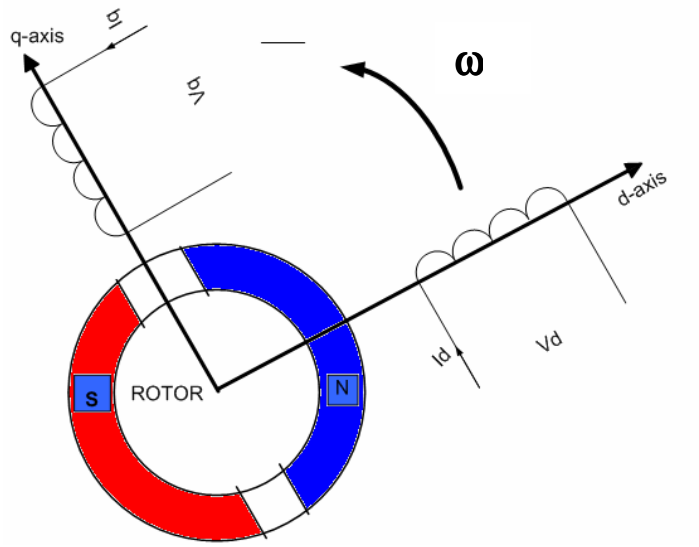

Figure 2.10 PMSM rotating two winding stator

The general Park transformation i_d and i_q are obtained directly from i_a, i_b and i_c. Here is the matrix equation corresponding to this transformation.

$$\begin{bmatrix} i_d \\ i_q \end{bmatrix} = \begin{bmatrix} \cos\theta_e & \cos(\theta_e - 2\pi/3) & \cos(\theta_e + 2\pi/3) \\ -\sin\theta_e & -\sin(\theta_e - 2\pi/3) & -\sin(\theta_e + 2\pi/3) \end{bmatrix} \begin{bmatrix} i_a \\ i_b \\ i_c \end{bmatrix} \tag{2.8}$$

Inverse park transformation has the following equations

$$\begin{aligned} i_a &= i_d \cos\theta_e - i_q \sin\theta_e \\ i_b &= i_d \cos(\theta_e - 2\pi/3) - i_q \sin(\theta_e - 2\pi/3) \\ i_c &= i_d \cos(\theta_e - 4\pi/3) - i_q \sin(\theta_e - 4\pi/3) \end{aligned} \tag{2.9}$$

2.6.3 Dynamic model of PMSM

For the control and simulation of the electrical machine a mathematical model is required. In a permanent magnet synchronous motor where inductances vary as a function of rotor angle, the 2 phase (d-q) equivalent circuit model is commonly used for simplicity and intuition. In this chapter, a two phase model for a PM synchronous motor is presented.

Throughout this sub-section, the following assumptions are made:

1) Saturation is neglected.
2) Stator windings produce sinusoidal mmf distribution.
3) Eddy currents and hysteresis losses are negligible.
4) Balanced three-phase supply voltage is considered.

Here is the derivation of the electrical equations which are greatly simplified due to the concept of rotating transformation. The two axis voltage equations for the stator winding which are of an IPMSM (but is the same for SPMSM where L_d and L_q have the same value) are given by equations (2.10) and (2.11). [25]

$$v_q = R_s i_q + \frac{d}{dt}(\psi_q) + \omega_e \psi_d \tag{2.10}$$

$$v_d = R_s i_d + \frac{d}{dt}(\psi_d) - \omega_e \psi_q \tag{2.11}$$

where $\psi_d = L_d i_d + \psi_m$ (2.12)

and $\psi_q = L_q i_q$ (2.13)

v_d *and* v_q are the (d, q) axis stator voltages, i_d *and* i_q are the (d, q) axis stator currents. L_d and L_q are the d, q axis inductances, while R_s is the stator winding resistance

and ω_e is the electrical speed of magnetic field, ψ_m is the flux linkage due to the rotor magnets linking the stator and ψ_d and ψ_q are stator flux linkages.

Now a more convenient equation for (2.10) and (2.11) can be rewritten as

$$v_q = (R_s + L_q \frac{d}{dt}) i_q + \omega_e L_d i_d + \omega_e \psi_m$$
$$v_d = (R_s + L_d \frac{d}{dt}) i_d - \omega_e L_q i_q \qquad (2.14)$$

Figure 2.11 shows a dynamic equivalent circuit of a PM synchronous machine based on equation 2.14.

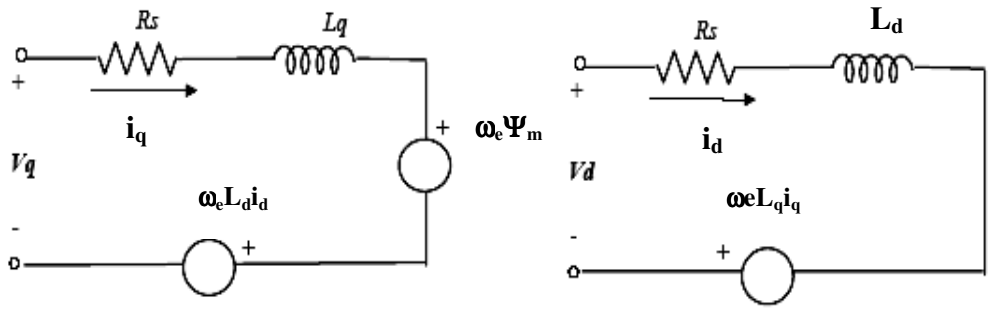

(a) q-axis circuit (torque) (b) d-axis circuit (field)

Figure 2.11- Equivalent Circuit of a PM Synchronous Motor

The relation between ω_e and ω is:

$$\omega_e = p\omega \qquad (2.15)$$

Where ω_e is the electrical angular velocity of the rotor, ω *is* the mechanical angular velocity of the rotor and *p is* the number of pole pairs.

Substitute equation (2.15) into equation (2.14), the mathematical model in terms of its state variable form will be

$$\begin{bmatrix} \frac{di_d}{dt} \\ \frac{di_q}{dt} \end{bmatrix} = \begin{bmatrix} \frac{-R_a}{L_d} & \frac{L_q p\omega}{L_d} \\ \frac{-L_d p\omega}{L_q} & \frac{-R_a}{L_q} \end{bmatrix} \begin{bmatrix} i_d \\ i_q \end{bmatrix} + \begin{bmatrix} \frac{v_d}{L_d} \\ \frac{-\psi_m p\omega}{L_q} + \frac{v_q}{L_q} \end{bmatrix} \tag{2.16}$$

Here is the derivation of torque equation.

Input power can be represented by

$$P_i = v_a i_a + v_b i_b + v_c i_c \tag{2.17}$$

For the above model, instantaneous power can be derived from equation 2.17 via transformation as

$$P_i = (3/2)[v_q i_q + v_d i_d] \tag{2.18}$$

Where scaling factor 2/3 guarantees power invariance.

Put equations (2.10) and (2.11) into equation (2.18) the power equation can be written as

$$P_i = \frac{3}{2}(R_s i_d^2 + R_s i_q^2) + \frac{3}{2}(i_d \frac{d\psi_d}{dt} + i_q \frac{d\psi_q}{dt}) + \frac{3}{2}\omega_e(\psi_d i_q - \psi_q i_d) \tag{2.19}$$

The first term of equation 2.19 is the power loss in the conductors, the second term is the time rate of change of stored energy in the magnetic fields and the third term is the energy conversion from electrical to mechanical energy. The torque can be derived from the third term of the power equation and written as:

$$P_e = \omega T_e = \frac{3}{2}\omega_e(\psi_d i_q - \psi_q i_d) \tag{2.20}$$

Substitute equation (2.15) into equation (2.20) the electromagnetic torque (T_e) for synchronous machines in the (d, q) axes is given by:

$$T_e = \frac{3}{2} p(\psi_d i_q - \psi_q i_d) \tag{2.21}$$

If equation (2.12) and (2.13) is substituted in equation (2.21), the torque can also be expressed in the following way and equated to the mechanical equation.

$$T_e = \frac{3}{2} p\left[\psi_m i_q + (L_d - L_q) i_q i_d\right]$$

$$= T_L + J\frac{d\omega}{dt} + B\omega \tag{2.22}$$

The first term is called "mutual reaction torque" occurring between i_q and the permanent magnet, while the second term corresponds to "reluctance torque" due to the difference in d-axis and q-axis reluctance (or inductance). The motor used in this project is surface mounted PMSM which means that $L_d \approx L_q$, due to the same reluctance paths in rotor d- and q-axis, and therefore the "reluctance torque" is equal to zero, so the torque expression for SPMSM is:

$$T_e = \frac{3}{2} p(\psi_m i_q) \tag{2.23}$$

Since the number of pole pairs and the magnetic flux linkages are constant, then the torque is directly proportional to q-axis current i_q. That is $T_e = K_t i_q$. The torque equation is now similar to that in a separately excited DC motor, where i_q corresponds to the armature current of the DC machine and torque can be controlled by controlling i_q. [9][17][18]

Constant torque control strategy is derived from field oriented control, where the maximum possible torque is desired at all times like the dc motor. This is performed by making the torque producing current i_q equal to the supply current I_s. This is achieved by controlling i_d to be equal to zero.

2.7 PMSM control structure

Rotor position information is very crucial for field oriented (vector) control. Since this control is based on projections which transform three-phase time and speed dependent system in to a two coordinate (d-q axis) time invariant system, position of a rotor is important. The Park and Inverse Park transformation use the value of the rotor position in order to handle the stator current vector projection in a rotating frame. The electrical position is not directly used in this transform but the sine and cosine values of it are used. It is known that electrical position of the rotor is linked to mechanical position of the rotor by the relation

$$\theta_{electricak} = \theta_{mechanical} * p \qquad (2.24)$$

Where p is number of pole pairs

Whether the control scheme is sensor based or sensor-less, position of the rotor is required.

Control of PMSM can be categorized in to two, the sensor based and sensor-less control.

1) *Sensor based control*: in this control method, sensors are used to indicate the position of the rotor, for instance incremental encoder, absolute encoder, resolver etc

2) *Sensor-less Control*: position of the rotor is estimated using algorithms (or vector control without a mechanical rotor position sensor) such as
    a) Back-emf measurement (Kalman filter and state Observer method)
    b) Inductance measurement (Voltage signal injection and Magnetic saliency)

The advantages of sensor based control system are: easiest way of speed and position measurement and simplification of the design complexity. On the contrary the demerits of this kind of control are it increases volume, weight and cost of the system, too many connection parts between motor and controller, sensors have noise and need space on the shaft of the motor for position measurement and error due to the inaccuracies of sensors.

Sensor-less control system has got some advantages. To mention; it overcomes the drawbacks of Sensor based control, it has better efficiency and lower cost without position transducer and it is reliable and faster response control method.

On the contrary this control system has got some demerits. This includes sophisticated design (e.g. Kalman filter), some methods fail at standstill (e.g. Back-emf method) and expensive for low cost applications and it will take time to develop.

This thesis is totally devoted on sensor based control of permanent magnet synchronous motor because of advantage mentioned above and the simplicity when compare to sensor less control.

In figure 2.12 PMSM drive system has been showed. The motor drive consists of four main components, the PM motor, inverter, control unit and the position sensor.

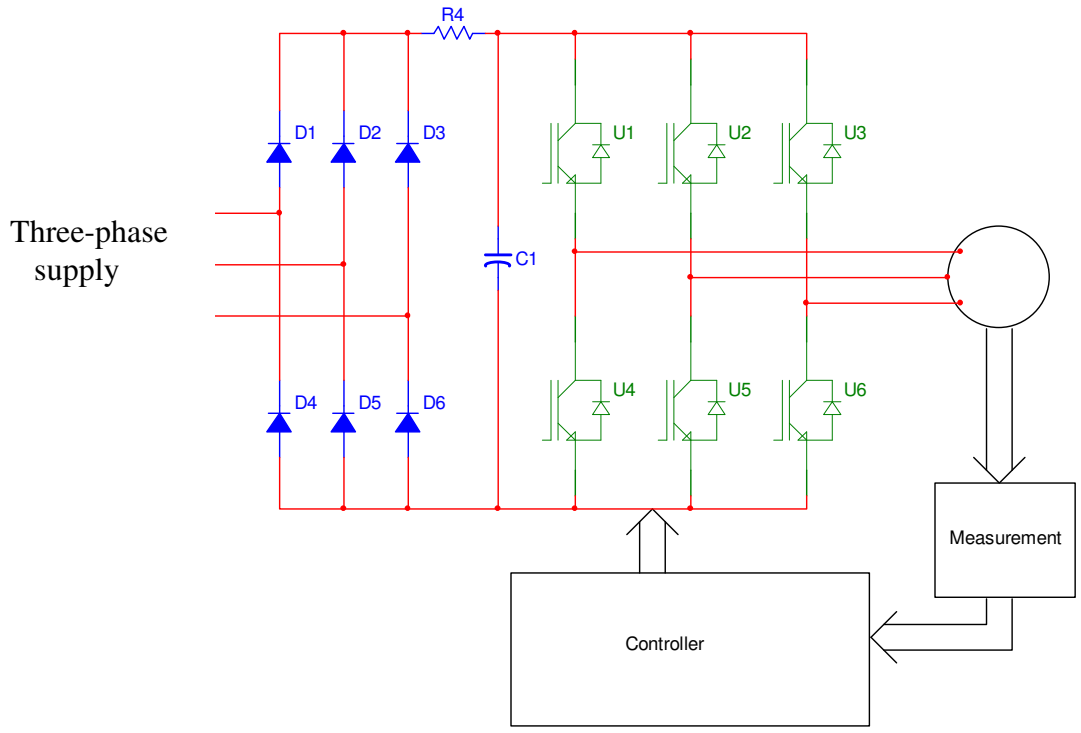

Figure 2.12 PMSM drive system

In this chapter descriptions of the different components of the drive system will be explained

Typical sensor based control scheme for the Field Oriented Control of PMSM drives is shown in the figure 2.13. The field oriented controller is based on current controlled voltage source inverter (VSI) structure. The function of an inverter is to change a dc input voltage to a symmetrical ac output voltage of desired magnitude and frequency. The output voltage could be fixed or variable at a fixed or variable frequency. A variable output voltage can be obtained by varying the input dc voltage and maintaining the gain of the inverter constant. On the other hand, if the dc input voltage is fixed and is not controllable, this is normally accomplished by pulse-width-modulation (PWM) control within the inverter.

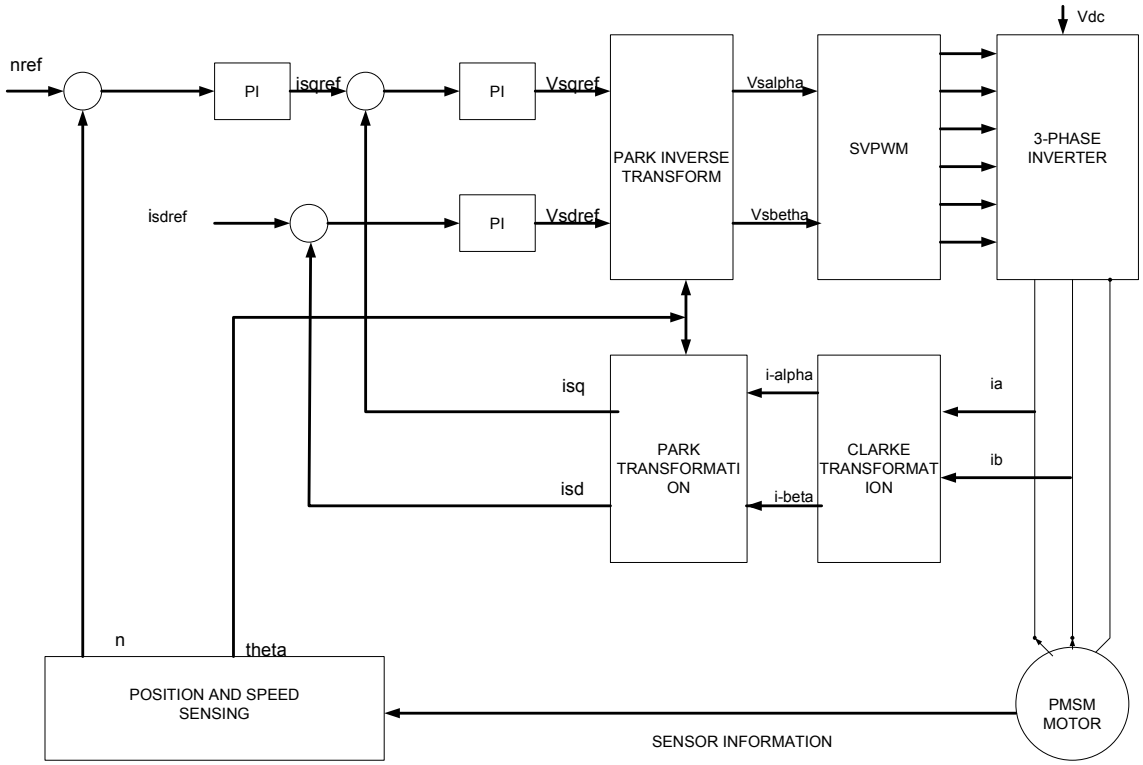

Figure 2.13 Sensor based Field Oriented Control for PMSM

The currents i_a and i_b are measured with two current sensors as shown in figure 2.13. Since current sensors are very costly, two current sensors are used. Besides, the third current i_c can be constructed from the two keeping the system is balanced. The Clarke transformation is applied to them to determine the stator current projection in the two co-ordinates α,β-axis (non-rotating frame). The Park co-ordinate transformation is then applied in order to obtain this projection in the d, q-rotating frame. The d,q projections of the stator currents are then compared to their reference values i_{Sqref} and i_{Sdref} (to get maximum torque, set to zero if there is no field weakening) and corrected by means of PI current controllers. The outputs of the current controller are passed through the inverse Park transform and a new stator voltage vector is impressed to the motor using the space vector pulse width modulation (SVPWM) technique. In order to control the mechanical speed of the motor, an outer loop is driving the reference current i_{Sqref}. The PI regulator

compares the speed set point with the measured mechanical speed of the rotor and produces the stator current quadrature axis reference, is_{qref}. That is the speed controller outputs a reference torque, which is proportional to the quadrature-axis stator current component i_{Sqref}. The mechanical speed reference is denoted "n_{ref}". The information about the phase current can be obtained by two current sensors and the information about the rotor position can be obtained by position sensor like incremental encoder.

The role of the DSP in such a system is to translate the stator variables (currents and angle) into the rotor coordinates as well as to compare the values with the reference values and update the PI controllers. After the transformation from rotor to stator coordinates the output voltage is impressed to the machine with a symmetric PWM, whereby the pulse pattern is computed on-line by the DSP. In some systems the position is measured by an encoder, this extra cost can be avoided by implementing an algorithm as an observer model. These algorithms are complex and therefore require a fast processor; a fixed-point DSP is able to perform the above controls with short cycle times. But this thesis is totally devoted on the sensor based control.

2.7.1 Space Vector Pulse Width Modulation (SVPWM)

At present, when fast and cheap semiconductor devices are available, it is more desirable to use the PWM technique in the low and middle power range since a PWM controlled inverter is able to control both the amplitude and frequency of the output voltage and does not require an additional voltage control on the DC side. This practice is based on multiple pulses in each half AC period, with variable width. Pulse width modulation is the process of modifying the width of the pulses in a pulse train in direct proportion to a small control signal. There are different types of pulse width modulations. Among them, the well known are Sinusoidal pulse width modulation (SPWM) and space vector pulse width modulation (SVPWM).

Sinusoidal PWM has been very popular technique used in AC motor control. This relatively unsophisticated method employs a triangular carrier wave compared with a

sine wave and the points of intersection determine the switching points of the power devices in the inverter. However, this method is unable to make full use of the inverter's supply voltage and the asymmetrical nature of the PWM switching characteristics produces relatively high harmonic distortion in the supply.

Figure 2.14 shows circuit model of a single-phase inverter with a center-taped grounded DC bus, and figure 2.15 illustrates principle of pulse width modulation.

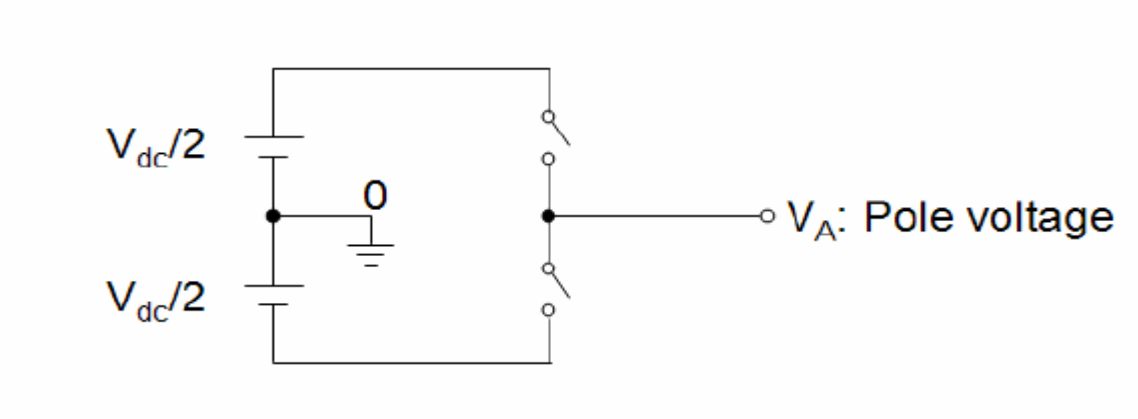

Figure 2.14 Circuit model of a single-phase inverter.

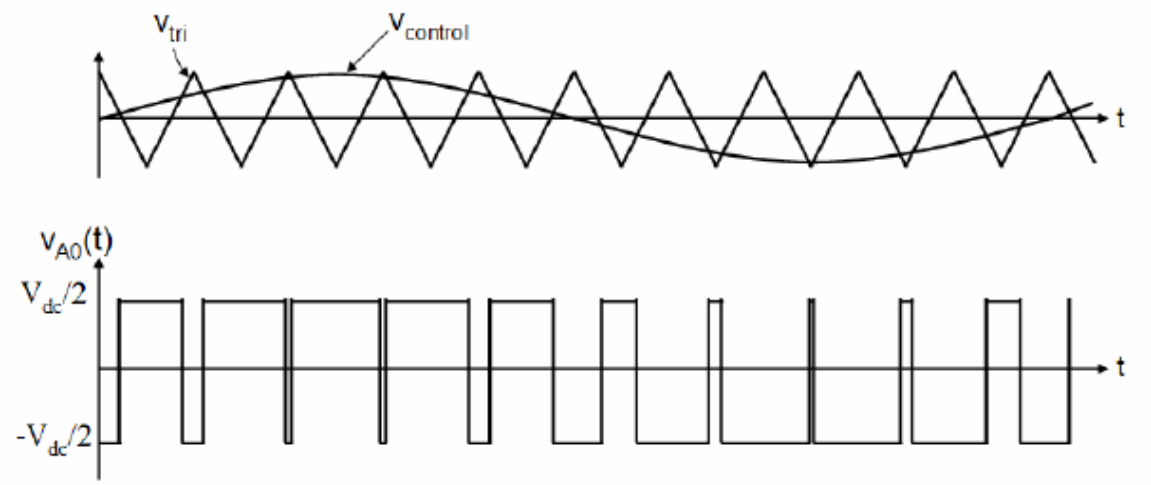

Figure 2.15 pulse width modulation

As depicted in figure 2.15, the inverter output voltage is determined in the following:

- When $V_{control} > V_{tri}$, $V_{A0} = V_{dc}/2$
- When $V_{control} < V_{tri}$, $V_{A0} = -V_{dc}/2$

The inverter output voltage in case of sinusoidal PWM has the following features:

- PWM frequency is the same as the frequency of triangular carrier wave.
- Amplitude is controlled by the peak value of sinusoidal wave.
- Fundamental frequency is controlled by the frequency of the sinusoidal wave.

Space Vector PWM (SVPWM) is a more sophisticated technique for generating a fundamental sine wave that provides a higher voltage to the motor and lower total harmonic distortion when compared to sinusoidal PWM. It is also well-suited for use in vector control (Field orientation) of AC motors. The space vectors technique is nowadays commonly known as space vector modulation (SVM).

The space vector pulse width modulation is used to generate the voltages applied to the stator phases. It uses a special scheme to switch the power transistors to generate pseudo sinusoidal currents in the stator phases. This method is increasingly used for AC drives with the condition that the harmonic current is as small as possible and the maximum output voltage is as large as possible[15][17][18]. The maximum output voltage based on the space vector theory is $2/\sqrt{3}$ times as large as the conventional sinusoidal pulse width modulation. The approach to pulse width modulation described here is based on the space vector representation of the voltage in the stationary reference frame.

In conventional sinusoidal pulse width modulation, locus of the reference vector is the inside of a circle with a radius of $1/2V_{dc}$. In the SV pulse width modulation it can be shown that the length of each of the six vectors is $2/3V_{dc}$. In steady state the reference vector magnitude might be constant. This fact makes the SV modulation reference vector locus smaller than the hexagon described above. To avoid low-order voltage harmonics, resulting from the non-circular shape of the envelop, the locus of the voltage vector is, in practice, narrows itself to the circle inscribed within the hexagon, thus having a radius of $1/\sqrt{3}V_{dc}$.[6] In figure 2.16 below the different reference vector loci are presented.

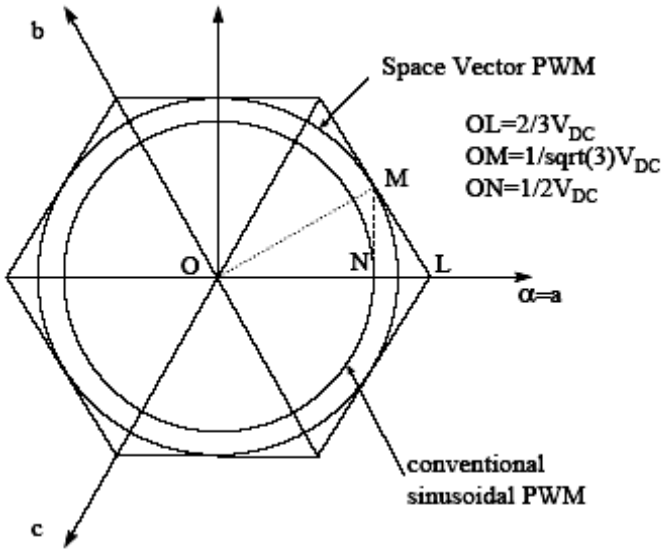

Figure 2.16 Locus comparisons of SVPWM with sinusoidal-PWM

The circuit model of a typical three-phase voltage source PWM inverter is shown in figure 2.17. S_1 to S_6 are the six power switches which are controlled by the switching variables a, a′, b, b′, c and c′ and shape the output. When upper transistor is switched on, i.e., when a, b or c is 1, the corresponding lower transistor is switched off, i.e., the corresponding a′, b′ or c′ is 0. Therefore, the on and off states of the upper transistors S_1, S_3 and S_5 can be used to determine the output voltage. For protection purpose dead band is required. Dead-band is the name given to the time difference between the commutations of the upper and lower transistor of one phase. The two transistors of each phase are then never conducting at the same time. The aim of the dead-band is to protect the power devices during commutation by avoiding conduction overlap and then high transient current.

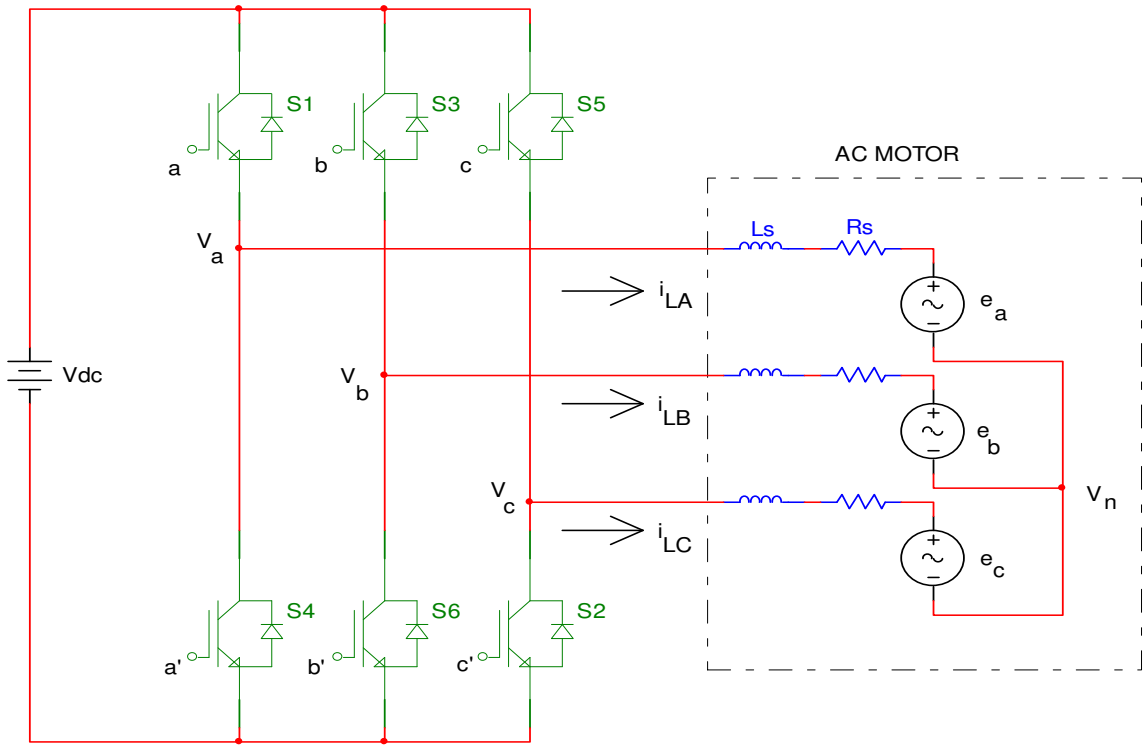

Figure 2.17 Three-phase voltage source PWM Inverter

The relationship between the switching variable vector [a, b, c]^t and the line-to-line voltage vector [V_{ab} V_{bc} V_{ca}]^t is given by equation (2.25).

$$\begin{bmatrix} V_{ab} \\ V_{bc} \\ V_{ca} \end{bmatrix} = V_{dc} \begin{bmatrix} 1 & -1 & 0 \\ 0 & 1 & -1 \\ -1 & 0 & 1 \end{bmatrix} \begin{bmatrix} a \\ b \\ c \end{bmatrix} \tag{2.25}$$

Also, the relationship between the switching variable vector [a, b, c]^t and the phase voltage vector [V_{an} V_{bn} V_{cn}]^t can be expressed below.

$$\begin{bmatrix} V_{an} \\ V_{bn} \\ V_{cn} \end{bmatrix} = \frac{V_{dc}}{3} \begin{bmatrix} 2 & -1 & -1 \\ -1 & 2 & -1 \\ -1 & -1 & 2 \end{bmatrix} \begin{bmatrix} a \\ b \\ c \end{bmatrix} \tag{2.26}$$

The quantities of direct-α and quadrature-β components of the 2-phase orthogonal coordinate system, describing the 3-phase stator voltages, are expressed by the Clarke transformation, arranged in a matrix form.

$$\begin{bmatrix} v_\alpha \\ v_\beta \end{bmatrix} = \frac{2}{3} \begin{bmatrix} 1 & \frac{-1}{2} & \frac{-1}{2} \\ 0 & \frac{\sqrt{3}}{2} & \frac{-\sqrt{3}}{2} \end{bmatrix} \begin{bmatrix} V_{an} \\ V_{bn} \\ V_{cn} \end{bmatrix} \tag{2.27}$$

Since only 8 combinations are possible for the power switches, v_α and v_β can also take only a finite number of values in the (α,β) frame according to the status of the transistor command signal (a,b,c).

As illustrated in figure 2.17, there are eight possible combinations of on and off patterns for the three upper power switches. The on and off states of the lower power devices are opposite to the upper one and so are easily determined once the states of the upper power transistors are determined. According to equations (2.25), (2.26) and (2.27), the eight switching vectors, output line to neutral voltage (phase voltage), and output line-to-line voltages in terms of DC-link V_{dc} and v_α and v_β are given in Table 2.1 and figure 2.18 shows the eight inverter voltage vectors (V_0 to V_7).

Table2.1. Switching vectors, phase voltages and output line to line voltages

vectors voltage	switching vectors			line to neutral voltage			line to line voltage				
	a	**b**	**c**	v_{an}	v_{bn}	v_{cn}	v_{ab}	v_{bc}	v_{ca}	v_α	v_β
v_0	0	0	0	0	0	0	0	0	0	0	0
V_1	1	0	0	2/3	-1/3	-1/3	1	0	-1	2/3	0
v_2	1	1	0	1/3	1/3	-2/3	0	1	-1	1/3	$1/\sqrt{3}$
V_3	0	1	0	-1/3	2/3	-1/3	-1	1	0	-1/3	$1/\sqrt{3}$
v_4	0	1	1	-2/3	1/3	1/3	-1	0	1	-2/3	0
V_5	0	0	1	-1/3	-1/3	2/3	0	-1	1	-1/3	$-1/\sqrt{3}$
V_6	1	0	1	1/3	-2/3	1/3	1	-1	0	1/3	$-1/\sqrt{3}$
v_7	1	1	1	0	0	0	0	0	0	0	0

(Note that the respective voltage should be multiplied by V_{dc})

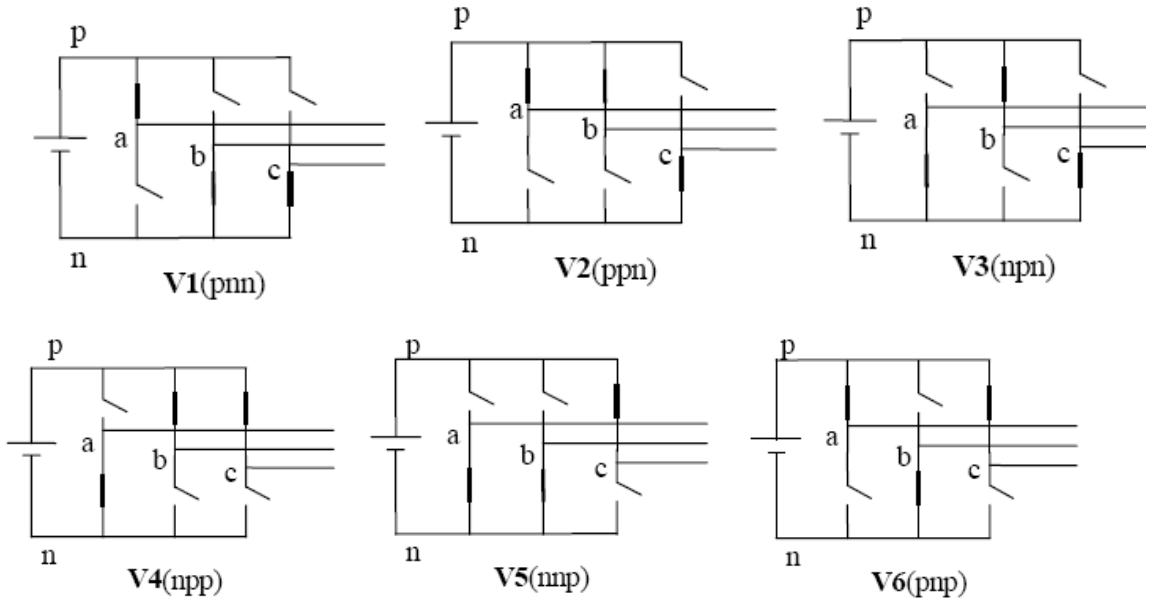

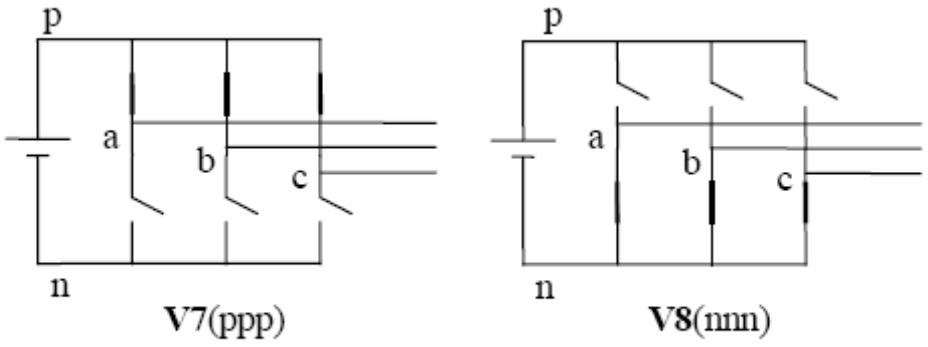

Figure 2.18 Eight switching state topologies of a voltage source inverter

Consider the topology 1 of figure 2.18 which is repeated in figure 2.19 (a) we see that the line voltages V_{ab}, V_{bc}, and V_{ca} are given by $V_{ab} = V_g$, $V_{bc} = 0$ and $V_{ca} = -V_g$. This can be represented in the α,β plane as shown in figure 2.19 (b), where voltages V_{ab}, V_{bc}, and V_{ca} are three line voltage vectors displaced 120° in space. The effective voltage vector generated by this topology is represented as **V1**(pnn) in figure 2.19(b). Here the notation 'pnn' refers to the three legs/phases a,b,c being either connected to the positive dc rail (p) or to the negative dc rail (n). Thus 'pnn' corresponds to 'phase a' being connected to the positive dc rail and phases b and c being connected to the negative dc rail.

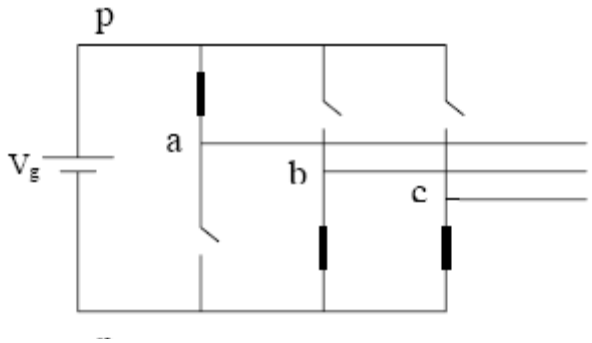

*Figure 2.19 (a) Topology 1-**V1**(pnn) of a voltage source inverter*

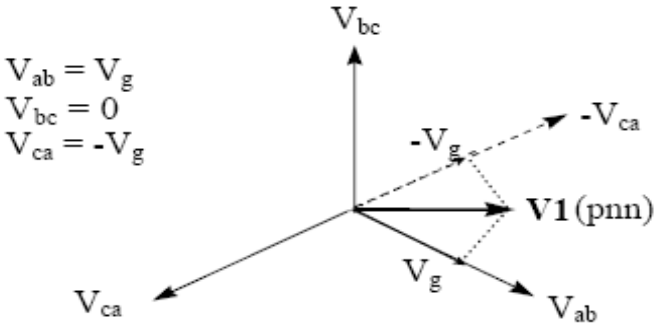

Figure 2.19 (b) Representation of topology 1 in the α,β plane

Proceeding on similar lines the six non-zero voltage vectors (**V1** - **V6**) can be shown in figure 2.20. We define the area enclosed by two adjacent vectors, within the hexagon, as a sector. Thus there are six sectors numbered 1 - 6 in figure 2.20.

Considering the last two topologies of figure 2.18. The output line voltages generated by this topology are given by $V_{ab} = 0$, $V_{bc} = 0$ and $V_{ca} = 0$. These are represented as vectors which have zero magnitude and hence are referred to as zero-switching state vectors or zero voltage vectors. They assume the position at origin in the α,β plane as shown in figure 2.20. The vectors V_1-V_8 are called the switching state vectors (SSVs).

.

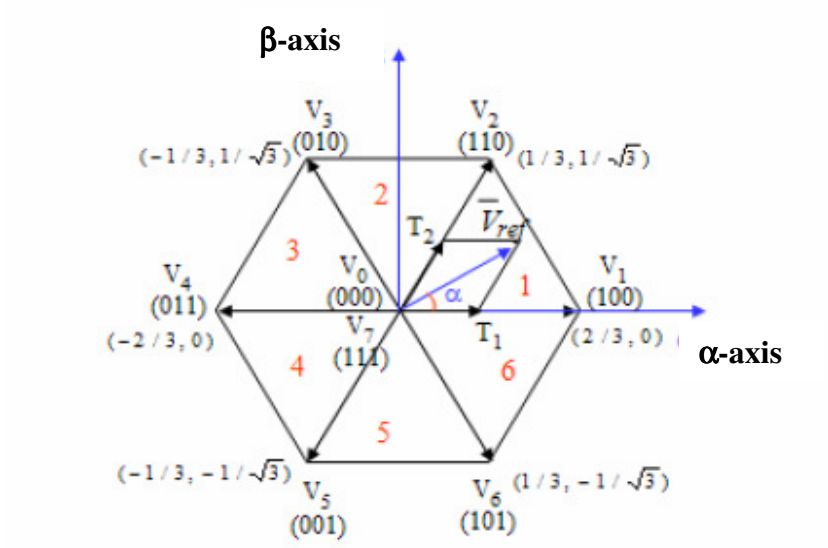

Figure 2.20 Basic switching vectors and sectors

Principle of Space Vector PWM

- Treats the sinusoidal voltage as a constant amplitude vector rotating at constant frequency.
- This PWM technique approximates the reference voltage Vref by a combination of the eight switching patterns(V_0 to V_7).
- Coordinate Transformation (abc reference frame to the stationary α-β frame). That is a three-phase voltage vector is transformed into a vector in the stationary α-β coordinate frame represents the spatial vector sum of the three-phase voltage.
- The vectors (V_1 to V_6) divide the plane into six sectors (each sector: 60 degrees).
- Vref is generated by two adjacent non-zero vectors and two zero vectors.

Comparison of Sine PWM and Space Vector PWM

- Space Vector PWM generates less harmonic distortion in the output voltage or currents in comparison with sine PWM
- Space Vector PWM provides more efficient use of supply voltage in comparison with sine PWM.
- In sine PWM the locus of the reference vector is the inside of the circle with the radius of 1/2 V_{dc}.
- In Space Vector PWM the locus of the reference vector is the inside of a circle with radius of $1/\sqrt{3}$ V_{dc}.

  ∴ Voltage Utilization: Space Vector PWM = $2/\sqrt{3}$ times of Sine PWM

To implement the space vector PWM, the voltage equations in the *abc* reference frame can be transformed into the stationary $\alpha\beta$ reference frame that consists of the horizontal (α) and vertical (β) axes, as a result, six non-zero vectors and two zero vectors are possible. Six nonzero vectors (V_1 - V_6) shape the axes of a hexagonal as depicted in figure 2.20, and feed electric power to the load or DC link voltage is supplied to the load.

The angle between any adjacent two non-zero vectors is 60 degrees. Meanwhile, two zero vectors (V_0 and V_7) are at the origin and apply zero voltage to the load. The eight vectors are called the basic space vectors and are denoted by V_0, V_1, V_2, V_3, V_4, V_5, V_6, and V_7. The same transformation can be applied to the desired output voltage to get the desired reference voltage vector V_{ref} in the d-q plane**.**

The objective of space vector PWM technique is to approximate the reference voltage vector V_{ref} using the eight switching patterns. One simple method of approximation is to generate the average output of the inverter in a small period, T to be the same as that of V_{ref} in the same period.[15][17][18]

2.7.2 Implementation of Space Vector PWM

Space vector PWM can be implemented by the following steps:

- ✓ **Step 1**. Determine V_α, V_β, V_{ref}, and angle (α)
- ✓ **Step 2**. Determine time duration T_1, T_2, T_0 where T_1, T_2 are the respective time for which the basic space vectors V_1 and V_2 should be applied within the time period T_z and T_0 is the course of time for which the null vectors V_0 and V_7 are applied.
- ✓ **Step 3**. Determine the switching time of each transistor (S_1 to S_6)

Step 1: Determine V_α, V_β, V_{ref}, and angle (α)

From figure 2.21, the V_α, V_β, V_{ref}, and angle (α) can be determined as follows:

$$V_\alpha = V_{an} - V_{bn} \cdot \cos 60 - V_{cn} \cdot \cos 60$$
$$= V_{an} - \frac{1}{2} V_{bn} - \frac{1}{2} V_{cn}$$

$$V_\beta = 0 + V_{bn} \cdot \cos 30 - V_{cn} \cdot \cos 30$$
$$= \frac{\sqrt{3}}{2} V_{bn} - \frac{\sqrt{3}}{2} V_{cn}$$

$$\begin{bmatrix} V_\alpha \\ V_\beta \end{bmatrix} = \frac{2}{3}\begin{bmatrix} 1 & -\frac{1}{2} & -\frac{1}{2} \\ 0 & \frac{\sqrt{3}}{2} & -\frac{\sqrt{3}}{2} \end{bmatrix}\begin{bmatrix} V_{an} \\ V_{bn} \\ V_{cn} \end{bmatrix} \quad (2.28)$$

$$\left|\overline{V}_{ref}\right| = \sqrt{V_\alpha{}^2 + V_\beta{}^2} \quad (2.29)$$

$$\alpha = \tan^{-1}\left(\frac{V_\beta}{V_\alpha}\right) = \omega t = 2\pi f t\,, \quad \text{where f=fundamental frequency} \quad (2.30)$$

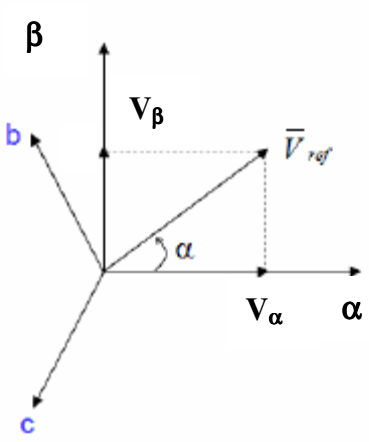

Figure 2.21 Voltage space vector and its components in (α,β)

Step 2: Determine time duration T_1, T_2, T_0

From figure 2.21, the switching time duration can be calculated as follows:

- Switching time duration at Sector I

$$\int_0^{T_Z} \bar{V}_{ref}\, dt = \int_0^{T_1} \bar{V}_1\, dt + \int_{T_1}^{T_1+T_2} \bar{V}_2\, dt + \int_{T_1+T_2}^{T_Z} \bar{V}_0$$

$$\therefore T_Z.\bar{V}_{ref} = (T_1.\bar{V}_1 + T_2.\bar{V}_2)$$

$$\Rightarrow T_Z.\left|\bar{V}_{ref}\right|.\begin{bmatrix}\cos(\alpha)\\ \sin(\alpha)\end{bmatrix} = T_1.\frac{2}{3}.V_{dc}.\begin{bmatrix}1\\ 0\end{bmatrix} + T_2.\frac{2}{3}.V_{dc}.\begin{bmatrix}\cos(\pi/3)\\ \sin(\pi/3)\end{bmatrix}$$

where, $0 \le \alpha \le 60°$

(2.31)

$$\therefore T_1 = T_Z.a.\frac{\sin(\pi/3-\alpha)}{\sin(\pi/3)}$$

$$\therefore T_2 = T_Z.a.\frac{\sin(\alpha)}{\sin(\pi/3)}$$

$$T_0 = T_Z - (T_1 + T_2), \quad \text{(where, } T_Z = \frac{1}{f_Z} \text{ and } a = \frac{\left|\bar{V}_{ref}\right|}{\frac{2}{3}V_{dc}}\text{)}$$

- Switching time duration at any Sector

$$\therefore T_n = \frac{\sqrt{3}.T_Z.\left|\bar{V}_{ref}\right|}{V_{dc}}\left(\sin\left(\frac{\pi}{3} - \alpha + \frac{n-1}{3}\pi\right)\right)$$

$$= \frac{\sqrt{3}.T_Z.\left|\bar{V}_{ref}\right|}{V_{dc}}\left(\sin\frac{n}{3}\pi - \alpha\right)$$

$$= \frac{\sqrt{3}.T_Z.\left|\bar{V}_{ref}\right|}{V_{dc}}\left(\sin\frac{n}{3}\pi\cos\alpha - \cos\frac{n}{3}\pi\sin\alpha\right)$$

$$\therefore T_{n+1} = \frac{\sqrt{3}.T_Z.\left|\bar{V}_{ref}\right|}{V_{dc}}\left(\sin\left(\alpha - \frac{n-1}{3}\pi\right)\right)$$
$$= \frac{\sqrt{3}.T_Z.\left|\bar{V}_{ref}\right|}{V_{dc}}\left(-\cos\alpha\sin\frac{n-1}{3}\pi + \sin\alpha\cos\frac{n-1}{3}\pi\right) \quad (2.32)$$

$$T_0 = T_Z - T_n - T_{n+1}$$

Where n = 1 through 6 (that is sector I to VI)

$$0 \le \alpha \le 60°$$

For sector I PWM output signal is shown in the figure 2.22

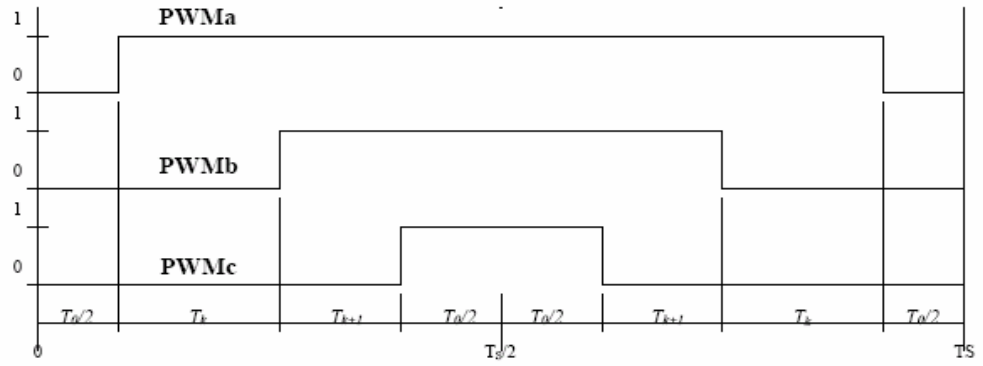

Figure2.22 PWM output signals for a reference vector sitting in sector I

Assuming that it is desired to produce a balanced system of sinusoidal phase voltages, it is known that the corresponding space vector locus is circular.

$$\bar{V}_{\mathrm{Re}f} = \left|\bar{V}_{ref}\right|e^{j\omega t} = \left|\bar{V}_{ref}\right|.(\cos(\omega t) + j\sin(\omega t)) \quad (2.33)$$

where ω is the angular frequency of the desired phase voltages.

From equation 2.33 follows that

$$\begin{pmatrix} T_n \\ T_{n+1} \end{pmatrix} = \frac{\sqrt{3}\left|V_{ref}\right|}{V_{dc}}.T_Z.\begin{bmatrix} \sin\frac{n\pi}{3} & -\cos\frac{n\pi}{3} \\ -\sin\frac{(n-1)\pi}{3} & \cos\frac{(n-1)\pi}{3} \end{bmatrix}.\begin{pmatrix} \cos(\omega t) \\ \sin(\omega t) \end{pmatrix} \tag{2.34}$$

While $0 \le \omega t \le \frac{\pi}{3}$ the reference vector lies in sector 1 and equation (2.34) reduces to

$$\begin{pmatrix} T_1 \\ T_2 \end{pmatrix} = \frac{\sqrt{3}\left|V_{ref}\right|}{V_{dc}}.T_Z.\begin{pmatrix} \sin(\frac{\pi}{3}-\omega t) \\ \sin(\omega t) \end{pmatrix} \tag{2.35}$$

The mean values of the inverter pole voltages averaged over one switching cycle are thus

$$\left.\begin{aligned} V_{A0}(\omega t) &= \frac{V_d}{2T_s}(-\frac{T_0}{2}+T_1+T_2+T_0+T_2+T_1-\frac{T_0}{2}) = \frac{\sqrt{3}}{2}\frac{\left|\overline{V}_{ref}\right|}{V_{dc}}.V_{dc}\cos(\omega t-\frac{\pi}{6}) \\ V_{B0}(\omega t) &= \frac{V_d}{2T_s}(-\frac{T_0}{2}-T_1+T_2+T_0+T_2-T_1-\frac{T_0}{2}) = \frac{3}{2}\frac{\left|\overline{V}_{ref}\right|}{V_{dc}}.V_{dc}\sin(\omega t-\frac{\pi}{6}) \\ V_{C0}(\omega t) &= -V_{A0}(\omega t) \end{aligned}\right\} \tag{2.36}$$

$$V_{A0}(\omega t) = \left\{\begin{array}{ll} \frac{\sqrt{3}}{2}\left|\overline{V}_{ref}\right|\cos(\omega t-\frac{\pi}{6}) & 0 \le \omega t \le \frac{\pi}{3} \\ \frac{3}{2}\left|\overline{V}_{ref}\right|\cos(\omega t) & \frac{\pi}{3} \le \omega t \le \frac{2\pi}{3} \\ \frac{\sqrt{3}}{2}\left|\overline{V}_{ref}\right|\cos(\omega t+\frac{\pi}{6}) & \frac{2\pi}{3} \le \omega t \le \pi \\ \frac{\sqrt{3}}{2}\left|\overline{V}_{ref}\right|\cos(\omega t-\frac{\pi}{6}) & \pi \le \omega t \le \frac{4\pi}{3} \\ \frac{3}{2}\left|\overline{V}_{ref}\right|\cos(\omega t) & \frac{4\pi}{3} \le \omega t \le \frac{5\pi}{3} \\ \frac{\sqrt{3}}{2}\left|\overline{V}_{ref}\right|\cos(\omega t+\frac{\pi}{6}) & \frac{5\pi}{3} \le \omega t \le 2\pi \end{array}\right. \tag{2.37}$$

$$V_{B0}(\omega t) = V_{A0}(\omega t-\frac{2\pi}{3})$$

$$V_{C0}(\omega t) = V_{A0}(\omega t-\frac{4\pi}{3})$$

$V_{A0}(\omega t)$ is shown below for one period

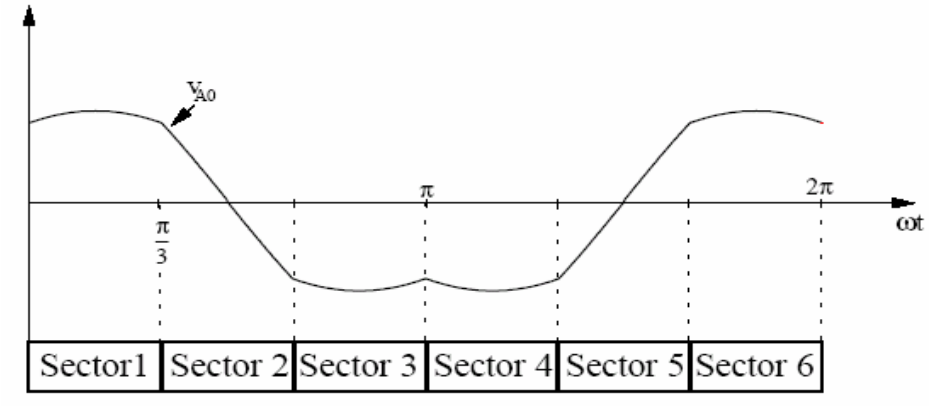

Figure 2.23 Pole voltage for the ideal SV-modulation

Evaluating the line-to-line voltages from equation 2.37 leads to

$$\left.\begin{aligned} V_{AB}(\omega t) &= V_{Ao}(\omega t) - V_{B0}(\omega t) = \sqrt{3}\left|\overline{V}_{ref}\right|\sin(\omega t + \frac{\pi}{3}) \\ V_{BC}(\omega t) &= V_{AB}(\omega t - \frac{2\pi}{3}) \qquad\qquad for \quad 0 \le \omega t \le 2\pi \\ V_{CA}(\omega t) &= V_{AB}(\omega t - \frac{4\pi}{3}) \end{aligned}\right\} \qquad (2.38)$$

Therefore it turns out that they are sinusoidal, as expected.

The method used to approximate the desired stator reference voltage with only eight possible states of switches is to combine adjacent vectors of the reference voltage and to modulate the time of application of each adjacent vector. Take the first sector.

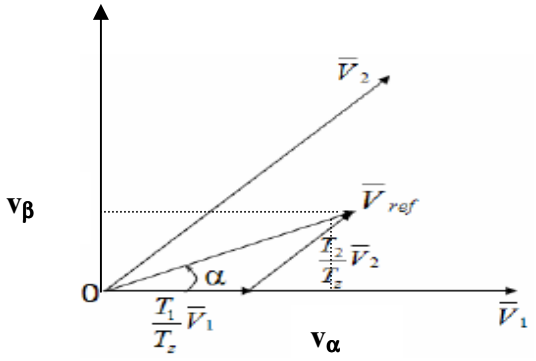

Figure 2.24 Reference vector as a combination of adjacent vectors at sector 1

From figure 2.24, the reference voltage $\bar{v}_{ref}$ is in the first sector and the application time of each adjacent vector is given by:

$$\begin{aligned} T_z &= T_1 + T_2 + T_0 \\ \bar{v}_{ref} &= \frac{T_1}{T_z}\bar{v}_1 + \frac{T_2}{T_z}v_2 \end{aligned} \tag{2.39}$$

The determination of times T_1 and T_2 is given by simple projections and with the (α,β) component values of the vectors, the amount of times of application of each adjacent vector is:

$$\begin{aligned} T_1 &= \frac{T_Z}{2V_{dc}}(3v_\alpha - \sqrt{3}v_\beta) \\ T_2 &= \sqrt{3}\frac{T_z}{v_{dc}}v_\beta \end{aligned} \tag{2.40}$$

Note that equation (2.40) is exactly the same as equation (2.31)

For every sector, commutation duration is calculated. The amount of times of vector application can all be related to the following variables:

$$\begin{aligned} X &= \sqrt{3}\frac{T_s}{2v_{dc}}v_\beta \\ Y &= \frac{\sqrt{3}}{2}\frac{T_s}{2v_{dc}}v_\beta + \frac{3}{2}\frac{T_s}{2v_{dc}}v_\alpha \\ Z &= \frac{\sqrt{3}}{2}\frac{T_s}{2v_{dc}}v_\beta - \frac{3}{2}\frac{T_s}{2v_{dc}}v_\alpha \end{aligned} \tag{2.41}$$

In the previous example for sector 1, T_1 = - Z and T_2 = X. For different sectors, the expressions of T_k and T_{k+1} are listed in the table below.

Table 2.2 Tk and T_{k+1} definition for different sectors in terms of X, Y and Z

Sector	I	II	III	IV	V	VI
T_k	-Z	Z	X	-X	-Y	Y
T_{k+1}	X	Y	-Y	Z	-Z	-X

In order to know which of the above variable apply, the knowledge of the sector in which the reference vector is needed. To determine this sector, a simple approach is to calculate the projections v_a, v_b and v_c of the reference voltage vector in the (a,b,c) plane. These projections are compared to zero.

The projections u_{ref1}, u_{ref2} and u_{ref3} are given by the Clarke^{-1} transform as follow:

$$\begin{aligned} u_{ref1} &= v_\beta \\ u_{ref2} &= \frac{1}{2}(\sqrt{3}v_\alpha - v_\beta) \\ u_{ref3} &= \frac{1}{2}(-\sqrt{3}v_\alpha - v_\beta) \end{aligned} \tag{2.42}$$

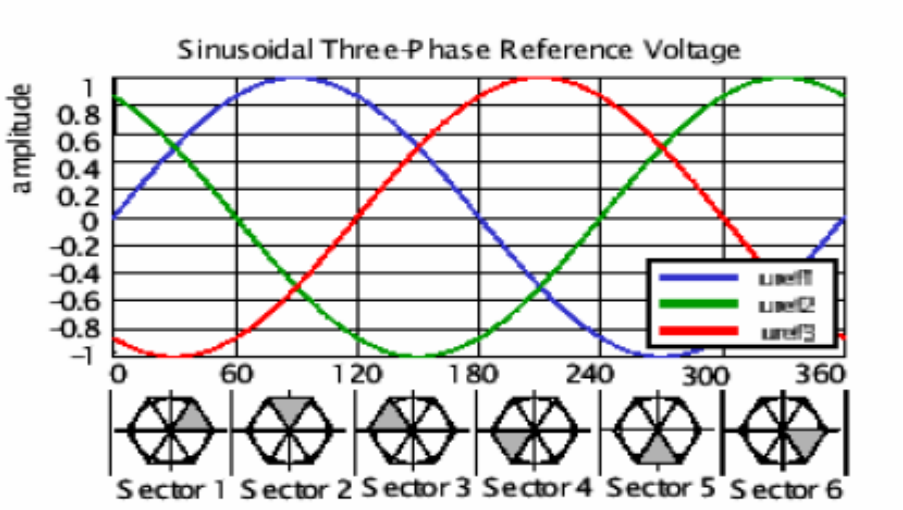

Figure 2.25 Reference voltages u_{ref1}, u_{ref2} and u_{ref3}

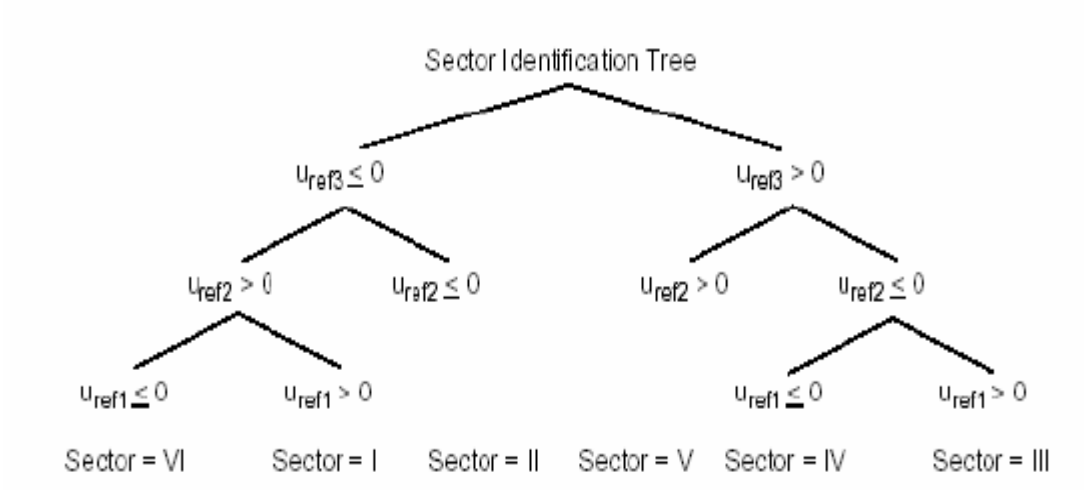

Figure2.26 Identification of sector number

To summarize, the desired three phase voltages at the output of the inverter could be represented by an equivalent vector **V** rotating in the counter clock wise direction as shown in figure 2.27. The magnitude of this vector is related to the magnitude of the output voltage (figure 2.28) and the time this vector takes to complete one revolution is the same as the fundamental time period of the output voltage. Figure 2.27 and 2.28 shows the relationship between the rotating vectors and sector in which this vector lies.

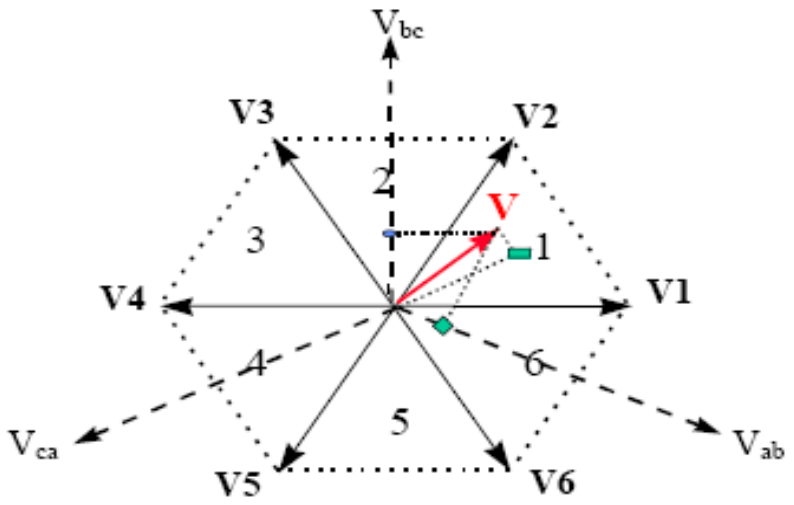

Figure 2.27 Output voltage vector in the α β plane

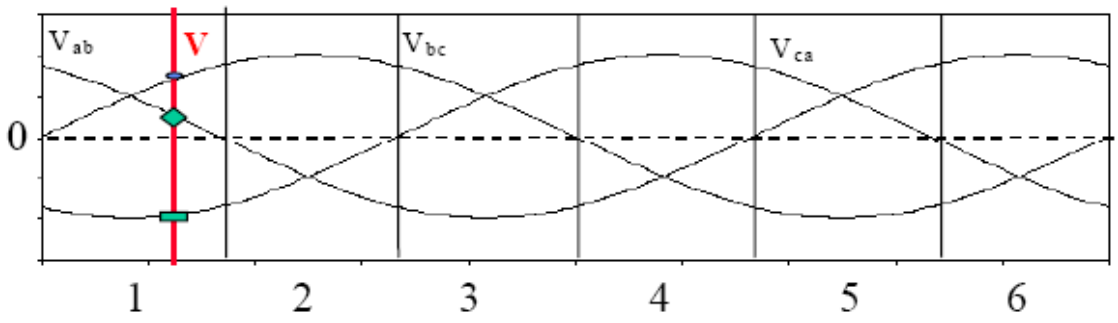

Figure 2.28 output line voltage in the time domain

Step 3: Determine the switching time of each transistor (S_1 to S_6)

Figure 2.29 shows space vector PWM switching patterns at each sector. This kind of switching patterns is called symmetrical PWM. From the figure $T_s = 2T_z$

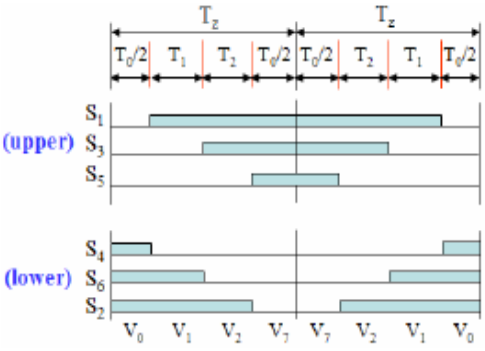

(a) Sector 1.

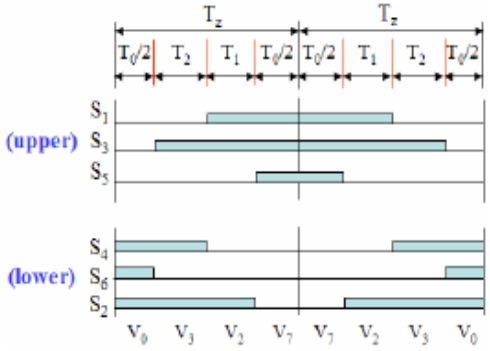

(b) Sector 2.

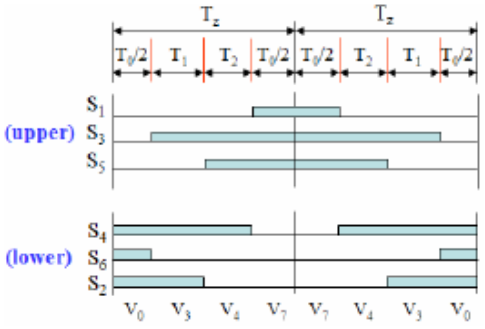

(c) Sector 3.

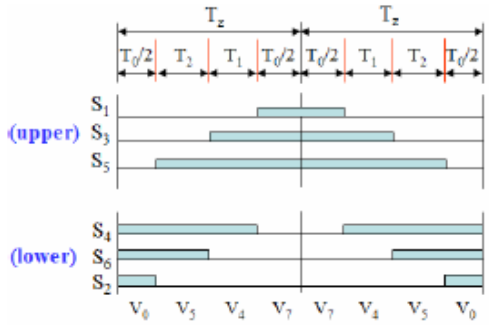

(d) Sector 4.

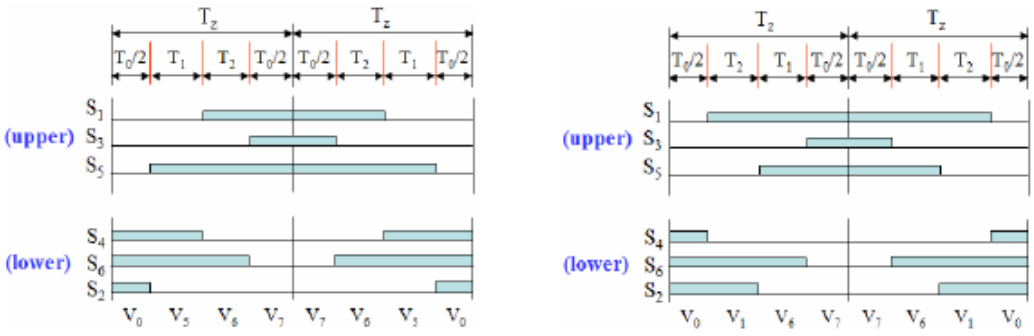

Figure 2.29 Space Vector PWM switching patterns at each sector

Based on figure 2.29, the switching time at each sector is summarized in Table 2.3.

Table 2.3 Switching Time Calculation at Each Sector

sector	Upper switches(S_1,S_3,S_5)	Lower switches(S_4,S_6, S_2)
1	$S_1 = T_1+T_2+T_0/2$ $S_2 = T_2+T_0/2$ $S_5 = T_0/2$	$S_4 = T_0/2$ $S_6 = T_1+T_0/2$ $S_2 = T_1+T_2+T_0/2$
2	$S_1 = T_1+T_0/2$ $S_2 = T_1+T_2+T_0/2$ $S_5 = T_0/2$	$S_4 = T_2+T_0/2$ $S_6 = T_0/2$ $S_2 = T_1+T_2+T_0/2$
3	$S_1 = T_0/2$ $S_2 = T_1+T_2+T_0/2$ $S_5 = T_2+T_0/2$	$S_4 = T_1+T_2+T_0/2$ $S_6 = T_0/2$ $S_2 = T_1+T_0/2$
4	$S_1 = T_0/2$ $S_2 = T_1+T_0/2$ $S_5 = T_1+T_2+T_0/2$	$S_4 = T_1+T_2+T_0/2$ $S_6 = T_2+T_0/2$ $S_2 = T_0/2$
5	$S_1 = T_2+T_0/2$ $S_2 = T_0/2$ $S_5 = T_1+T_2+T_0/2$	$S_4 = T_1+T_0/2$ $S_6 = T_1+T_2+T0/2$ $S_2 = T_0/2$
6	$S_1 = T_1+T_2+T_0/2$ $S_2 = T_0/2$ $S_5 = T_1+T_0/2$	$S_4 = T_0/2$ $S_6 = T_1+T_2+T_0/2$ $S_2 = T_2+T_0/2$

2.7.3 Position sensor

Knowledge of the rotor flux angle is essential for accurately applying the Clarke and Park transforms. If this angle is incorrect, the flux and torque producing components of the stator current are not decoupled and true field oriented control is not achieved. The need of knowing the rotor position requires the development of devices for position measurement. There are different types of rotor position measuring device like potentiometer, linear variable differential transformer, optical encoder, resolver, and tachogenerator. The ones most commonly used for motors are encoders and resolver. Depending on the application and performance desired by the motor a position sensor with the required accuracy can be selected.

Whenever mechanical rotary motions have to be monitored, the optical encoder as shown in the figure 2.30 is the most important interface between the mechanics and the control unit. Encoders transform rotary movement into a sequence of electrical pulses. An encoder consists of a rotating disk, a light source, and a photo detector (light sensor). The disk, is mounted on the rotating shaft, has coded patterns of opaque and transparent sectors. As the disk rotates, these patterns interrupt the light emitted onto the photo detector, generating a digital pulse or output signal.

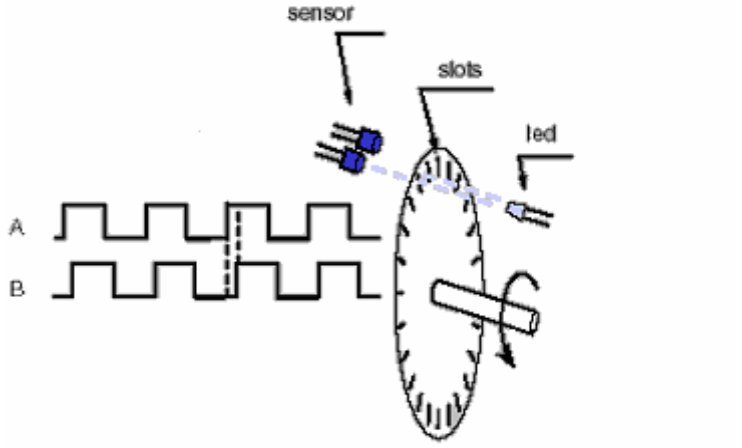

Figure 2.30 Optical encoder

Optical encoders offer the advantages of digital interface. There are two types of optical encoders, incremental encoder and absolute encoder. Figure 2.31 shows both incremental and absolute encoder.

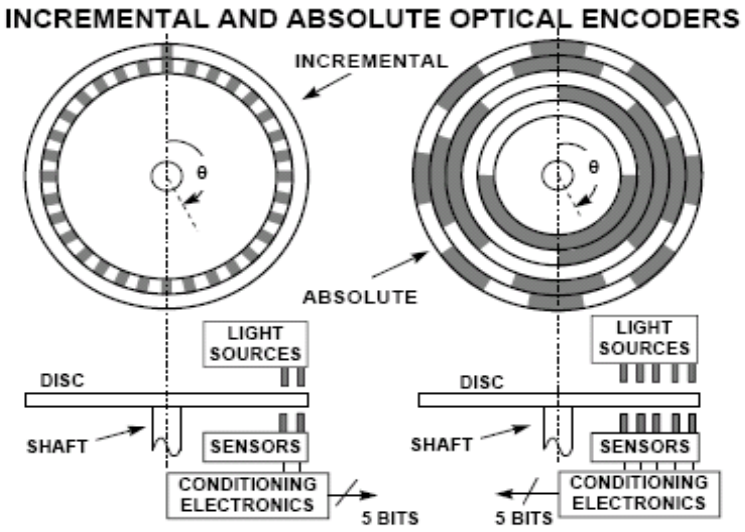

Figure 2.31 Incremental and absolute encoder

The absolute encoder, as shown in figure 2.31 captures the exact position of the rotor with a precision directly related to the number of bits of the encoder. It can rotate indefinitely and even if the motor stops the position can be measured or obtained.

Absolute encoders can measure the position of an object relative to a reference position at any time. The output signal of the absolute encoder presents the absolute positions in a digital code format. An incremental encoder can measure the change in position, not the absolute position. Therefore, the incremental encoder cannot tell the position relative to a known reference. If absolute position information is needed from incremental encoder measurement, the device must perform the so-called “home-ing” motion sequence in order to establish its reference position after the power up. From that point on, the absolute position can be tracked by digital counting. An absolute encoder doesn’t need a counting circuit if the total position change is within the range covered by the absolute encoder.

Incremental encoders have good precision and are simple to implement but they suffer from lack of information when the motor is at rest position and in order for precise position the motor must be stopped at the starting point.[5]

The resolution (number of counts per revolution) of the absolute encoder is determined by the number of photo detectors. If the absolute encoder has eight photo detectors (8-bits), the smallest position change that can be detected is $360°/2^8 = 360/256°$. If the encoder is 12-bits, the resolution is $360°/2^{12} = 360/4096°$. For each position, the absolute encoder outputs a unique code. Gray code is known to have better noise immunity and is less likely to provide wrong reading compared with binary code.

Advantage of optical encoder is it has high resolution and its disadvantages are high cost and lack of robustness.

The other very commonly used position sensor is position revolver as shown in figure 2.32, also called rotary transformers, works on the transformer principle. The resolver is basically a rotary transformer with one rotating reference winding (V_{ref}) and two stator windings (90° out of phase). The primary winding is placed on the rotor and depending upon the rotor shaft angle the induced voltage at the two secondary windings of the transformer shifted by 90° would be different. The magnitude of the induced voltage is a function of the angular position of the rotor. The position can be calculated using the two voltages.

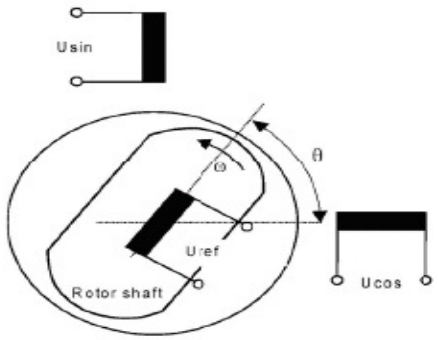

Figure 2.32 Resolver

2.7.4 Current Controlled inverter

Usually the motor is fed from a voltage source inverter with current control. The control is performed by regulating the flow of current through the stator of the motor. Current controllers are used to generate gate signals for the inverter. Proper selection of the inverter devices and selection of the control technique will guarantee the efficiency of the drive.

Voltage Source Inverters are devices that convert a DC voltage to AC voltage of variable frequency and magnitude. The output voltage could be fixed or variable at a fixed or variable frequency. A variable output voltage can be obtained by varying the input DC voltage and maintaining the gain of the inverter constant. On the other hand, if the DC input voltage is fixed and is not controllable, a variable output voltage can be obtained by varying the gain of the inverter, which is normally accomplished by pulse width modulation (PWM) control within the inverter. The inverter gain may be defined as the ratio of the AC output voltage to DC input voltage.

They are very commonly used in adjustable speed drives and are characterized by a well defined switched voltage wave form in the terminals. Figure 2.33 shows a voltage source inverter. The AC voltage frequency can be variable or constant depending on the application.

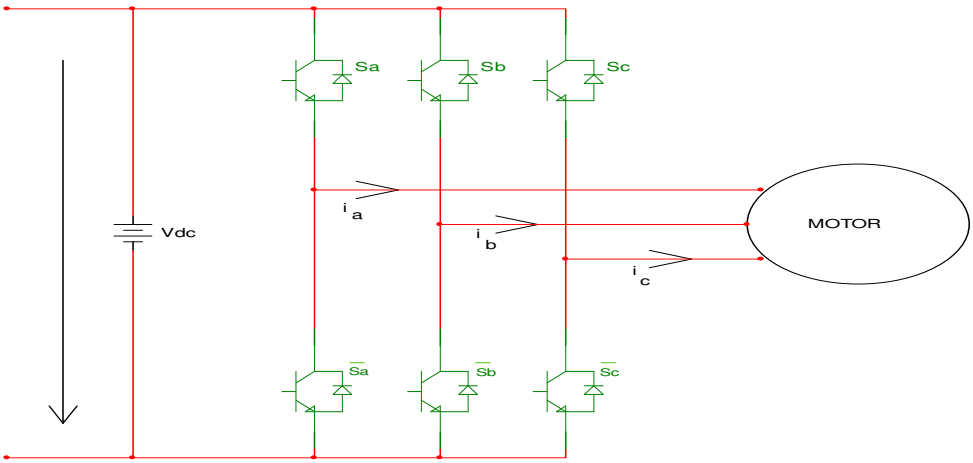

Figure 2.33 Voltage source inverter connected with a motor

Three phase inverters consist of six power switches connected as shown in figure 2.33 to a DC voltage source. The inverter switches must be carefully selected based on the requirements of operation, ratings and the application. There are several devices available today and these are thyristors, bipolar junction transistors (BJTs), MOS field effect transistors (MOSFETs), insulated gate bipolar transistors (IGBTs) and gate turn off thyristors (GTOs). The devices list with their respective power switching capabilities are shown in table 2.4. MOSFETs and IGBTs are preferred by industry because of the MOS gating permits high power gain and control advantages. While MOSFET is considered a universal power device for low power and low voltage applications, IGBT has wide acceptance for motor drives and other application in the low and medium power range. The power devices when used in motor drives applications require an inductive motor current path provided by anti-parallel diodes when the switch is turned off.

Table 2.4 Devices power and switching capabilities

Sl.No	Devices	power capability	switching speed
1	BJT	Medium	Medium
2	GTO	High	Low
3	IGBT	Medium	Medium
4	MOSFET	Low	High
5	THYRISTOR	High	Low

2.7.5 -PI Controller

PI or two-term controllers are the most widely used controllers in industries today. The name PI comprises the first letter P stands for Proportional term in the controller and I stands for the Integral term in the controller. PI control is applied in speed, current, and position control.

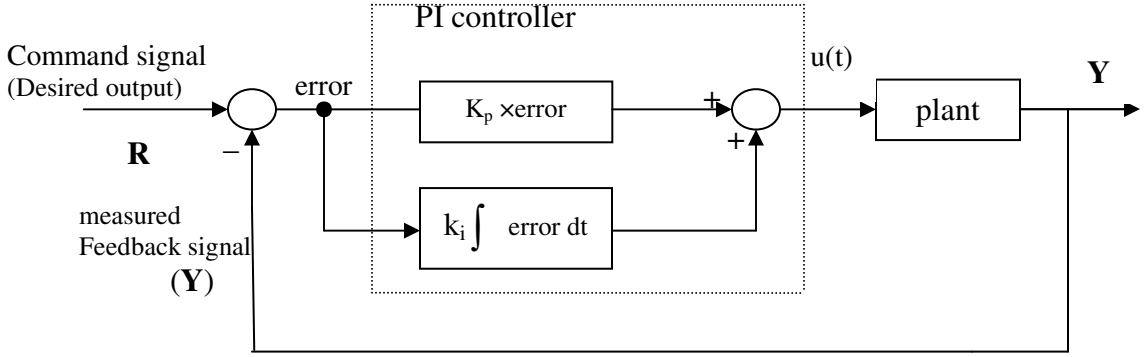

Figure 2.34 PI controller

The expression of PI control in time domain is:

$$u(t) = k_p[R(t) - Y(t)] + k_i \int_0^t [R(t) - Y(t)]dt$$
$$= k_P e(t) + k_i \int_0^t e(t)dt \qquad (2.43)$$

where:

$u(t)$ is the controller's output signal

$e(t)$ is the controller's input error signal

k_P is proportional control gain

k_i is integral control gain

The Field Oriented Control of a PMSM needs three PI controllers. One for each current in rotating frame (i_d and i_q) and one for the angular speed. (See figure 2.12).

The Laplace transform of equation (2.43) and the structure of PI controller will be

$$U(s) = k_p(R(s) - Y(s)) + \frac{k_i}{s}(R(s) - Y(s))$$
$$U(s) = k_P E(s) + \frac{k_i}{s}E(s) \qquad = E(s)\left(k_P + \frac{k_i}{s}\right) \tag{2.44}$$

$$D(s) = \frac{U(s)}{E(s)} = k_P + \frac{k_i}{s} = \frac{k_P s + k_i}{s}$$

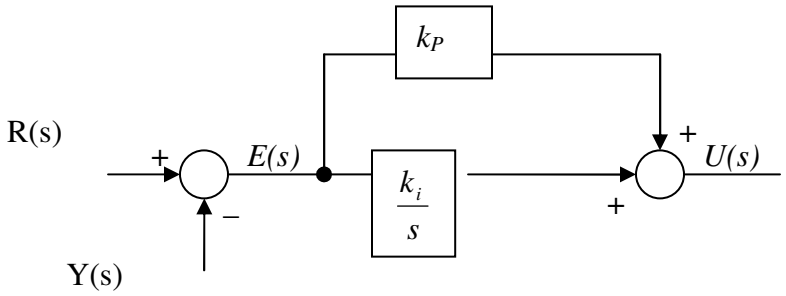

Figure 2.35 Structure of PI controller

A proportional controller (k_p) will have the effect of reducing the rise time and will reduce, but never eliminate the steady state error. If k_p is increasing the steady state error will be decreased but may cause the controller signal to be large which may lead to saturation or limiting problems with the system actuator. An integral control (k_i) will have the effect of eliminating the steady-state error, but it may make the transient response worse.[12][13]

This is how a PI controller is modeled, where the two parameters or gains k_p and k_i are chosen to give the desired system dynamics. For this controller the gain ki is about an order of magnitude of 10 less than the gain kp,

Table 2.5 -Summery of PI controller characteristic

Controller	Benefit	Drawbacks
P(k_p)	-Simple, cheap	-Steady state error -large overshoot and settling time - poor transient response -prone to instability(large gains)
I(k_i)	-eliminates steady state error	-poor damping -large overshoot and settling time -poor transient response & reduces stability

Approximating the integral by rectangular approximation and if the sampling period, k, is small enough, the proportional-integral (PI) control algorithm for a discrete implementation can be written:

$$U_{PI}(k) = U_P(k) + U_I(k) = k_P e(k) + k_i \sum_{j=0}^{k-1} e(j)$$
$$U_{PI}(k-1) = U_P(k-1) + U_I(k-1) = k_P e(k-1) + k_i \sum_{j=0}^{k-2} e(j) \quad (2.45)$$

From equation (2.45), the incremental form of the PI algorithm is expressed as:

$$\Delta U_{PI}(k) = U_{PI}(k) - U_{PI}(k-1) = k_p[e(k) - e(k-1)] + k_i e(k)$$

$$U_{PI}(k) = U_{PI}(k-1) + k_P[e(k) - e(k-1)] + k_i e(k-1) \qquad (2.46)$$

Where the correction signal U_{PI} for k is derived from the error signal e and it is the actual iterative used.[11][17] The two free parameters which need to be set prior to operation are k_P and k_i, the gains controlling the proportional and integral parts of the algorithm. k_P determines the size of the response to a change in the error signal state, and k_i controls the steady-state correction response. The two parameters need to be adjusted to provide an optimum balance between a fast initial correction and a high resolution steady-state correction.

Several limitations of proportional control are resolved by integral control. As long as the system remains stable, the system output equals the desired output regardless of the value of k_p. In general, even though integral control improves the steady state response, it has the effect of slowing down the response while the overshoot is kept constant.

2.7.6 Current sensing

In most of the inverter system with close loop current control, phase current information is required. The method of obtaining those currents is to directly sense them but this requires, depending on the load schematic, at lease two sensors applied directly on the motor phases.

On the inverter (DL 2646) which is intended to use for field weakening control, there are two current sensors. The measurement of the current is only carried out at two outputs since in a balanced three-phase system the sum of the instantaneous values of the three currents is always zero. The out put for this current sensor is in terms of voltage. [30]

$$V_{11} = 0.3I_1(A)$$
$$V_{22} = 0.3I_3(A) \qquad (2.47)$$

Most of the sensor convert the current in to the voltage information and hence sample the voltage from the sensor output and use software to convert it to current based using sensor characteristics equation (equation 2.47)

2.8 Field weakening strategies

Air gap flux control of PM machines can generally be accomplished by two means: control techniques and suitable modification of the machine topology. Conventional PM machines have a fixed magnet excitation which limits the drive's capability and becomes a significant limitation. The machines are operated at constant volt/hertz operation up to base speed and constant voltage operation which requires weakening of the field at higher speeds to extend the speed range. Above base speed, vector control techniques are typically used to weaken the air gap flux.

2.8.1 Concept of field weakening operation

When a vehicle is cruising at high speed, the required torque is normally low, and the supply voltage to the motor has a certain limit. Therefore, field weakening is an essential requirement for motors used for electric vehicle drive.[1] The concept of field weakening in a permanent magnet machine is for the purpose of providing a constant power region at speeds above base speed.

The separately excited DC commutator motor drive shows an ideal field-weakening characteristic. Therefore it is appropriate to consider the principle of field-weakening operation using this familiar motor characteristic.

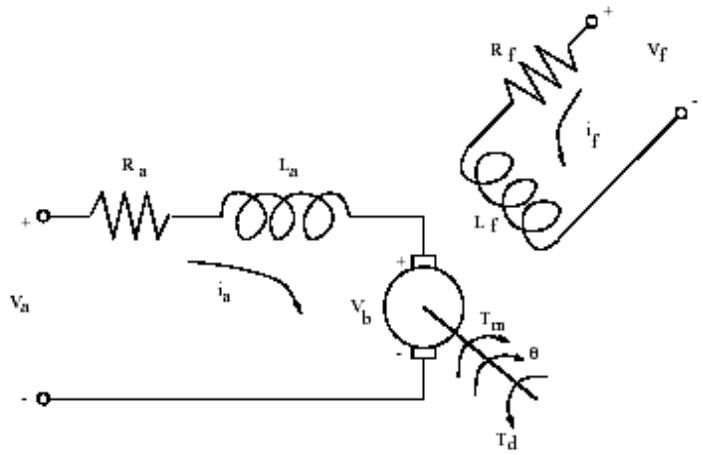

Figure 2.36 Separately excited dc commutator motor drive

Here are the basic equations for torque developed by the motor, back emf of the armature and the relationship between field current and field flux before saturation reaches respectively

$$T_m(t) = K_m i_f(t) i_a(t) \tag{2.48}$$

$$E_b = K_b \Phi_f \omega \tag{2.49}$$

$$\phi_f = f(i_f) \tag{2.50}$$

In this motor the field and armature currents are set to their maximum permissible values, then, from equation 2.48, in order to get maximum torque possible, field and armature current is maximum. This constraint sets the limit curve #1 on figure 2.37 [9]

When the speed of the dc motor increases, the voltage applied to the motor must increase to match the back emf of the dc motor as defined by equation 2.49. Eventually, at some speed, for any practical power supply, the voltage can not be further increased to maintain the current at the limit value $I_{a,max}$. If the field current is not changed at this point the current will rapidly drop to zero, i.e. at the speed where $V_{dc(max)} = E_{b,}$ where $V_{dc(max)}$ is the dc output voltage of the power supply. Torque can continue to be maintained however, if the emf of the motor is held at a value lower than $V_{dc(max)}$. The

minimum value of field current at any speed is set by the maximum permissible value of I_a. Hence, another boundary curve, curve #2 in Figure 2.37, can be identified which is set by the saturation of the dc power supply. This curve is usually labeled as the constant power region.

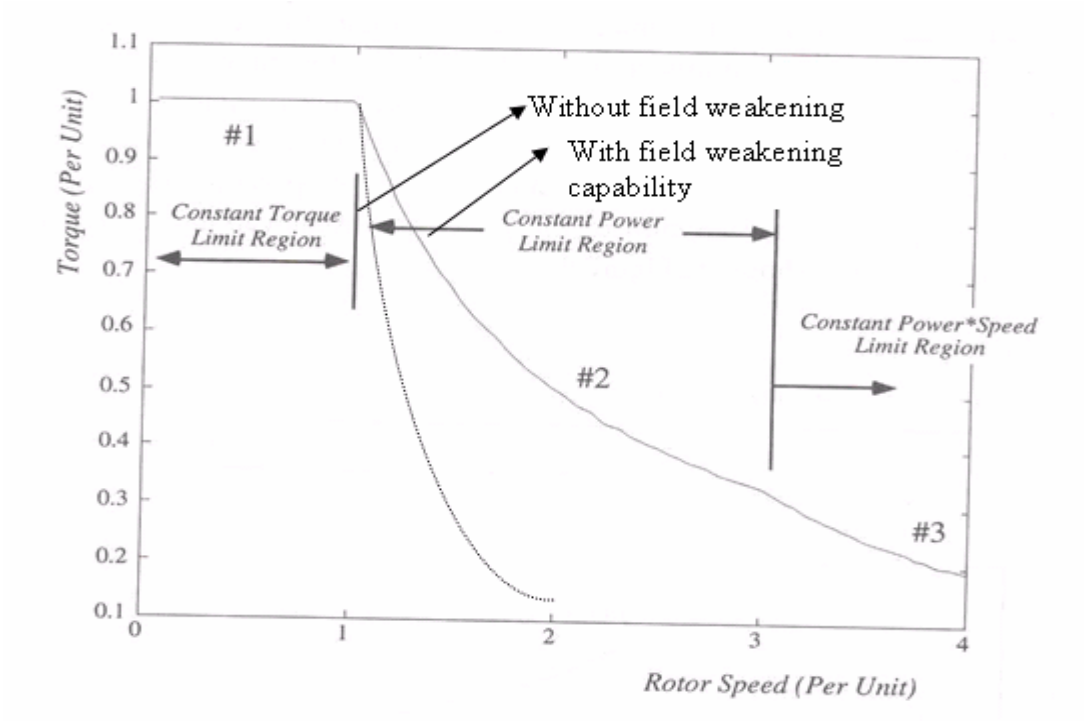

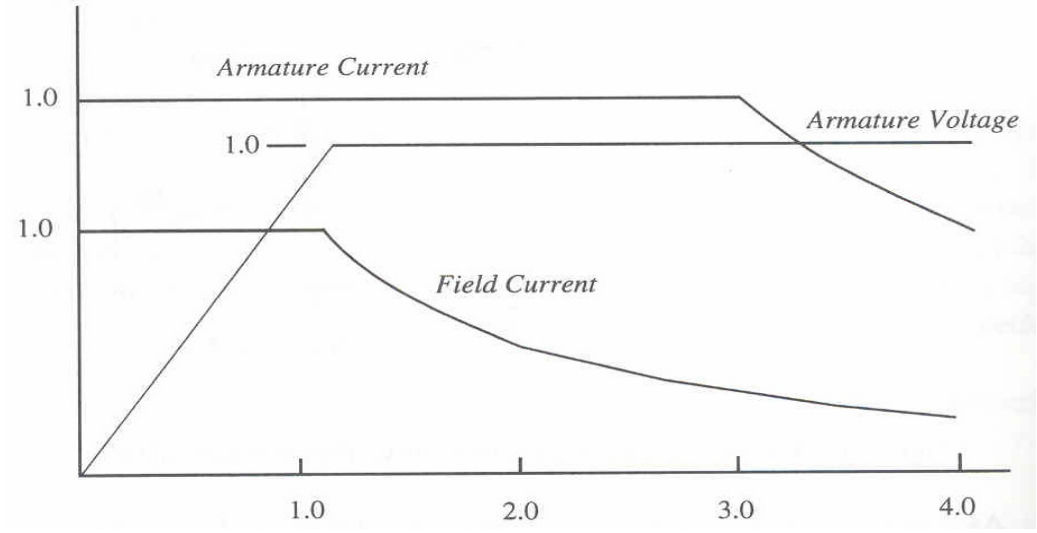

Figure 2.37 Torque vs. speed capability curve for dc motor drive
Figure 2.38 electrical variables corresponding to figure 2.37 as a function of speed

As speed continues to increase the minimum value of field current needed to supply rated armature current decreases in accordance with equation 2.49 which specifies that as speed increases, the field flux linkage must decrease inversely with speed if E_b is to be maintained constant. However, as the field current is decreased, the distortion of the airgap flux caused by the armature current increases creating a very non-uniform distribution of bar to bar voltage on the commutator. This distortion at the high speed eventually cause bar to bar commutator voltages to reach unacceptable levels, Sparking begins to occur usually terminated by spectacular fireworks, a flashover of the brush and commutator rigging. Hence, above a certain speed the reduction of the field current to maintain constant armature current must be curtailed. The armature current must now begin to decrease. Since the need for commutating ability is proportional to the current to be commutated, the field current now becomes proportional to the armature current resulting in a third mode of operation termed series field operation, curve #3. The corner point at which the machine reaches crossover between curve #2 and curve #3 is generally considered to be rated maximum speed. Operation along curve #3 is rarely used since commutating ability is marginal and the motor enters a speed region where physical integrity of the commutator bars becomes difficult to maintain. In addition the torque capability in this region is not much more than windage and friction losses making the additional complexity of operating in this region difficult to justify. The variation of the motor electrical variables needed to obtain figure 2.38 is shown in figure 2.39.

It should be noted that since the armature current and field current are constant the constraint set by curve #1 on figure 2.38 inherently produces a constant torque limit on the speed-torque plane while constant armature current and constant back emf constraint of curve #2 imposes inherently a constant power limit. Neglecting armature resistance, Curve #3 imposes an inverse square law torque characteristic. Popular acceptance of these capability limitations of a dc machine has caused users of electrical equipment to define these same characteristics from the point of view of torque requirements not only

to be imposed on a dc machine but any type of motor drive. It remains to be seen whether the maximum capability curves of an induction machine are consistent with torque requirements, as adopted from the maximum capability curves of a dc machine.

Real motors do not have flat output power against speed characteristics above rated speed ω_b. In Figure 2.39 the dashed line is the ideal field-weakening characteristic and the solid line is the actual characteristic. Rated power is the output power at rated speed ω_b with rated torque T_b. The inverter utilization is the ratio of rated power to the ideal output power. This is less than unity as the motor does not have unity power factor and 100% efficiency under rated operating conditions. The constant-power speed range (CPSR) is the speed range over which rated power can be maintained.

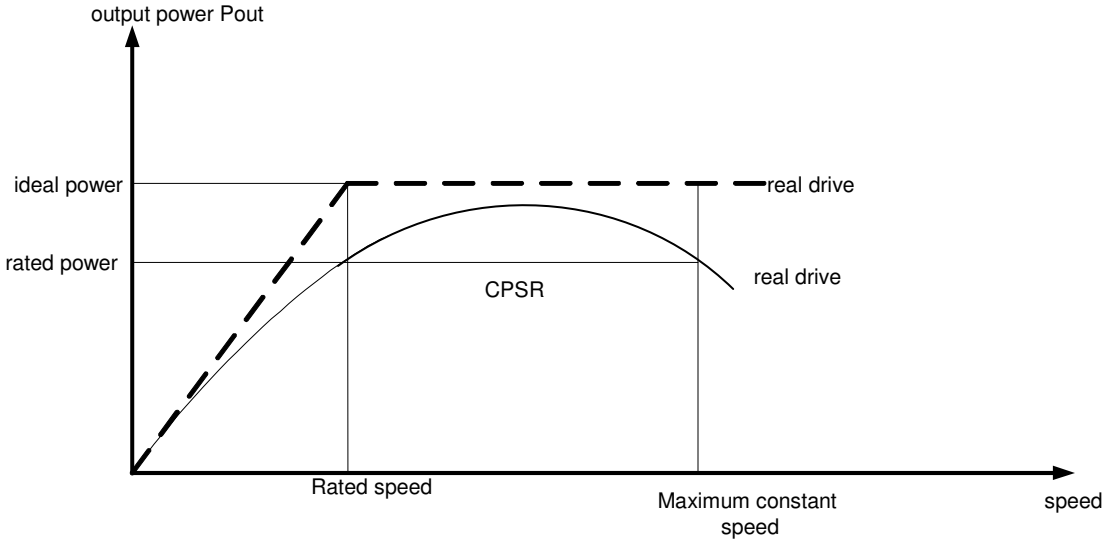

Figure 2.39 *Ideal and practical field weakening characteristics*

In short in case of separately excited DC motor the method by which the field is weakened simply involves a reduction in the field current. Thanks to brush and commutator, this simplicity came from the fact that the fluxes due to field current and armature current are decoupled and stationary with respect to each other. However, to weaken the fields in machines were the excitation is provided by permanent magnet like PMSM is not so straightforward.

2.8.2 Field-weakening analysis of Permanent Magnet Motors

The principle of flux-weakening control of PMSM is to increase negative direct axis current and use armature reaction to reduce air gap flux, which equivalently reduces flux and achieves the purpose of flux-weakening control.

In permanent magnet motors, the excitation flux is produced by the magnets. As the magnets look a lot like "fixed excitation flux" source, the magnetic field cannot be varied as in a separately excited DC motor by controlling the field current. The approach commonly used is to control the stator armature current to produce an intentional component of mmf which acts in opposition to the permanent magnet field thereby reducing the field in the air gap. It is achieved by increasing a negative d-axis current i_d, as illustrated in figure 2.40. As a consequence i_q and then the torque are reduced in order not to exceed the maximum output current (which is greater than or equal to $\sqrt{(i_d^{\,2} + i_q^{\,2})}$).

As shown in the figure 2.40 the direction of air gap flux due to a permanent magnet rotor is opposite to the flux due to the negative d-axis current. Therefore, the air gap flux will weaken thereby wide speed range is achieved.

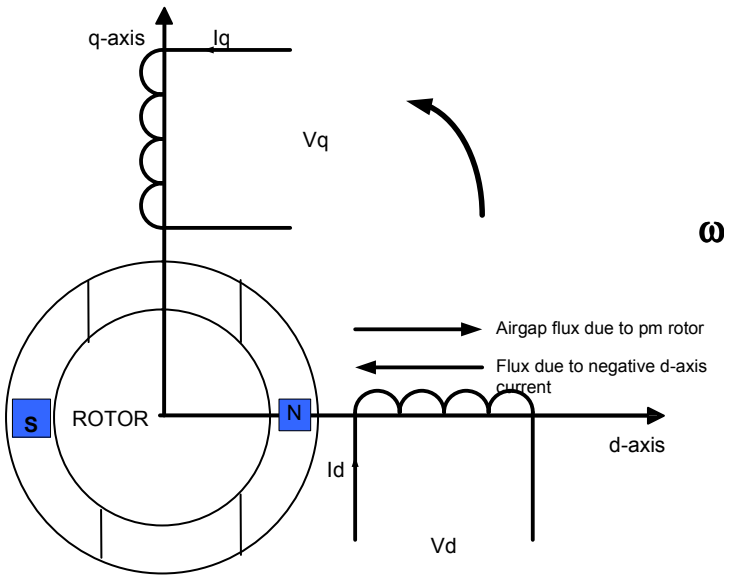

Figure 2.40 Field weakening of permanent magnet motor

This concept can be further clarified with simple vector diagrams of a non-salient PM motor. Figure 2.41 (a) shows the phasor diagram when the motor is running at a low speed well below the rated speed. When the motor is operating at the rated condition with the maximum possible voltage *V*, it can be noted that the voltage vector is on the voltage limit contour, as shown in figure 2.41 (b). It is virtually impossible to increase the speed further once the voltage limit is reached. In order to increase the speed beyond the rated speed, an introduction of the negative d-axis current I_d is then necessary. As depicted in figure 2.41 (c), with the help of the imposing current I_d, the voltage vector *V* is "brought back" within the voltage limit.

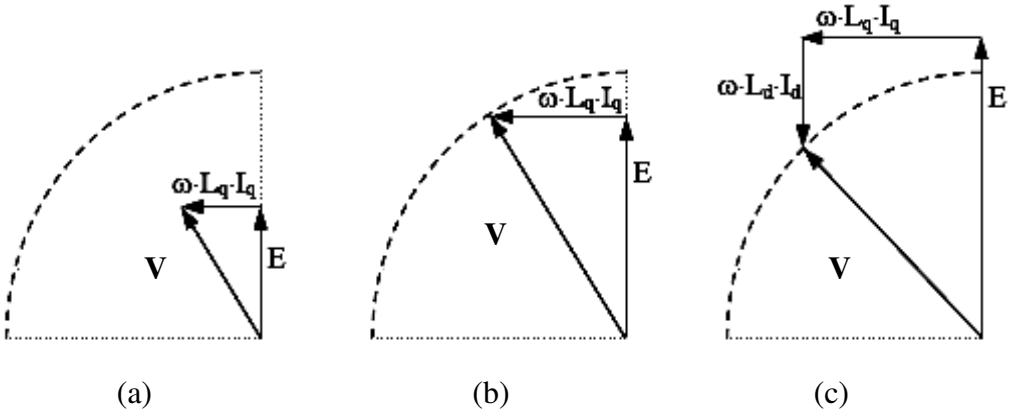

Figure 2.41 Phasor diagram of the PM motor (ideal condition assumed): (a) At low speed; (b) At rated speed; (c) Beyond rated speed with Id.

2.8.3 Operation in flux weakening region

For operation above base speed, the back EMF, due to permanent magnets on the rotor, can exceed the available inverter voltage. For PMSM drives, the impact of the back EMF can be reduced by adding a demagnetizing current component, i.e $i_d < 0$. This allows the operation above base speed, although the obtainable torque is reduced due to the demagnetizing current component.

The properties of operation above base speed, i.e., field-weakening operation, are commonly described in terms of limitations in the current dq-plane. The current is limited by

$$\sqrt{{i_d}^2 + {i_q}^2} \le I_{\max} \tag{2.51}$$

Where I_{max} is the limit set by either the inverter rating or the thermal constraints of the PMSM. Similarly the available inverter voltage is limited by

$$\sqrt{{v_d}^2 + {v_q}^2} \le v_{\max} \tag{2.52}$$

Where v_{max} is the maximum available inverter voltage. Keeping the inverter voltage inside the largest circle possible within the voltage hexagon (see figure 2.16), v_{max} is related to the available DC-link voltage as $v_{\max} = \frac{v_{dc}}{\sqrt{3}}$, where v_{dc} is the DC-link voltage.

The way (2.53) sets a limit on the available currents is easily found by substituting the expression for v_d and v_q in equation (2.52). Neglecting the current derivatives, the following condition is obtained.

$${v^2}_{\max} = (R_s i_d - \omega_e \psi_q)^2 + (R_s i_q + \omega_e L_d i_d + \omega_e \psi_m)^2 \tag{2.53}$$

As the resistive voltage drop is relatively very small, it can be neglected and equation (2.53) can be simplified to

$$\left(i_d + \frac{\psi_m}{L_d}\right)^2 + \left(\frac{L_q}{L_d} i_q\right)^2 = \left(\frac{v_{\max}}{\omega_e L_d}\right)^2 \tag{2.54}$$

which describes an ellipse (or a circle in the case of non-salient PMSM) in the dq-palne, with its center at $i_d = -\psi_m / L_d$ and ellipticity L_q / L_d. Thus, the current is not only limited within the circle $\sqrt{{i_d}^2 + {i_q}^2} \le I_{\max}$, but also within this voltage limit ellipse. As the speed increase, the voltage limit ellipse shrinks towards its center. The voltage and current limit circles is shown in figure 2.42.

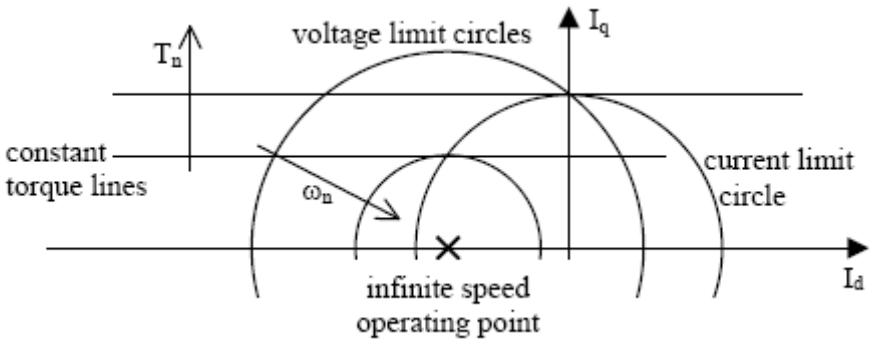

Figure 2.42 Voltage and current limit circle

2.8.4 Common flux weakening strategies

The PMSM motor is represented here by the steady-state part of its state-space voltage equations (2.55) to (2.59).

$$v_d = -pL_q \omega i_q \tag{2.55}$$

$$v_q = R_s\, i_q + k_t \omega \tag{2.56}$$

$$T_e = T_L + J_m \frac{d\omega_e}{dt} + B.\omega_e = \frac{3p}{2}(\psi_m i_q) = \frac{3}{2} k_t i_q,\ k_t = p\psi_m \tag{2.57}$$

$$v_S = \sqrt{v_d^2 + v_q^2} = V_{ph} \quad ; v_{S\max} = mV_{dc}\ ,\ \text{m=2/3} \tag{2.58}$$

$$i_S = \sqrt{i_d^2 + i_q^2} = I_{ph} \tag{2.59}$$

Using equations (2.55) and (2.56), a PMSM voltage d-q vector diagram is developed as shown in figure 2.43 for maximum torque operating region (for the sake of simplicity, it was approximated with $i_d = 0$), figure 2.43 (a) and the flux weakening region as in figure (2.43 (b)). The current and voltage vectors cannot exceed the limits from figure 2.42.

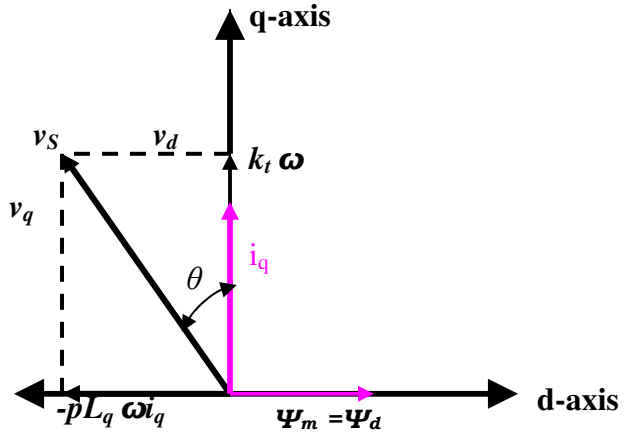

a) $i_d = 0$

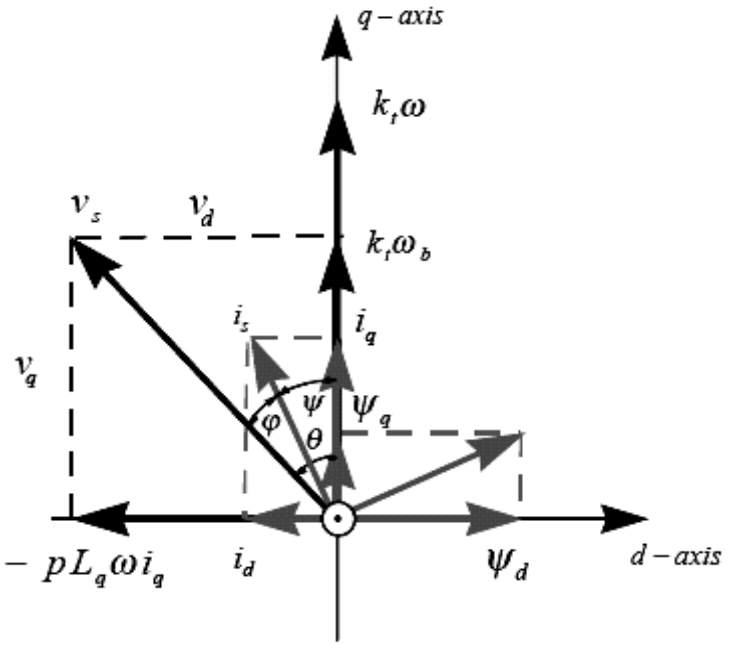

b) $i_d \neq 0$

Figure 2.43 PMSM voltage d-q vector diagram for a) $i_d = 0$, and b) $i_d \neq 0$

In order to produce the maximum torque, which main component is proportional to q-axis component of the armature current, it is convenient to control the inverter-fed PMSM by keeping the direct, *d-axis*, current component to be $i_d = 0$ as long as the inverter output voltage doesn't reach its limit. At that point, the motor reaches its maximum speed, so-called *rated speed* (called also *base speed* when talking about flux-weakening). Beyond that limit, the motor torque decreases rapidly toward its minimum value, depending on a load torque profile.

To expand the speed above the rated value, the motor torque must be reduced. In PM synchronous motors the air gap flux is weakened by producing a negative d-axis stator current component, i_d. This control method is called *flux-weakening*. Above base speed, i_d is typically limited by [26]

$$i_d \le -\frac{\psi_m}{L_d} + \frac{1}{L_d}\sqrt{\frac{v_{\max}^{\ 2}}{\omega_e^{\ 2}} - (L_q i_q)^2} \qquad (2.60)$$

which is found by solving i_d in equation (2.54)

As a basis for this analysis, the PMSM current and voltage d-q vector diagram in figure 2.43 is used.

During flux-weakening, because the demagnetizing (negative) i_d current increases, a phase current vector i_s rotates toward the *negative d-semi axis*. The rotation of the phase voltage vector is determined by a chosen flux weakening strategy, but at the end of flux-weakening it always rotates toward the *positive q-semi axis* because of i_q current, i.e. v_d voltage magnitude decrease. A big concern of flux-weakening control is a danger of permanent demagnetization of magnets. However, large coercitivity of materials such as Samarium-Cobalt allows significant i_d current which can extend the motor rated speed up to two times. Three commonly used flux-weakening control strategies are:[9][28]

- Constant-voltage-constant-power (CVCP) control;
- Constant-current-constant-power (CCCP) control; and
- Optimum-current-vector (OCV or CCCV - constant-current-constant-voltage) control.

Before investigating each flux-weakening control strategy, concept of normalization is very crucial. It is often convenient to express the quantities of an AC system, such as a motor, in a dimensionless form, in so-called per unit values. This way motor of different dimensions can easily be compared with each other. The parameter normalization is based on the definition of three "base'' quantities T_b, ω_b, and V_b ,which are respectively ,the amplitudes of the torque T, the electrical speed ω ,and the speed-voltage vector V at full load operation and at the maximum speed of the constant-torque region. The base quantities are assumed as follows:

- The base torque T_b is the limit torque of the constant torque region, which is the rated torque.
- The base angular frequency ω_b is the maximum electrical speed of the constant torque region (base or rated speed)
- The base voltage V_b is the voltage amplitude (of the space vector) under base torque ($T=T_b$) and base angular frequency ($\omega = \omega_b$). The base voltage is also referred to as rated voltage.

The normalized quantities (subscript n indicates normalized parameters) are therefore expressed by the following equations.

$$T_n = T/T_b \tag{2.61}$$

$$\omega_n = \omega/\omega_b \tag{2.62}$$

$$V_n = V/V_b \tag{2.63}$$

$$I_n = I / I_b \quad , \quad I_b = \frac{2.T_b.\omega_b}{3.p.V_b} \tag{2.64}$$

$$L_n = L / L_b \, , \qquad L_b = \frac{3.p\,V_b^2}{2.T_b.\omega_b^2} \tag{2.65}$$

$$\psi_{mn} = \psi_m / \psi_b \quad , \quad \psi_b = L_b.I_b = V_b / \omega_b \tag{2.66}$$

Where p is the number of pole pairs of the motor. As far as the current and the motor parameters (Equation 2.64 to Equation 2.66) are concerned, their base values are derived from the power balance.

$$T_b . \frac{\omega_b}{p} = \frac{3}{2} . V_b . I_b \tag{2.67}$$

Having in mind the concept of normalization, each flux-weakening control strategy will be explained in detail with appropriate figure.

2.8.4.1 Constant Voltage Constant Power (CVCP) Control strategy

This flux-weakening control method is based on two constraints - constant power and constant phase voltage vector, implemented in the PMSM drive d-q model to define the i_d and i_q current reference algorithms. For the sake of simplicity, the i_d current base value is set to be zero.

This strategy is very popular in industry because of its simplicity. It is based on keeping the voltage steady-state d and q components constant:

$$
\begin{aligned}
&P_m = T_m\omega = \frac{3}{2}(v_d i_d + v_q i_q) = const.\\
&v_d \approx -pL_q\omega\ i_q = -pL_q\omega_b I_{qb} = const.\\
&v_q \approx k_t\omega\ + pL_d\omega\ i_d = k_t\omega_b = const.\\
&v_s = V_{s\max} = V_{qb} = const.
\end{aligned}
\tag{2.68}
$$

Values v_{qb} , i_{qb} and ω_b are base voltage, base current and base (rated) speed in the beginning of flux-weakening, respectively. Usually, $I_{qb} = I_{s\,max}$.

Reference i_d and i_q currents are derived from equation (2.68):

$$
\begin{aligned}
&i_d = -\frac{k_t}{pL_d}\left(1 - \frac{\omega_b}{\omega}\right)\\
&i_q = I_{qb}\frac{\omega_b}{\omega}
\end{aligned}
\tag{2.69}
$$

Regarding the complexity, this is the easiest flux-weakening control, due to i_d / i_q linearity which is obvious from equation (2.69). By this strategy, the voltage vector V_s on the PMSM voltage vector diagram, figure 2.43 (b), is supposed to keep a constant position, while the vertex of the current vector, i_s , moves from point (0, I_{qb}) down the slope i_q/i_d, derived from equation (2.69) toward the *negative d-semiaxis*. The current and voltage d-q vector tendencies in CVCP flux-weakening control strategy are shown in figure 2.44. However, when the phase current limit, figure 2.42, is reached, i.e. after passing the critical speed, ω_{cr}, the strategy fails and vector I_s follows the limitation circle, while vector V_s naturally rotates toward the v_q -axis. The critical speed, where the current reaches its limit is:

where

$$\omega_{cr} = \frac{I_p^2 + I_{qb}^2}{I_p^2 - I_{qb}^2}\omega_b = \frac{V_{qb}^2 + V_d^{'2}}{V_{qb}^2 + V_d^{'2}}\omega_b \qquad (2.70)$$

$$I_p = \frac{k_t}{pL_d}; \qquad V_d^{'} = \frac{L_d}{L_q}V_d$$

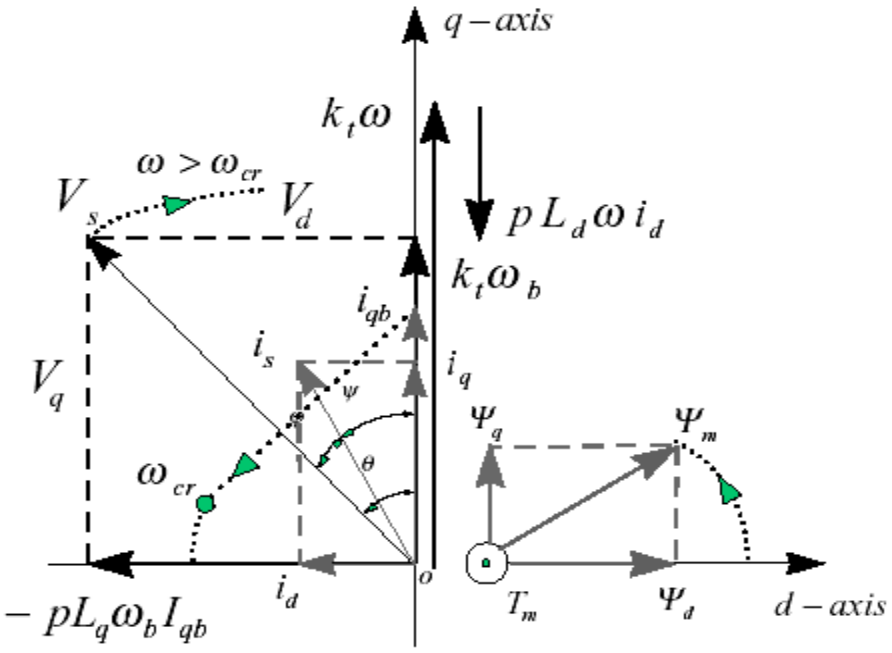

Figure 2.44 PMSM voltage d-q vector diagram for CVCP flux-weakening control

2.8.4.2 Constant Current Constant Power (CCCP) Control strategy

Besides the constant power, this strategy tries to maintain a constant magnitude of the phase current vector. A characteristic of this method is that neither i_q, nor i_d current depends on the motor parameters. The i_q current has the same expression as in the previous strategy, due to keeping the power constant. That implies that v_d voltage is also constant, figure 2.45. However, the phase voltage *q-axis* component, v_q, depends on both, motor parameters and the current *q-axis* component base value.

The references for this control method are:

$$\begin{aligned} i_s &= I_{qb} = const. \\ P_m &= T_m \omega = \frac{3}{2}(v_d i_d + v_q i_q) = const. \end{aligned} \tag{2.71}$$

From equation (2.71), reference i_d and i_q currents for the current control loops are:

$$\begin{aligned} i_q &= I_{qb} \frac{\omega_b}{\omega} \\ i_d &= -\sqrt{I_{qb}^2 - i_q^2} \end{aligned} \tag{2.72}$$

The d-q voltage equations in steady-state, extracted from equation (2.71) are:

$$\begin{aligned} v_d &= -pL_q \omega\, i_q = const. \\ v_q &= -pL_d \omega\, i_d + k_t \omega \end{aligned} \tag{2.73}$$

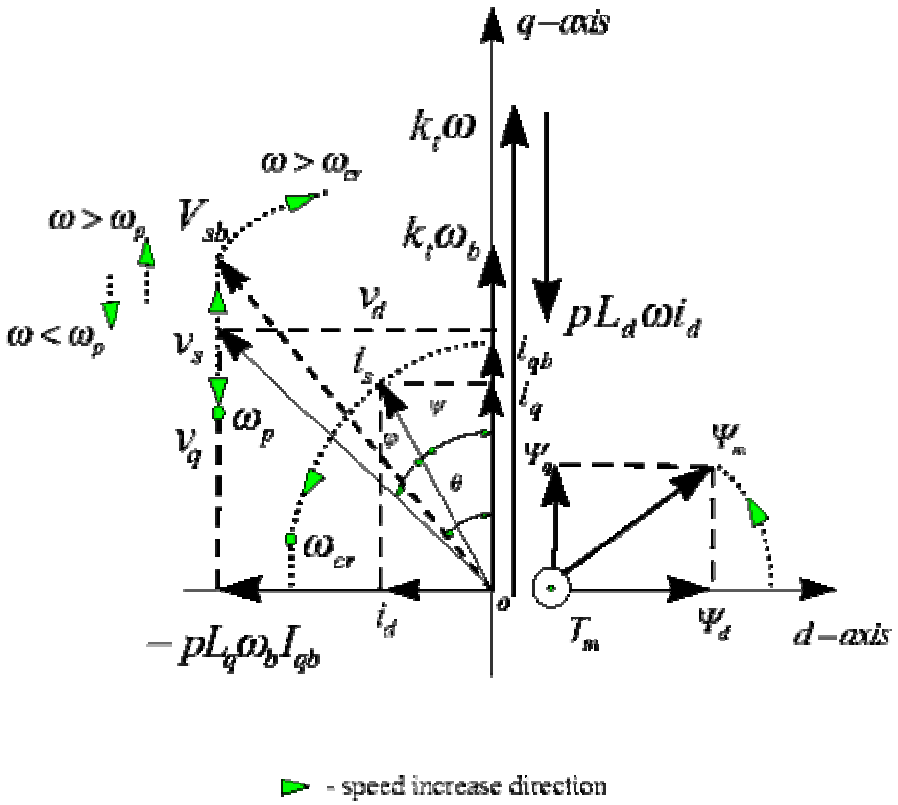

Figure 2.45 PMSM voltage d-q vector diagram for CCCP flux weakening control

By applying this strategy, the phase current vector i_s rotates around its origin, and phase voltage vector V_s, vertex moves along the V_d line, figure 2.45.The *prevailing speed*, ω_p, where voltage V_q passes its minimum is

$$\omega_p = \frac{\omega_b}{\sqrt{1-\left(-\frac{V_d^{'}}{V_{qb}}\right)^2}} \Rightarrow v_q = v_{q\min} \tag{2.74}$$

where $V_d^{'} = \frac{L_d}{L_q} V_d$ and $V_{qb} = k_t\omega_b$.

A critical speed when voltage V_S reaches its maximum value is the same as in the previous example, but now the phase current i_s reaches its limit:

$$\omega_{cr} = \frac{I_p^2 + I_{qb}^2}{I_p^2 - I_{qb}^2}\omega_b = \frac{V_{qb} + V_d^{'}}{V_{qb} + V_d^{'}}\omega_b \qquad (2.75)$$

When $\omega=\omega_{cr}$,the phase voltage reaches its limit and stays constant under higher speed.

In comparison with the constant voltage strategy, this strategy is more complex because of the reference i_d/i_q non-linearity. Its advantages are constant phase current and constant power in flux-weakening region between ω_b and ω_{cr}.

2.8.4.3 Optimum Current Vector (OCV) Control

Unlike the constant power flux-weakening control strategies, where phase voltage or current were reduced in order to keep constant active power, in this method the active power is allowed to change with a change of the power factor, *cos φ*, while the magnitudes of phase current and phase voltage vectors are set to their maximum values:

$$i_S = I_{qb} = I_{s\,max} = const. \qquad (2.76)$$
$$v_S = V_{qb} = V_{S\,max} = const.$$

In other words, by this control strategy the maximum allowable apparent power is used, although the active power is not constant. Hence, both vector trajectories are along their limiting circles, figure 2.42. The superimposed current, voltage and flux vector diagrams are shown in figure 2.46. The expressions for the abovementioned conditions are:

$$v_S^2 = v_d^2 + v_q^2 = V_{S\max}^2 \tag{2.77}$$

$$i_S^2 = i_d^2 + i_q^2 = I_{S\max}^2 = I_{qb}^2 \tag{2.78}$$

The consequent expressions for reference currents i_d and i_q, are:

$$i_d = -I_{qb} K_1 \left(1 - \frac{\omega_b^2}{\omega^2}\right) \tag{2.79}$$

$$i_q = I_{qb} \sqrt{1 - \left[K_1 \left(1 - \frac{\omega_b^2}{\omega^2}\right)\right]^2} \tag{2.80}$$

where $$K_1 = \frac{I_{qb}}{2I_p} + \frac{I_p}{2I_{qb}} \tag{2.81}$$

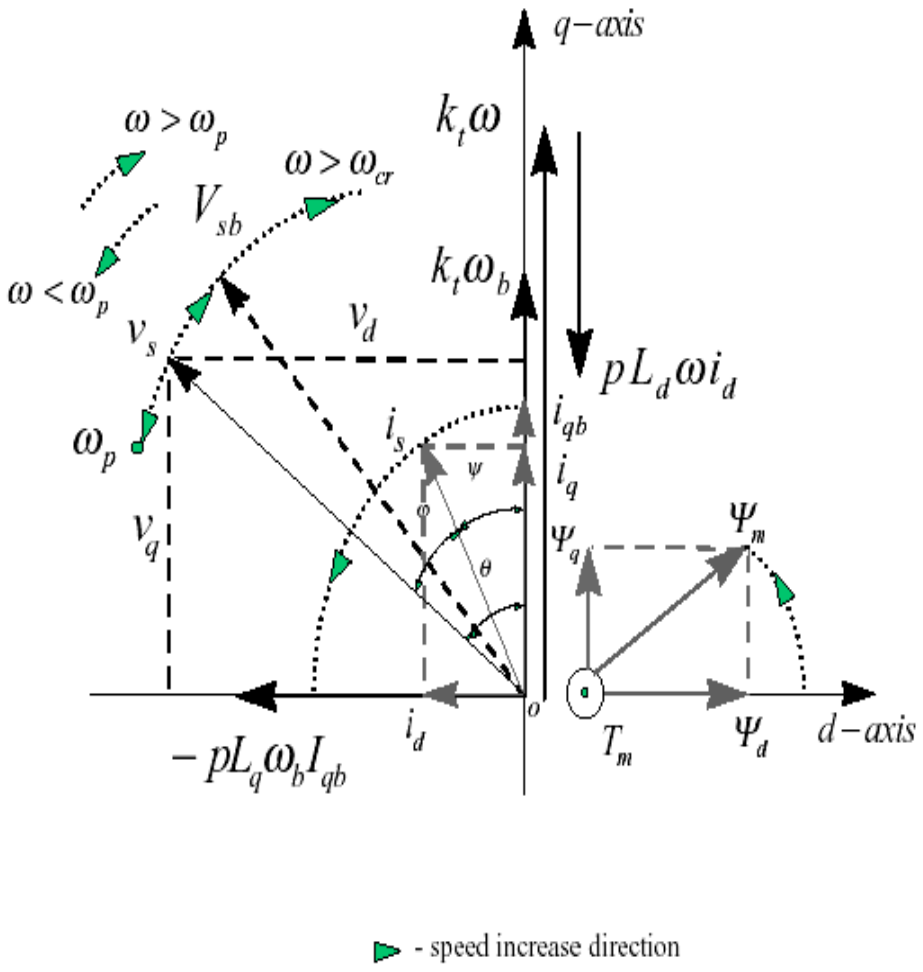

Figure 2.46 PMSM voltage d-q vector diagram for OCV flux-weakening control

For non-salient PMSM, where $L_d = L_q = L$, and

$$i_d = I_p^{'}\left[1-\sqrt{1+K_2\left(1-\frac{\omega_b^2}{\omega^2}\right)}\right] \tag{2.82}$$

$$i_q = I_{qb}\sqrt{1-\left(\frac{I_p^{'}}{I_{qb}}\right)^2\left[1-\sqrt{1+K_2\left(1-\frac{\omega_b^2}{\omega^2}\right)}\right]^2}$$

(2.83)

CHAPTER 3

SIMULATION AND EXPERIMENTAL SET UP

This section of the thesis is concerned with the simulation results of the closed loop control of the system under field weakening using Matlab/Simulink. In the simulation part both below and above base speed will be explained. In addition to the simulation an attempt is made to formulating software that will be used to develop the open loop control of the system and the target board generates the PWM pulses that are given to the inverter.

3.1 Simulation result and discussion

This section deals with the simulation results of PMSM drive system. The parameters of the motor that are used in the simulation are shown in table 3.1. The system built in Simulink for a PMSM drive system has been tested at the constant torque and flux-weakening regions of operation.

The simulation of the surface mounted PMSM was done using the software package MATLAB/SIMULINK. For this purpose, the motor's block diagram, inverter, different transformations, PI controller are constructed. After running the simulation, the speed of a motor, torque, current waveforms were recorded and analyzed. The motor parameters are found from matlab documentation.

Table 3.1 Surface mounted permanent magnet motor parameters

Dc link voltage	310V
Inertia	0.0008Kg.m*2*
magnetic flux linkage	0.175Wb
pole pairs	4
rated power	700W
Base speed	175rad/s
stator resistance	2.875ohm
q-axis inductance	8.5mH
d-axis inductance	8.5mH
Rated current	3.8 Amp

friction coefficient	5.396×10^{-5} Nm/rad/s

The motor is operated with constant torque up to its base speed and beyond that base speed flux-weakening mode is adopted. Simulation results are given at the speeds of 150 radians per second which is below base speed and 233 radians per second which is above base speed of the motor.

Figure 3.1 (a) is the simulation set up that is going to be used.

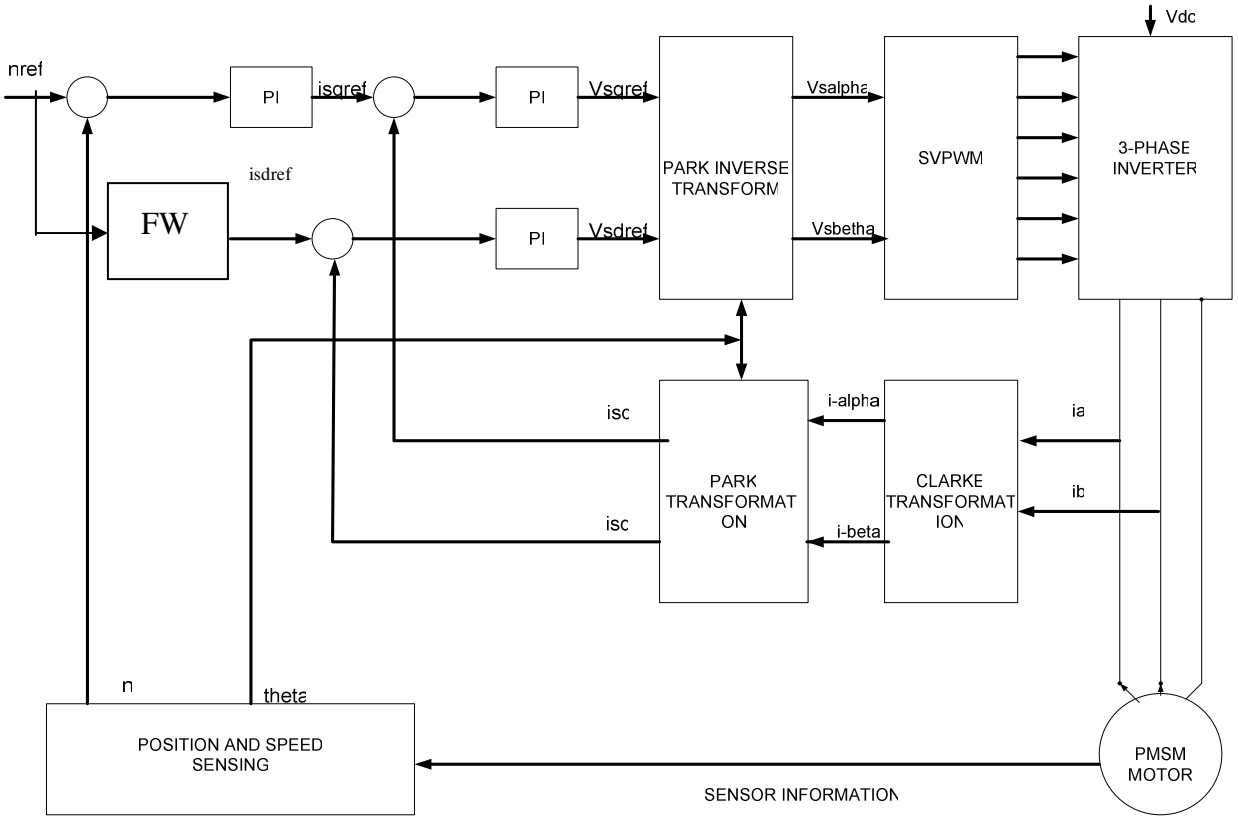

Figure 3.1 (a) The complete simulation set up

3.1.1 Simulation for Operation at 150 rad/s (without field weakening)

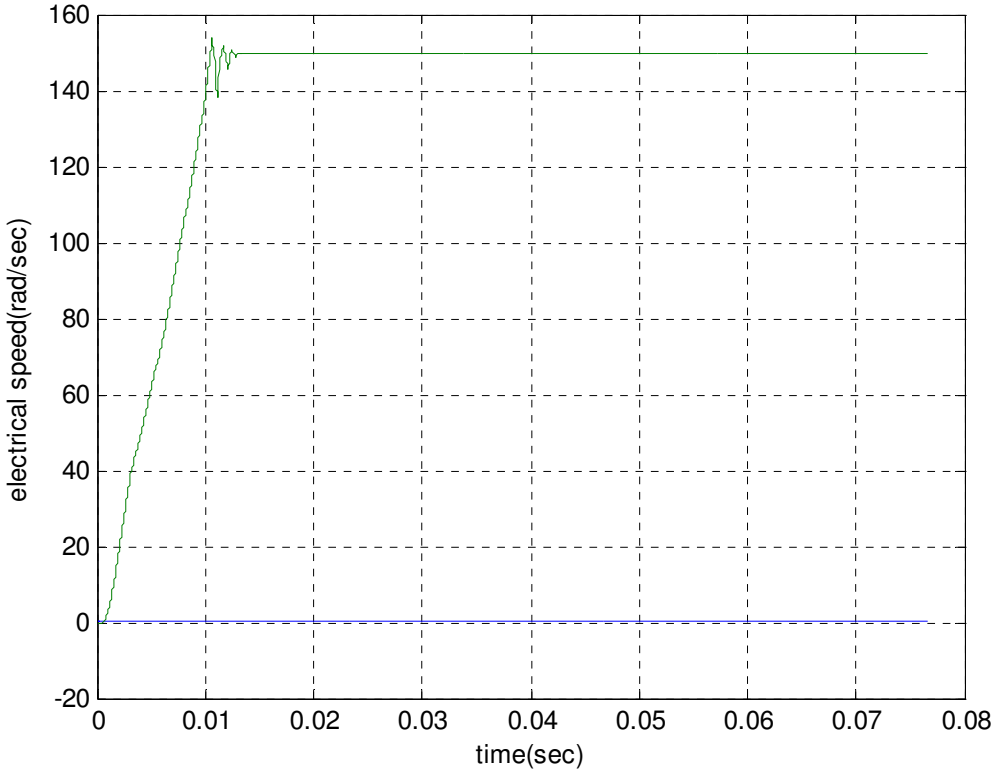

Figure 3.1 motor accelerating to Speed 150 rad/s

Figure 3.1 shows a variation of the speed with time. The steady state speed is the same as that of the commanded reference speed.

Figure 3.2 shows the developed torque of the motor. The developed torque is the same as the load torque under steady state condition. The starting torque is higher when compare to the steady state value. The steady torque is 4 Nm.

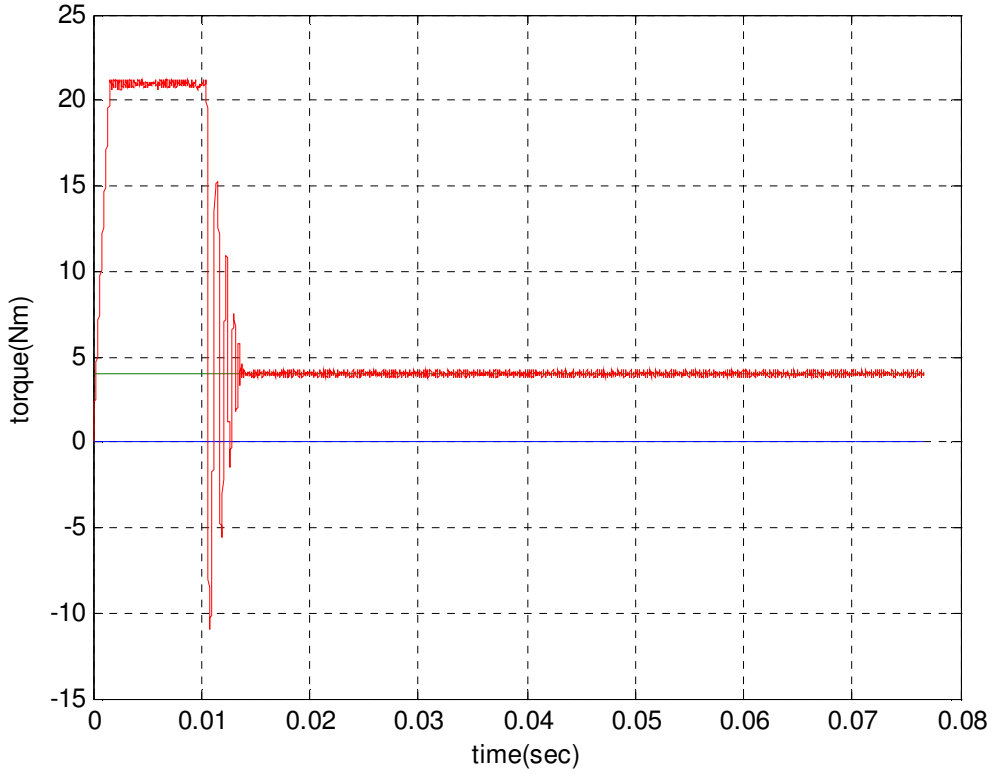

Figure 3.2 Developed Torque at 150 rad/s

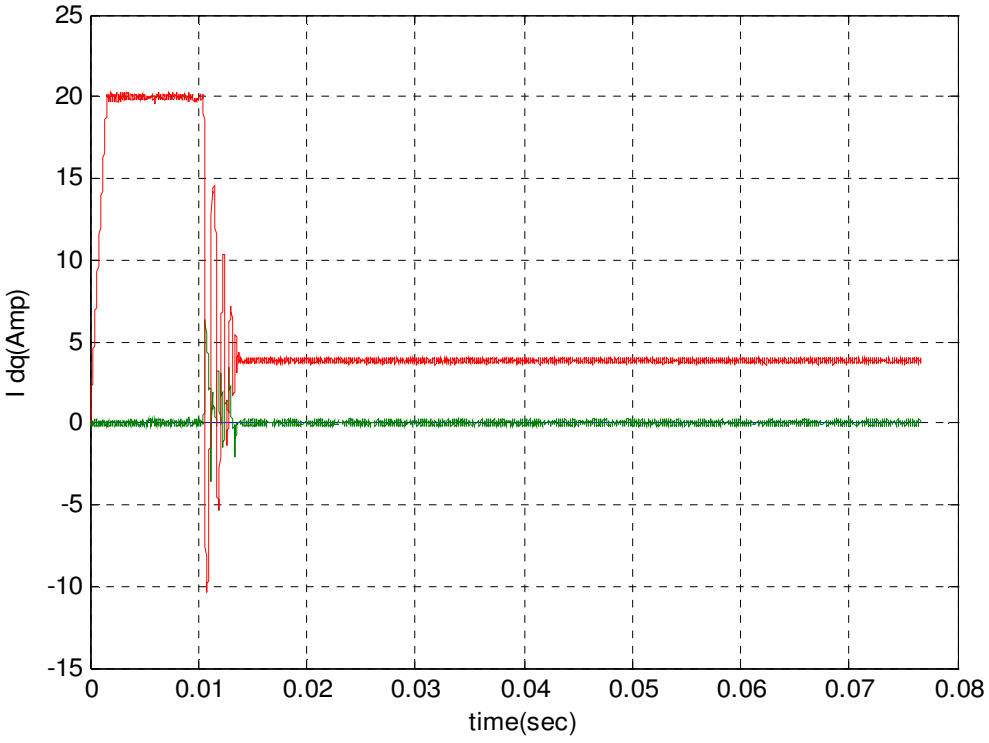

Figure 3.3 I_{dq} Currents at 150 rad/s

The d and q component of current is given in figure 3.3. Since field oriented control is used the value of i_d is zero for constant torque operation. Because of vector control the q and d-axis current is just like a dc armature and field current respectively. So the control concept lies here. That is it can control the d and q-axis current to get the desired speed.

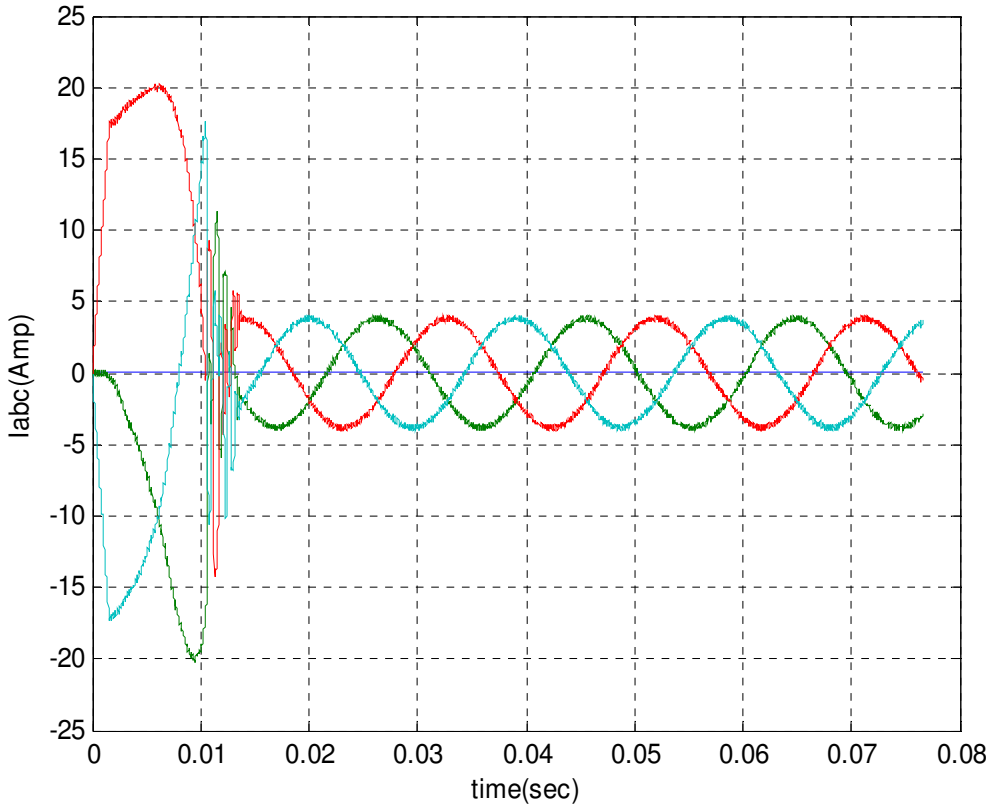

Figure 3.4 Iabc Currents as motor accelerating to 150 rad/s

Figure 3.4 shows the three phase currents drawn by the motor. The currents are obtained using Park's reverse transformation. It is clear that the current is non sinusoidal at the starting and becomes sinusoidal when the motor reaches the controller command speed at steady state.

3.1.2 Simulation for Operation at Higher Speed of 233 rad/s (with field weakening)

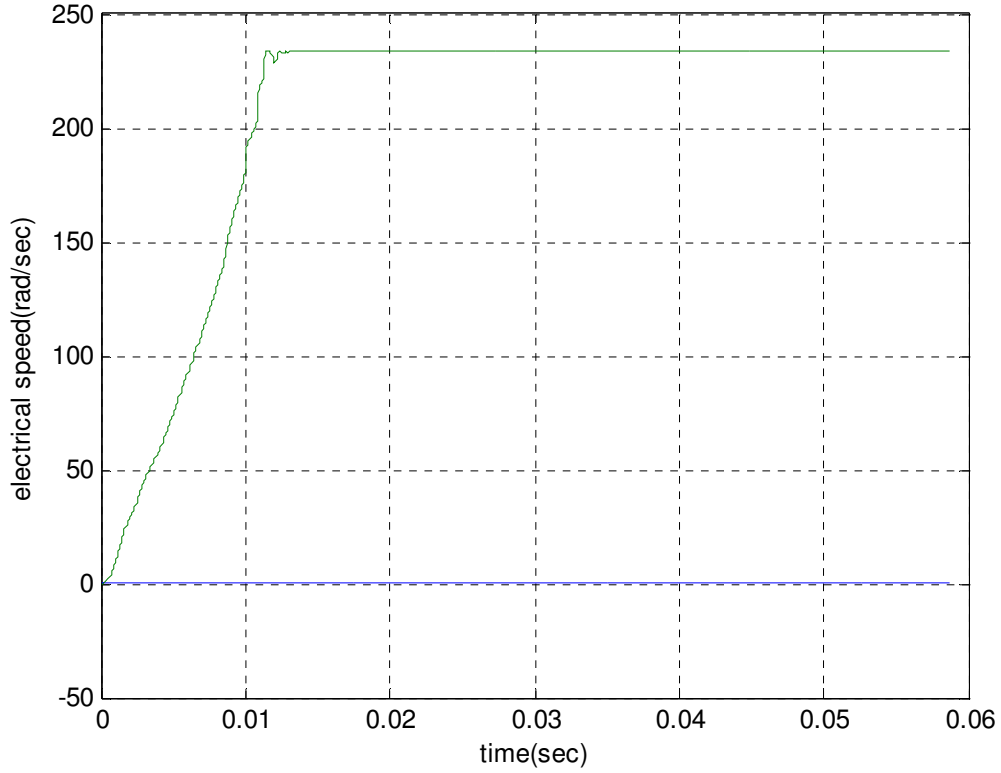

Figure 3.5 Motor accelerating to Speed 233 rad/s

Figure 3.5 shows a variation of the speed with time. The steady state speed is the same as that of the commanded reference speed of 233 rad/sec.

Figure 3.6 shows the developed torque of the motor. The starting torque is quiet high and the steady state value of torque is reduced at this speed. At this speed the motor is operating in the constant power region.

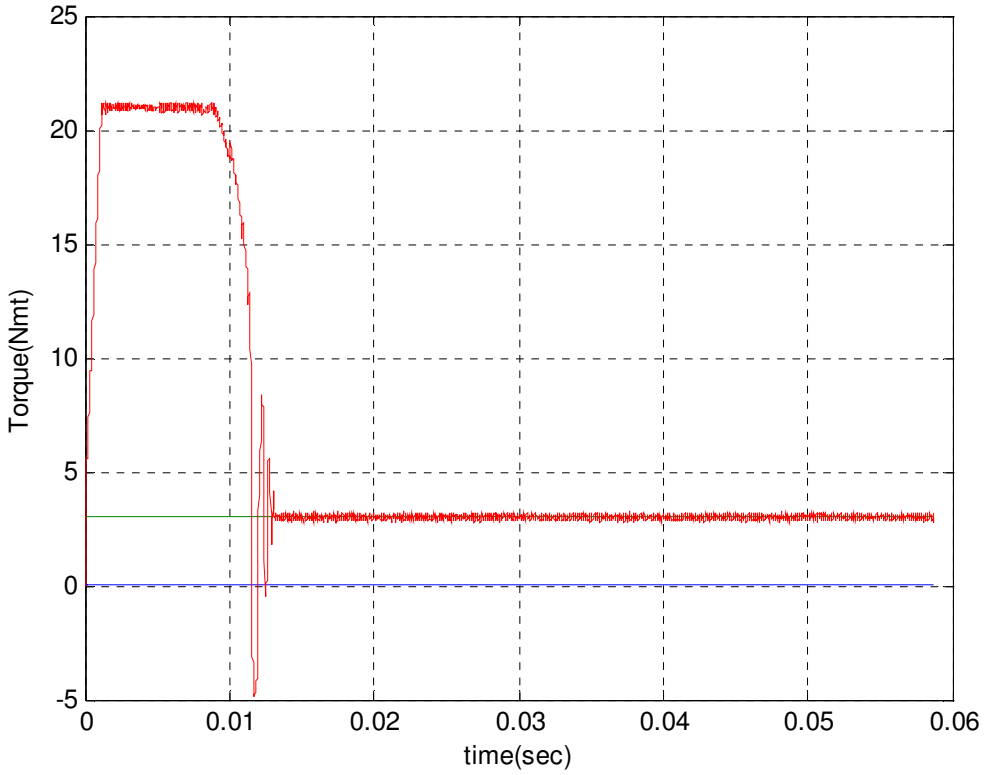

Figure 3.6 Developed torque at 233 rad/s

The dq component of current is given in figure 3.7. Both d and q axis current are present. However the q axis current is very small since the torque gets reduced at higher speed, operating at constant power region. In this region negative d-axis current is applied to weaken the air gap flux.

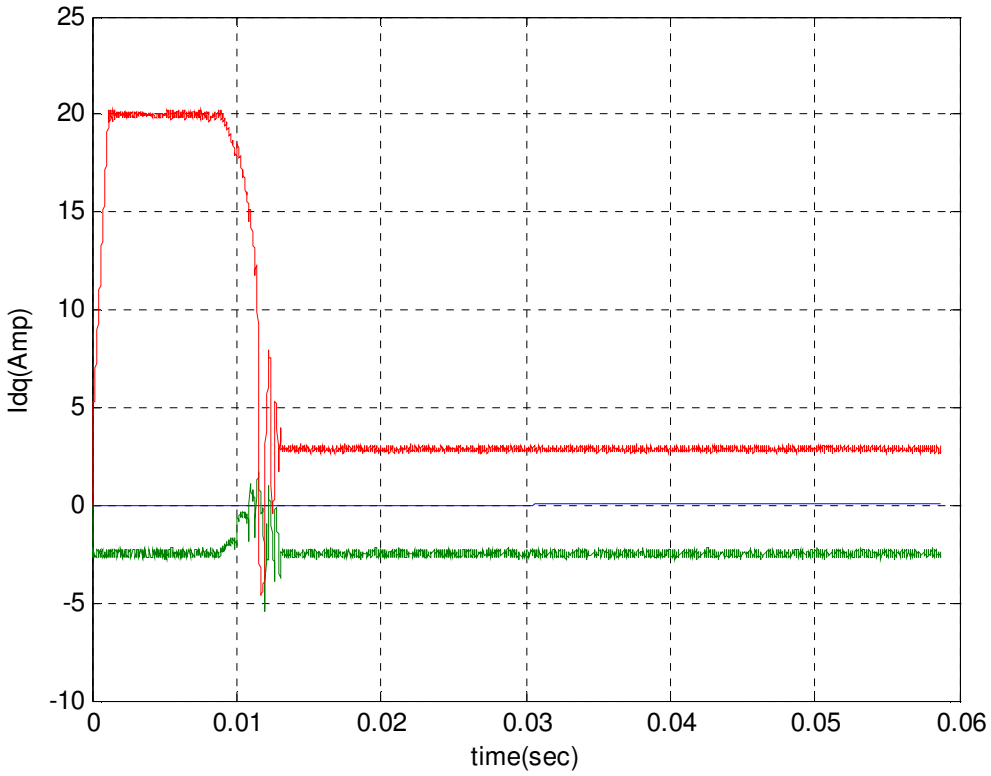

Figure 3.7 I dq currents at 233 rad/sec

Figure 3.8 shows the three phase currents obtained from Park's reverse transformation. It is clear that the current is non sinusoidal at the starting and becomes sinusoidal when the motor reaches the controller command speed of 233 rad/sec at steady state

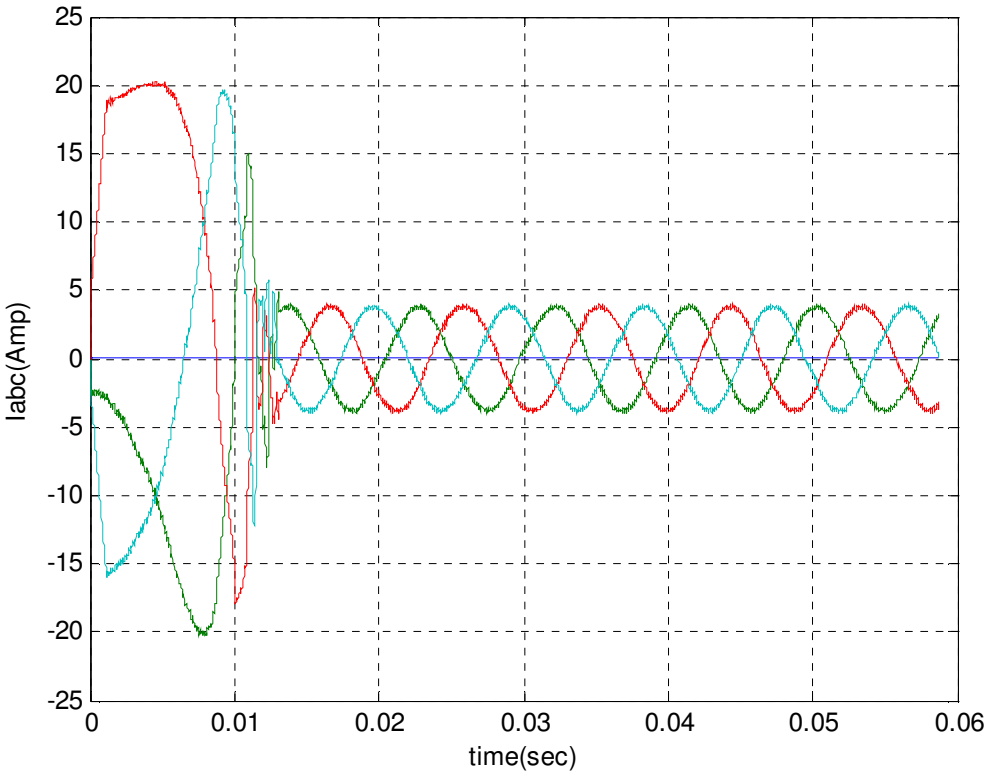

Figure 3.8 Iabc Currents as motor accelerating to 233 rad/s

Figure 3.9 shows a motor speed when there is a change of torque for forward rated torque(4 Nmt) to reverse rated torque (-4Nmt). This is one of the performance tests that indicate the simulation is quite alright.

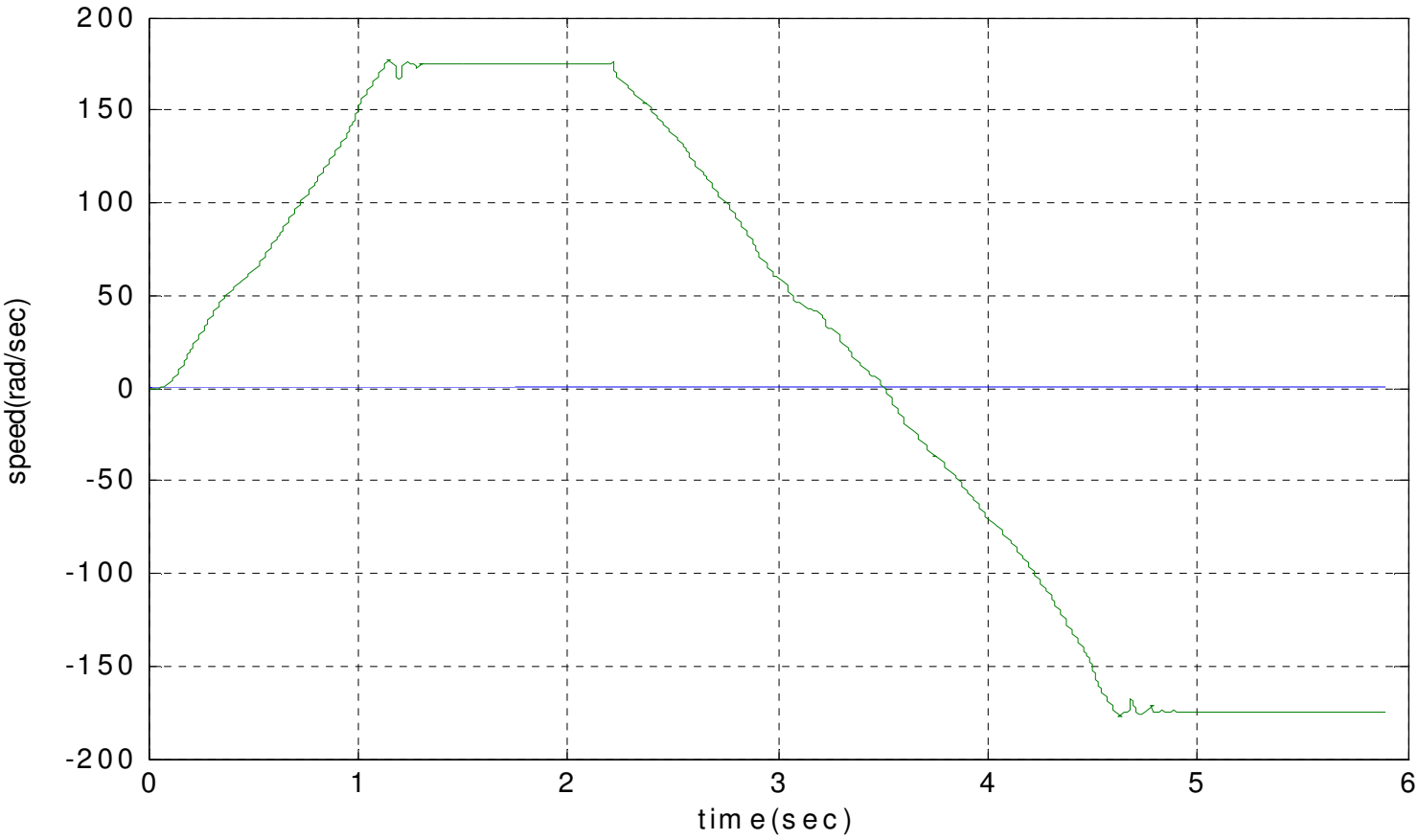

Figure 3.9 Motor electrical speed when change of torque

In electrical vehicle giving the small torque below rated torque make the vehicle to run beyond base speed. Figure 3.10 shows the speed change if the torque is decreasing from 4 Nmt (rated motor torque) to 3.5 Nmt.

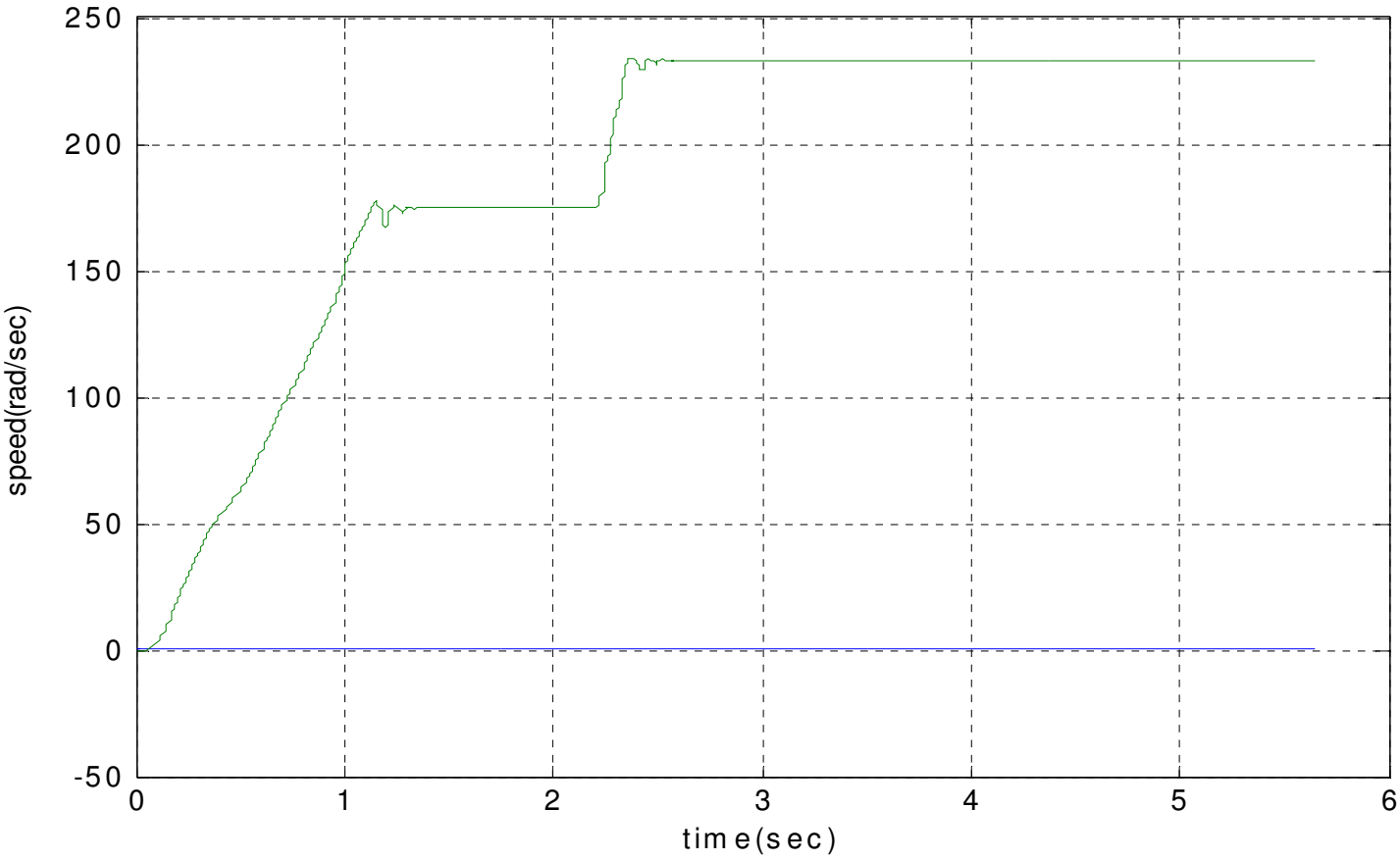

Figure 3.10 Sudden decreasing of torque from Trated (4 Nmt) to 3.5 Nmt

The torque speed characteristic for both with and without field weakening capability is shown in figure 3.11. The reason why the speed range beyond base speed is not wide is that here in this thesis the type of motor that is used is surface mounted permanent magnet synchronous motor. Since the air gap is large when compare to interior permanent magnet motor, wide speed range is not possible.

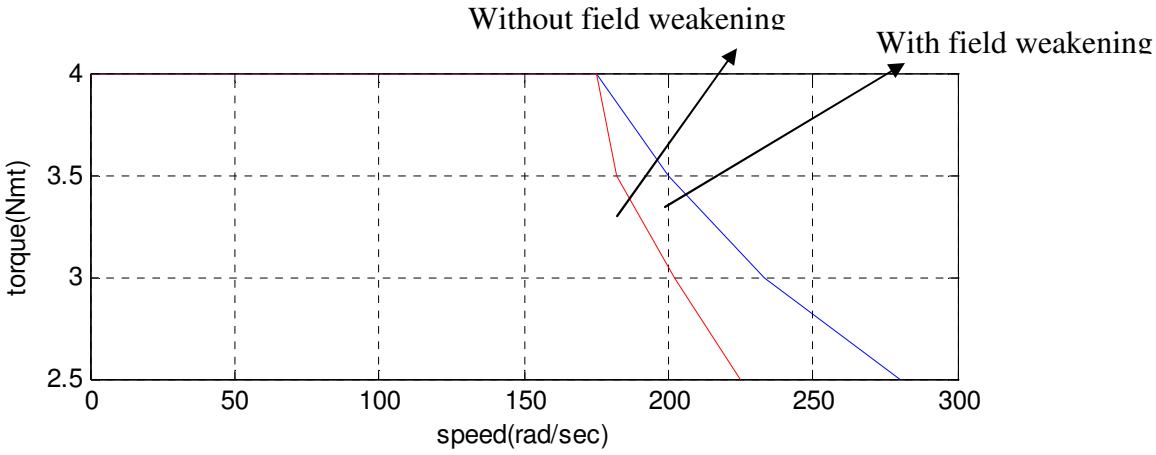

Figure 3.11 The speed-torque characteristics curve with and without field weakening capability

3.2 System hardware and software organization

3.2.1 System hardware

3.2.1.1 The DSP(TDS 2407 EA) in motor control

A more appropriate definition for DSP as it applies toward the computer industry can be derived from the name digital signal processing itself–DSP is the processing of analog signals in the digital domain. Real-world signals, such as voltages, pressures, and temperatures, are converted to their digital equivalents at discrete time intervals using ADC for processing by the CPU of a digital computer. The result is an array of numerical values stored in memory, ready to be processed. DSP is useful in almost any application that requires the high-speed processing of a large amount of numerical data. The data can

be anything from position and speed information for a closed loop control system, to two-dimensional video images, to digitized audio and vibration signals. The common factor in all of these applications is the need to do extremely high-speed calculations on large amounts of data in real time.

If an application to be controlled or analyzed requires that time-critical functions be completed within a given time interval, then a system can be called a real-time system if it will completely execute the necessary functions within the given time interval for all cases. More specifically, real time implies real time within the constraints of the system of interest.

Traditionally motor control was designed with analog components as they are easy to design and can be implemented with relatively inexpensive components. However, there are several drawbacks with analog systems. Aging and temperature can bring about component variation causing the system to need regular adjustment, as the part count increases, the reliability of the system decreases. Analog components raise tolerance issues and upgrades are difficult, as the design is hardwired.

Digital systems offer improvements over analog designs. Drift is eliminated since most functions are performed digitally, upgrades can easily be made in software and part count is also reduced since digital systems can handle several functions on chip.

Generally fixed point DSPs are preferred for motor control for two reasons. Firstly, fixed point DSPs cost much less than the floating point DSPs. Secondly, for most applications a dynamic range of 16 bits is enough. If and when needed, the dynamic range can be increased in a fixed-point processor by doing floating-point calculations in software.

The performances of an AC synchronous motor are strongly dependent on its control. DSP controllers enable enhanced real time algorithms as well as sensorless control. The combination of both allows a reduction in the number of components and optimizes the design of silicon to achieve a system cost reduction.

A powerful processor such as a DSP controller does the following:

- Favours system cost reduction by an efficient control in all speed ranges implying right dimensioning of power circuits.

- Performs high-level algorithms due to reduced torque ripple, resulting in lower vibration and longer time.
- Enables a reduction of harmonics using enhanced algorithms, to meet easier requirements and to reduce filters cost.
- Removes speed or position sensors by the implementation of sensorless algorithm.
- Decrease the number of look-up tables which reduces the amount of memory required.
- Real-time generation of smooth near-optimal reference profiles and move trajectories, resulting in better-performing.
- Controls power switching inverters and generates high-resolution PWM outputs.
- Provides single chip control system.

Figure 3.12 is an overview of the hardware required to implement a Field-Oriented Control System for Permanent-Magnet Synchronous Motor using digital signal processor. The hardware comprises of DSP(TDS2407 EA) board with its JTAG emulator, inverter (DL 2646), current sensors which are found on the inverter (DL 2646), one PMSM, tachogenerator, computer and digital oscilloscope. Six PWM outputs from the DSP are used to drive a 3-phase power inverter**.** The DSP samples ia and ib using current sensor. In the DSP the Clarke transformation is applied to determine the stator current projection in a two-coordinate non-rotating frame. The Park coordinate transformation is then applied to obtain this projection in the d, q rotating frame. The stator phase current's d, q projections are then compared to their reference values i^*_q and i^*_d (set to 0) and corrected by mean of PI current controllers. The outputs of the current controllers are passed

through the inverse Park transformation and a new stator voltage vector is applied to the motor using the Space Vector Modulation technique.

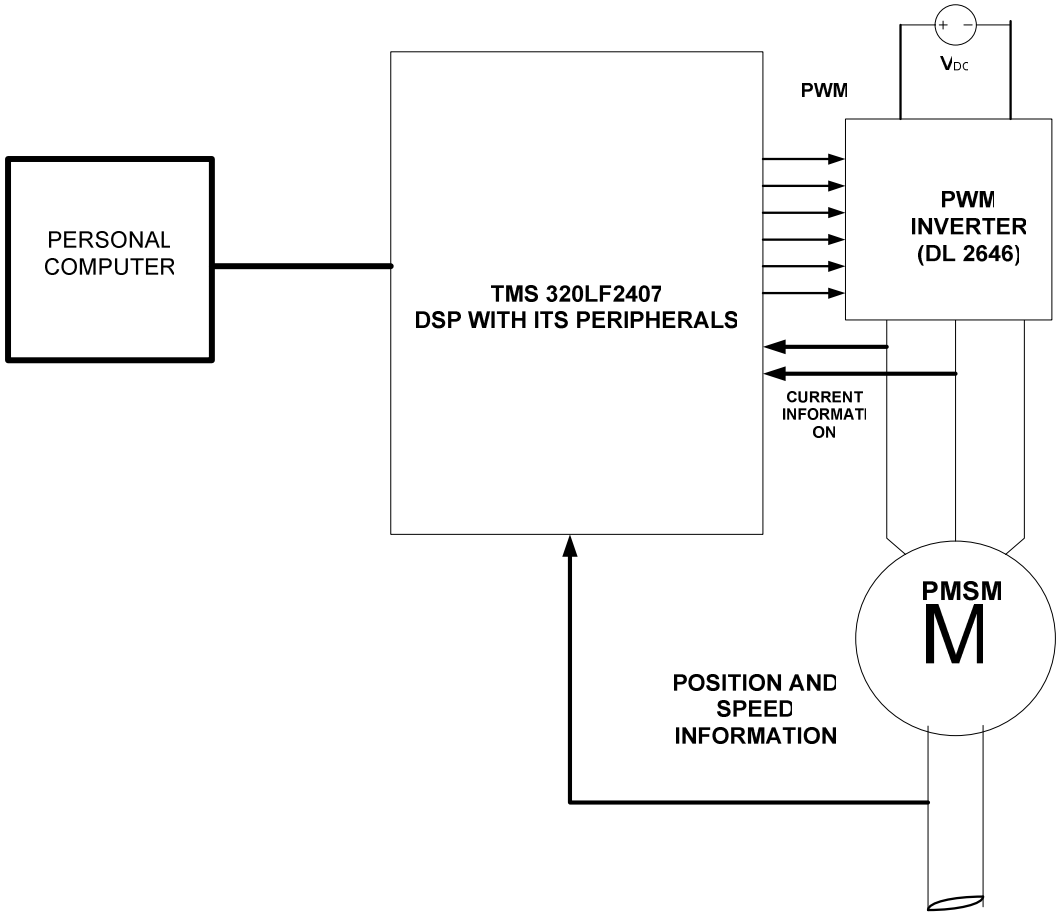

Figure 3.12 PMSM system control structure

The TDS2407 EA is a stand-alone card allowing evaluators to examine the TMS320LF2407 digital signal processor (DSP) to determine if it meets their application requirements. Furthermore, the module is an excellent platform to develop and run software for the TMS320LF2407 processor. The TDS2407 EA is shipped with a

TMS320LF2407A DSP. The DSP allows full speed verification of LF2407A code. To simplify code development and shorten debugging time, a C2000 Tools Code Composer driver is provided with a JTAG emulator.

Here are the main Key Features of TDS2407 EA:

- TMS320LF2407A Digital Signal Processor
- JTAG emulator
- 30 MIPS operating speed
- 1K words on-chip RAM
- 8K words on-chip Flash memory
- Onboard 7.28 MHz. CPU clock from gate array
- 2 Expansion Connectors (analog, I/O)
- 5-volt only operation with supplied AC adapter
- TI Code Composer tools driver

The TDS2407 EA consists of four major blocks of logic:

- Analog Interface Connector
- I/O Interface Connector
- Parallel Port JTAG Controller Interface
- Voltage Control

Figure 3.13 shows a block diagram of the basic configuration for the TDS2407 EA. The major interfaces of the target board include the external program and data RAM, JTAG interface, and expansion interface.

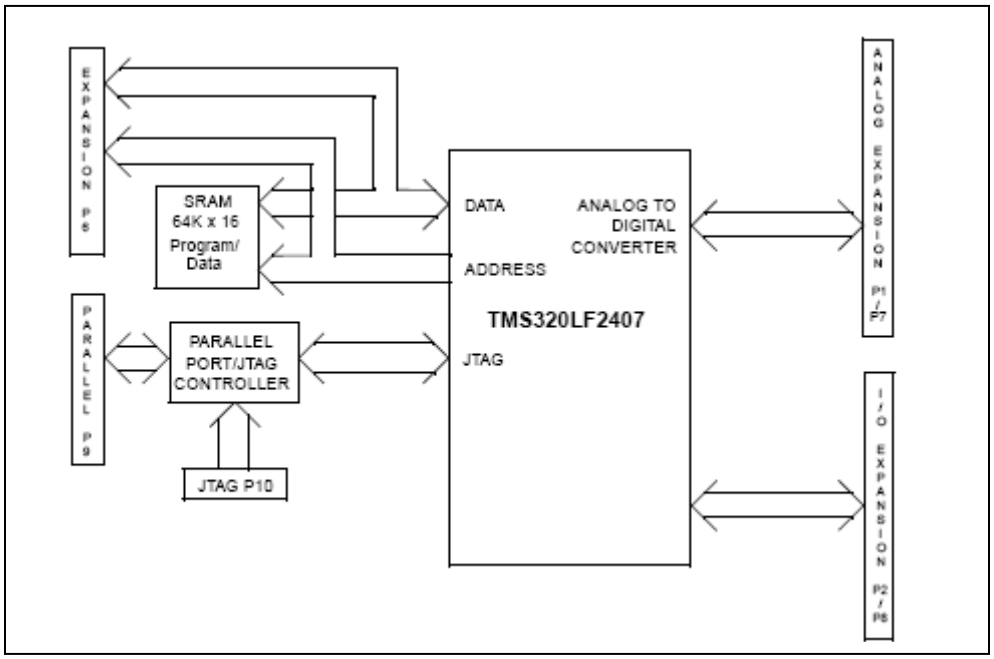

Figure 3.13 Block diagram of TDS2407 EA

3.2.1.2 A large range of applications

The target applications for a fixed point DSP controller having the necessary features are where the above-mentioned advantages meet the customer's needs. Typical end equipment applications with an advanced control are:

· Appliances (washers, blowers, compressors)
· HVAC (heating, ventilation and air conditioning)
· Industrial servo drives (Motion control, Power supply inverters, Robotics)
· Automotive control (Power steering, Anti-lock brakes, Suspension controls) etc.

Figure 3.14 is shown the complete picture of the experimental set up that is used in this thesis. Here to achieve open loop control system the main components that are needed are inverter with its current sensor (output of the sensor is voltage), DSP with its JTAG emulator, personal computer, surface mounted PMSM and to see the PWM pulses, there should be digital oscilloscope.

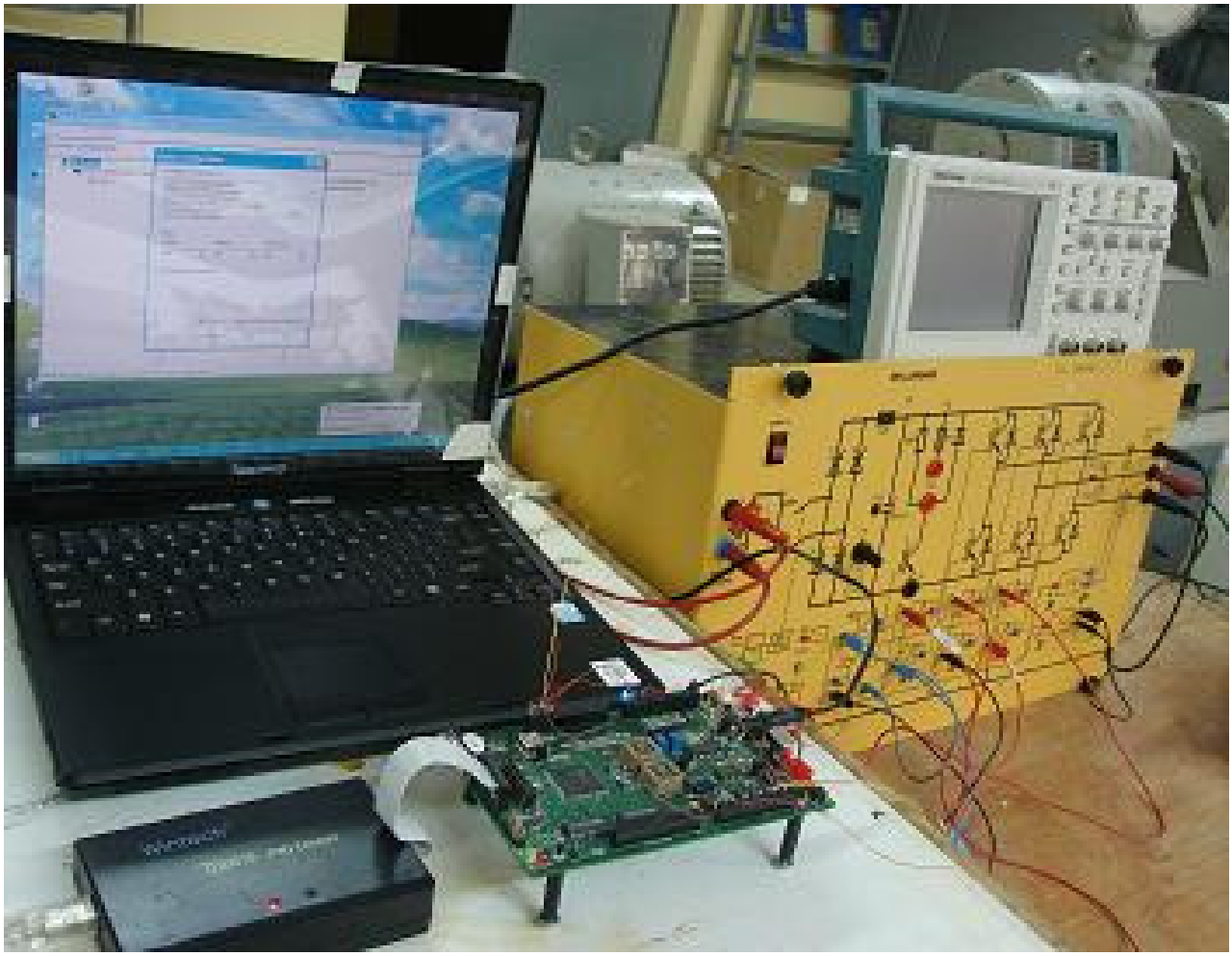

Figure 3.14 Complete experimental setup open loop control

3.2.2 SYSTEM SOFTWARE ORGANIZATION

The program is based on two modules: initialization module and the interrupt module. After a processor reset, the initialization module perform the following tasks: DSP setup, variable initializations, interrupt source selection and enable and waiting loop.

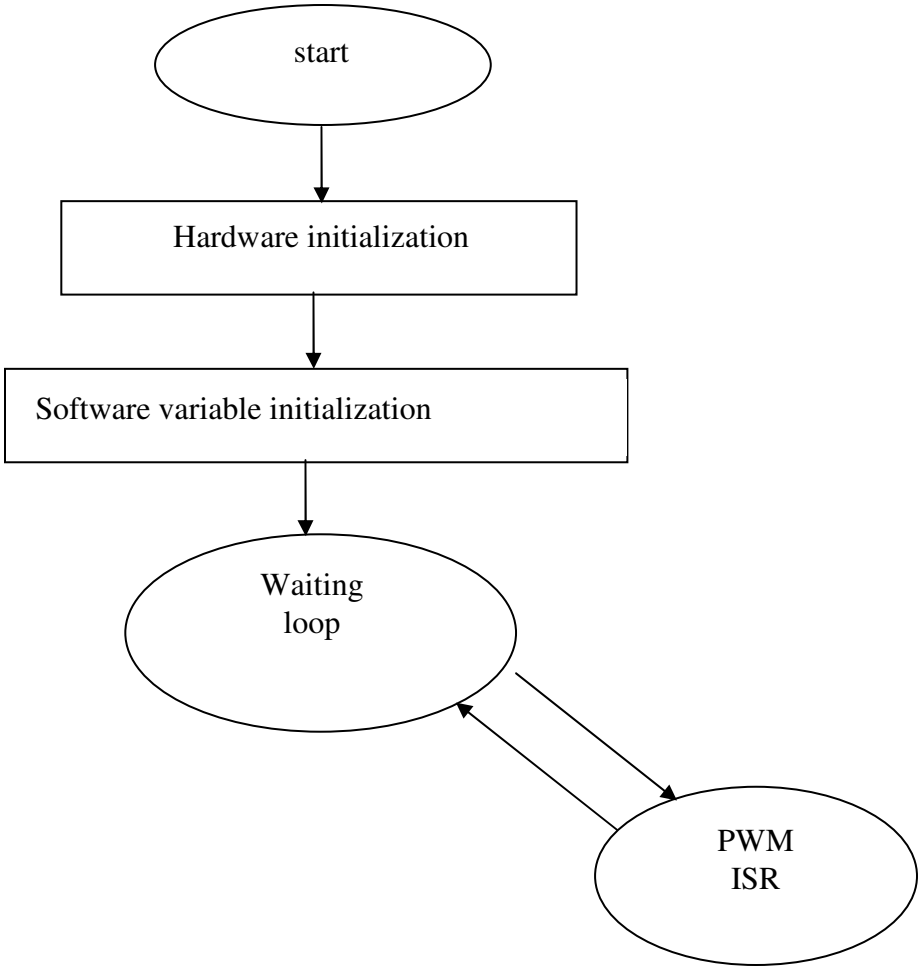

Figure 3.15 General software flowcharts

The ISR(Interrupt Service Routine) is a function executed when interrupt occurs. Here the role of the DSP in such a closed loop system is to translate the stator variables (current and angles) in to rotor coordinates as well as the values with the reference values and update the PI controller.

The program is based on two modules:

1. the initialization module

2. the interrupt module.

1. Initialization Module Description

After a processor reset, the initialization module performs the following tasks:

- DSP setup : core, watchdog, clocks, ADC, SCI, general purpose IO, event manager
- Variables initializations : default values
- Interrupt source selection and enable
- Waiting loop

3. Interrupt Module Description

The interrupt module handles the whole FOC algorithm (in this thesis interrupt module handles open loop control). It is periodically computed according to a fixed PWM (pulse width modulation) period value. The goal of the interrupt module is to update the stator voltage reference and to ensure the regulation of stator currents and rotor mechanical speed.

Block diagram for open loop control system and base don the block diagram the flow chart for open loop control are shown in the figure 3.16

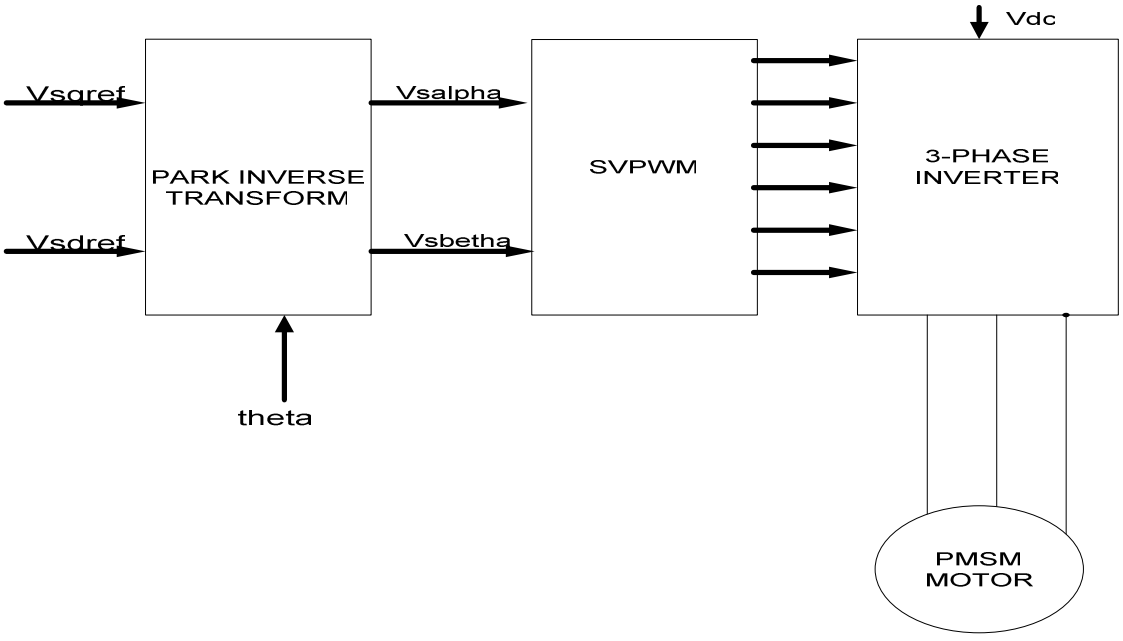
Vdc
Vsqref
Vsalpha
PARK INVERSE TRANSFORM
SVPWM
3-PHASE INVERTER
Vsdref
Vsbetha
theta
PMSM MOTOR

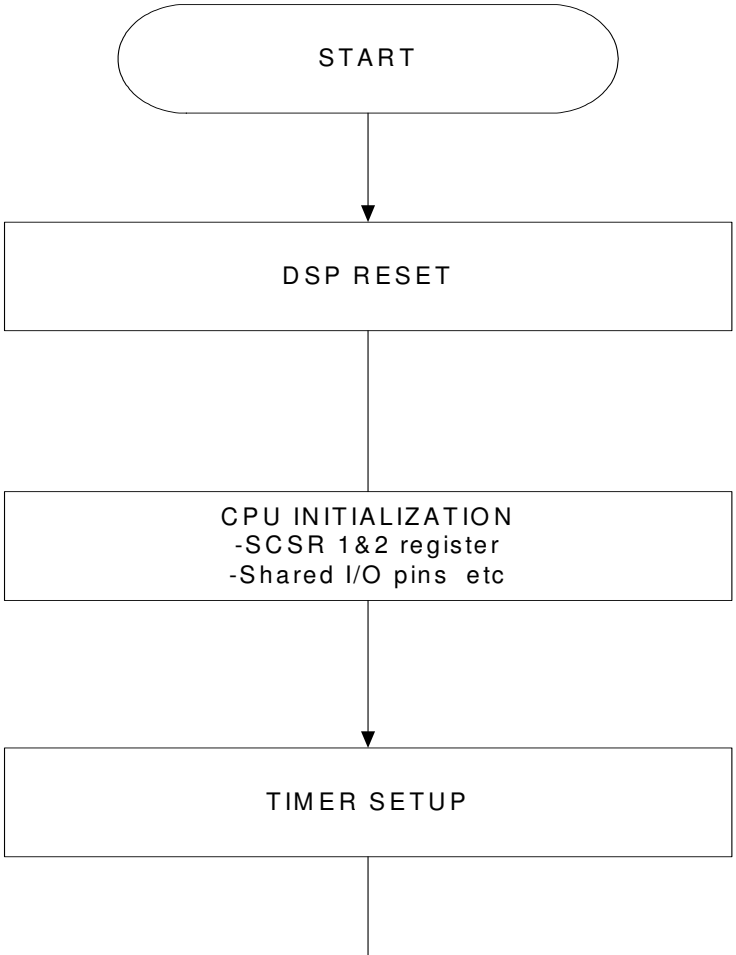
START
DSP RESET
CPU INITIALIZATION
-SCSR 1&2 register
-Shared I/O pins etc
TIMER SETUP

ISR

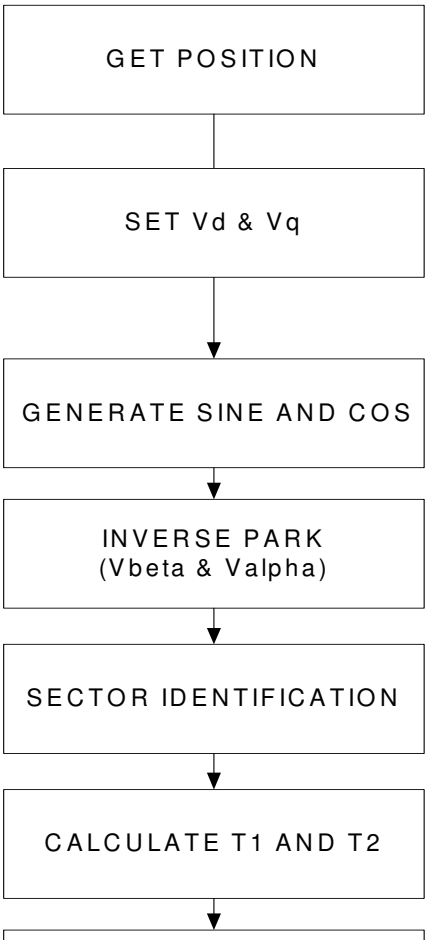
GET POSITION
SET Vd & Vq
GENERATE SINE AND COS
INVERSE PARK
(Vbeta & Valpha)
SECTOR IDENTIFICATION
CALCULATE T1 AND T2

Figure 3.16 The flow chart and block diagram for open loop control of PMSM

CHAPTER 4
CONCLUSION AND RECOMMENDATION

4.1 Conclusions

A detailed Simulink model for a PMSM drive system with field weakening control has been developed and operation below and above rated speed has been studied. Simulink has been chosen because it is capable of showing real time results with reduced simulation time and debugging.

The performance of field weakening control of PMSM motor has been studied. In the simulation it has been observed that in constant power region extended speed range beyond base speed (approximately two times) is achieved. The demagnetizing effect of the negative direct axis current to weaken the air gap flux was presented in detail.

The field weakening has not been implemented using DSP due to time constraint and some technical problems on the DSP used. It has been tried to do the open loop control and the DSP target board generate the PWM pulses.

It was also observed that total system will be efficient if field weakening controlled permanent magnet synchronous motor is implemented in electric vehicle. Gear system loss and additional load to the vehicle are totally avoided.

4.2 Recommendation

The main recommendations for this dissertation are summarized as:

- If all equipments are available, sensor based control of field weakening can be implemented using the DSP board.
- Sensorless control can also be (with no rotor position sensor) implemented.